Huang, T.; Ling, Z.; Ma, J.; Macdonald, R.; Gao, H.; Tao, S.; Tian, C.; Song, S.; Jiang, W.; Chen, L.; Chen, K.; Xie, Z.; Zhao, Y.; Zhao, L.; Gu, C.; Mao, X.:
Human exposure to polychlorinated biphenyls embodied in global fish trade.
In: Nature Food. Vol. 1 (2020) 5, 292 - 300.
First published online by Nature Research: 11.05.2020

https://dx.doi.org/10.1038/s43016-020-0066-1

Human exposure to polychlorinated biphenyls embodied in the global marine fish trade

Tao Huang[1*], Zaili Ling[1], Robie W. Macdonald[3,4], Hong Gao[1], Shu Tao[2], Chongguo Tian[5], Shijie Song[1], Wanyanhan Jiang[1], Lulu Chen[1], Kaijie Chen[2], Zhiyong Xie[6], Yuan Zhao[2], Liuyuan Zhao[1], Chen Gu[1], Xiaoxuan Mao[1], Jianmin Ma[2,1*]

[1] Key Laboratory for Environmental Pollution Prediction and Control, Gansu Province; College of Earth and Environmental Sciences, Lanzhou University, Lanzhou 730000, P. R. China

[2] Laboratory for Earth Surface Processes, College of Urban and Environmental Sciences, Peking University, Beijing 100871, P. R. China

[3] Department of Environment and Geography, Centre for Earth Observation Science, University of Manitoba, Manitoba R3T 2N2, Canada

[4] Fisheries and Oceans Canada, Institute of Ocean Sciences, Sidney, British Columbia V8L 4B2, Canada

[5] Key Laboratory of Coastal Zone Environmental Processes and Ecological Remediation, Yantai Institute of Coastal Zone Research, Chinese Academy of Sciences, Yantai 264003, P. R. China

[6] Helmholtz-Zentrum Geesthacht, Centre for Materials and Coastal Research GmbH, Institute of Coastal Research, Max-Planck Straße 1, DE-21502 Geesthacht, Germany

Abstract The international food trade poses food safety risks through the collateral transport of persistent organic pollutants (POPs). Here we assess the human exposure to a representative polychlorinated biphenyl (PCB) congener, PCB-153, through consumption of marine fish traded globally. Higher PCB exposure was identified in Europe, historically a major PCB use region with extensive fishery and fish export, than other places of the world, making higher contribution to the estimated daily intake (EDI) of PCB-153 via fish consumption of residents in those countries importing fish from Europe. Our results reveal that 84% of PCB-153 exposure in Sub-Saharan fish consumers is attributed to fish imported from Europe. In contrast, European fish consumers face reduced exposure to PCB-153 by consuming fish imported from countries fishing in less contaminated waters. We find that farmed salmon involved in global trade fed with marine ingredients from PCB-153 contaminated seawaters results in high PCB exposure. Our finding demonstrates that food trade is an important pathway of POPs between food origins and consumption.

Main

A large body of evidence has accumulated showing that humans and animals are subject to health risks due to exposure to toxic chemicals released to the environment. Chemicals that are persistent, bioaccumulative, and toxic are of particular concern because wide dispersal into global receptors in soil, air, and water leads to subsequent contamination of food webs[1]. In cases where large quantities of persistent organic pollutants (POPs) have been released (e.g., polychlorinated biphenyls (PCBs)), the

concentrations found in predatory animals are sufficient to put wildlife, humans and ecological integrity at risk[2]. Large reservoirs of some POPs, like PCBs, remain in aquatic sediment and soil for decades after they have been banned from use where they continue to be taken up by plants and animals. Owing to the persistence of large reservoirs of these chemicals in aquatic sediments, soils, and snow/ice, and continuing exchange between these media, concentrations of POPs in predatory species, especially those from aquatic environments, remain high[3]. Current use of many restricted chemicals and the development of new chemicals are of further concern[4,5]. Over 90% of human exposure to PCBs occurs by ingestion of chemically contaminated food items[5,6], many of them of animal origin. The ingestion of sufficient quantities may lead to neurological, reproductive, carcinogenic, and immunological effects[7]. PCB levels in seafood are generally higher than those in meat and can be 4-fold higher than those in rice[5,6]. The level of exposure depends on the quantity of contaminated seafood consumed. Considering that seafood is a prominent component of the human food chain, there should be a concern about seafood from origins where PCB concentrations are known to be higher.

Extensive investigations of long-range atmospheric and oceanic transport of POPs show that many of these chemicals end up in remote receptor regions where they become magnified into food webs supporting humans[8,9]. Yet, it remains unclear to what extent POPs then become further distributed within the marine food trade. Local and regional fish are caught in large fisheries and are transported in pathways set by global economies and food requirements. For those foods harvested in regions contaminated

by POPs, the food trade likely provides a direct and efficient pathway from harvest to consumption[10]. Efforts have been made to track food contamination from its origin using models and model simulations[11,12]. However, these models usually are empirical and of sufficiently coarse spatial resolution that they cannot provide an accurate global picture of the fish import/export among countries relative to the trade within countries at the national scale, or assume that POPs concentrations in diets come from the local and remote sources. Here, we incorporate a food-trade pathway into a global-scale atmospheric transport model for POPs (*Methods*). As a first step to quantify human exposure arising from the global food trade, this study implemented global fish trade data from the UN Global Comtrade (https://comtrade.un.org) and global marine fish catch data (*Methods*) in a coupled POPs atmospheric transport, multi-compartment exchange and marine food web model. This model was then used to predict exposure to marine fish embodied in global trade contaminated by a representative PCB congener, PCB-153. PCB-153 is one of the best characterized POPs with respect to physicochemical properties and emission estimates. Extensive investigations for PCB-153 provided abundant datasets which could be used to verify and compare the results from this study[11,12]. Due to its high lipophilicity[13,14], recalcitrance to metabolism in higher organisms[14], and high abundance in commercial PCB mixtures (e.g. 4.3% in Aroclor 1254 and 10.2% in Aroclor 1260)[15], PCB-153 has higher detection frequencies than other PCB congeners in the environment and in humans in many places across the globe[16,17], such as in the United States of America (USA) where PCB-138, 153, and 180 contributed 65% of total PCB body burdens[17]. PCB-153 is also among six PCB

98 congeners having marked effects on animal and human health[17], particularly in marine
99 food webs. Higher PCB-153 or hexa-PCB homologs detected in fish can be attributed
100 to the greater octanol-water partition coefficient $\log K_{OW}$, ranging from 6.3 – 8.4 or 7.0
101 for hexa-PCB homologs, and bio-concentration factor logBCF (4.66 – 5.3 for fish) or
102 5.4 (fish) for hexa-PCB homologs. These values are larger than tri-PCB ($\log K_{OW}$ = 5.8,
103 logBCF = 4.2 for fish) and tetra-PCB ($\log K_{OW}$=6, logBCF=4.6 for fish), suggesting
104 stronger partitioning of PCB-153 into fish tissue[13,14]. As a result, fish consumption is
105 an important route of human exposure to PCB-153. The present study aims to inform
106 fish consumers of the exposure to PCBs associated with consumption of marine fish
107 caught and imported from various marine locations, rather than attempt to assess the
108 risk because a risk assessment of PCB-153 or any chemical, or mix of chemicals
109 involves the complete identification of the chemical hazards and probabilities of
110 exposure to that hazard. In this context, we shall quantify the potential for the
111 international food trade to contribute to exposure of human fish consumers to PCBs,
112 focusing this initial effort on PCB-153.

113 Below, our results refer to annual mean PCB-153 concentrations in air, water,
114 sediment, and fish species on a spatial resolution of $1^o \times 1^o$ latitude/longitude across the
115 global oceans averaged over modeled daily concentrations, and their potential influence
116 on human health via 7 selected major marine fish species (*Methods*, **Supplementary**
117 **Text 1-5, Supplementary Fig. 1-8, Supplementary Table 1-4**). The modeled mean
118 levels of PCB-153 embodied in traded fish species were then used to calculate the EDI.
119 To isolate the impact of the global fish trade on human exposure, we compared two

120 distinct model scenarios. Scenario 1 incorporates international fish trade, hereafter
121 referred to as "Trade" simulation whereas Scenario 2 neglects fish trade, referred to as
122 "NO-Trade" simulation. Here we specify that all marine fish are harvested locally for
123 coastal countries and are not involved in fish trade for land-locked countries (or zero
124 fish trade), assuming the same quantity of fish consumption between the two scenarios
125 and that the fish is traded only once with no further trade for deep-processed fish.

126 **PCB-153 concentrations in environmental media**

127 Model simulations for 2012 show higher PCB-153 concentrations in air and higher
128 deposition (**Supplementary Fig. 9**) in Western Europe (WE) and the eastern seaboard
129 of the USA, in line with higher emissions of this PCB congener from these two
130 regions[18]. Higher average PCB-153 concentrations were simulated for water and
131 sediment off the west and east coasts of the North Atlantic Ocean compared with the
132 coasts of North Pacific and Indian Oceans, agreeing with observations[19-21]. PCB-153
133 entering oceans via surface runoff is discussed in *Methods* and **Supplementary text 3**.

134 As a result of the higher water and sediment concentrations, the simulated
135 concentration of PCB-153 averaged in all selected fish species was considerably higher
136 for European coastal waters (Atlantic and Mediterranean) than for the rest of the global
137 ocean (**Supplementary Fig. 10**). Therefore, fish from European coastal waters
138 exported in global trade presented the greatest burdens of PCB-153.

139 **Exposure to PCB-153 embodied in the global marine fish trade**

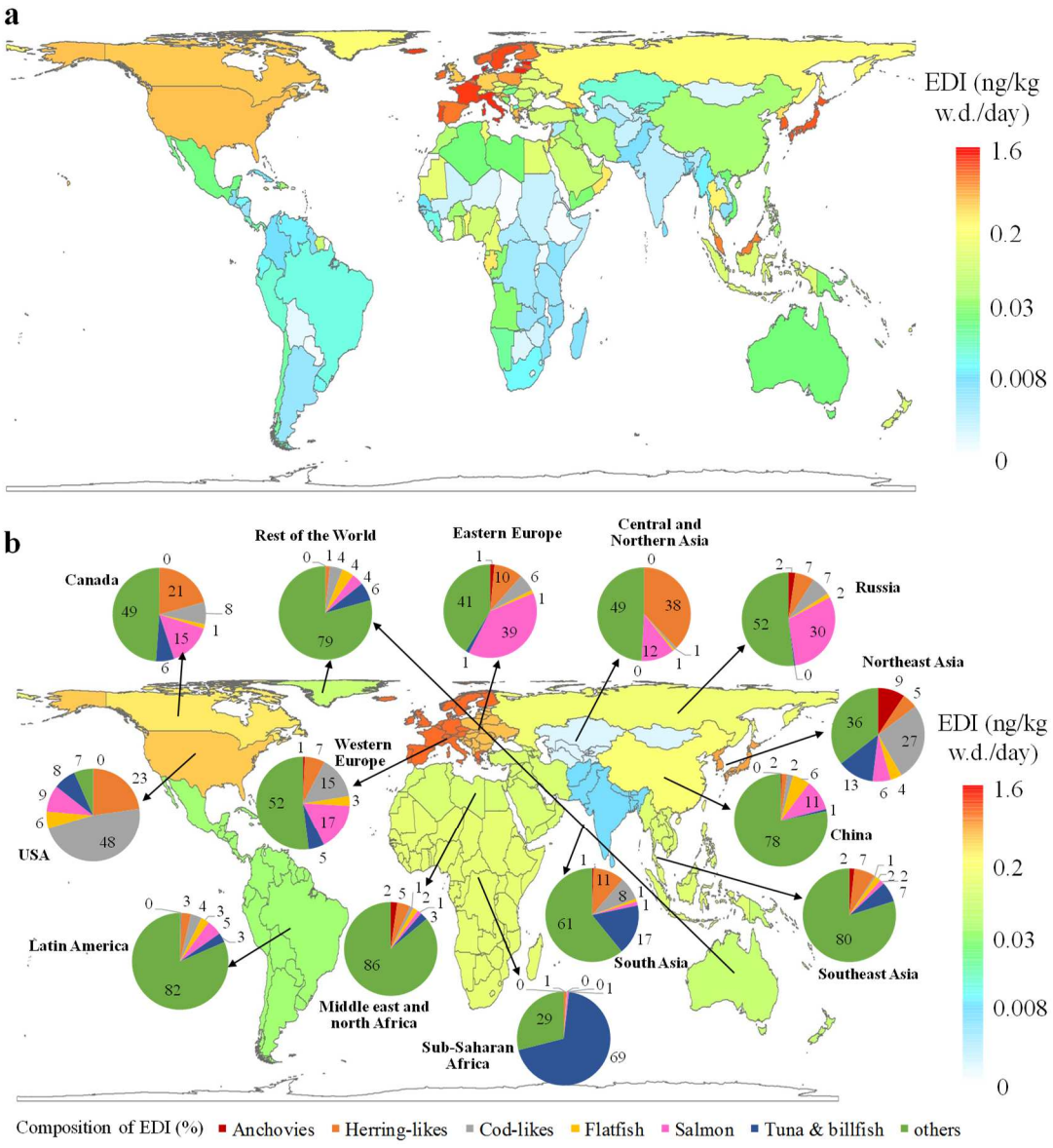

Fig. 1 Estimated daily intake (EDI (ng/kg b.w./day)) and fractions of PCB-153 in 2012. (**a**) EDI due to locally caught and traded fish intake for an average adult with 65 kg body weight, estimated using the Devine formula[22] from for different countries; (**b**) pie chart in **Fig. 1b** shows percentage of the EDI induced by consuming different marine fish species imported from 14 regions (**Supplementary Fig. 11**) across the globe (%). The color shading of background map shows EDI due to locally caught and traded fish intake for an average adult from 14 regions. The color bars on the bottom of **Fig. 1b** show different fish species.

The "Trade" simulations (**Fig. 1a**) show higher EDIs (ng/kg b.w./day) in WE and Northeast Asia, with the highest ranked countries being Malta (1.52), Estonia (1.28), Denmark (1.26), Netherlands (1.17), Lithuania (1.17), and Italy (0.9). These high EDIs directly reflect the higher PCB-153 concentrations in the fish consumed (**Supplementary Fig. 10**) and the high fish consumption in these countries (**Supplementary Fig. 13**). According to Breivik et al.[23,24], the total global production of PCBs (1.324 million tonnes between 1930 and 1993), occurred mostly in WE, followed by the USA, Japan, and the former Soviet Union. Accordingly, WE emitted the largest amount of PCBs, followed by the USA, Eastern Europe, Japan, South Korea, and other countries[18], which can be identified by high levels of PCB-153 measured near the coasts of these countries (**Supplementary Fig. 9**). The residents of WE tended to consume more marine fish than others, leading to higher EDI values (**Fig. 1a**). **Figure 1b** shows the percentage of the EDI induced by consuming different marine fish. In the majority of countries, except for Sub-Saharan Africa, and the USA, the EDI was mainly from intake of marine fish species other than the seven major fish species (referred to as "other marine fish" hereafter). Especially, other marine fish contributed more than 75% to the total fish consumption (TFC) EDI in the Middle East and North Africa, Latin America, Southeast Asia, the rest of the World, and China (**Supplementary Fig. 13**). Partly owing to greater production as shown in **Supplementary Fig. 14**, cod-like fish contributed 47.8% to TFC EDI in the USA, 26.9% in Northeast Asia, and 14.9% in WE. **Supplementary Fig. 14f** shows that global salmon were produced in high latitude areas of the Northern Hemisphere, resulting in a high exposure of salmon

consumers to PCB-153 in these areas. Among the seven fish categories, salmonids were mostly farmed and fed using feed containing lessmarine ingredient, and therefore were not strictly in the marine food web. . It is important to note that the TFC EDI fraction via tuna & billfish consumption accounted for 69.2% of the TFC EDI in Sub-Saharan Africa, which was attributed to tuna & billfish import from WE (**Supplementary Fig. 15**). A recent study yielded model results with considerably lower concentrations of PCB-153 in human milk than found in samples from West African countries. The low model results were attributed to ignoring imported fish consumption from Europe, especially since marine fish consumption accounted for over 50% of PCB exposure in African residents[25]. The "other marine fish" category contributes more than 75% to the TFC EDI in the Middle East and North Africa, Latin America, Southeast Asia, the rest of the World, and China.

Impact of global marine fish trade on human health exposure

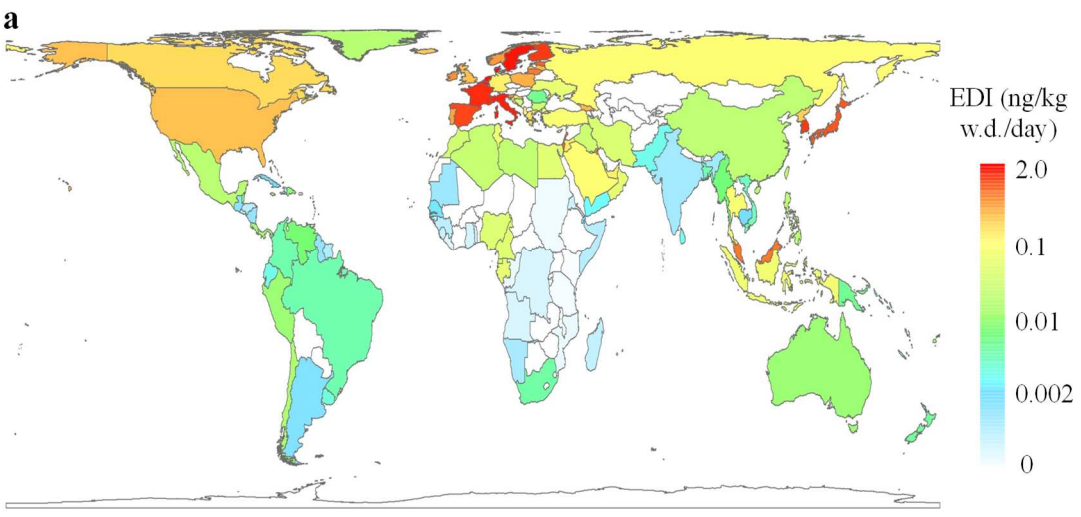

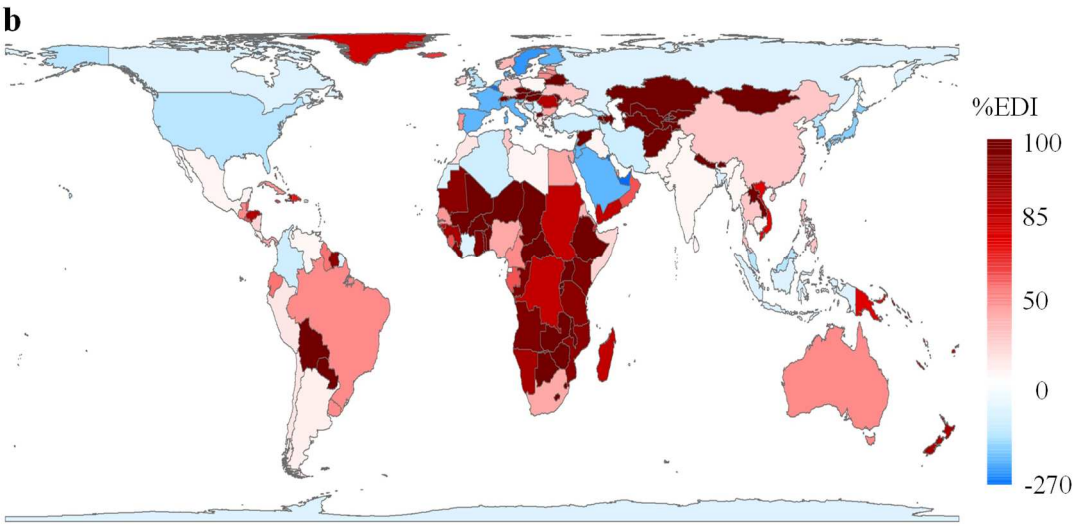

Fig. 2 Estimated daily intake (EDI ng/kg b.w./day) and fractions of PCB-153 via fish intake in 2012. **(a)** EDI from No-trade simulation; **(b)** fractions of "Trade" scenario simulated EDI to the "NO-Trade" scenario simulated EDI, estimated as (ΔEDI × 100)/EDIT, where ΔEDI = EDIT-EDINT, referring respectively to Trade and NO-Trade simulated EDI. ΔEDI is equivalent to the intake due to consumption of fish acquired through global trade.

The "NO-Trade" simulations quantified the contribution of all marine fish consumption from local production to human exposure to PCB-153. When global trade was not accounted for in the model, WE countries and South Korea had the greatest exposure to PCB-153 via fish consumption, caused by its high levels (**Supplementary Fig. 10**) in fish and high population densities. In WE countries, the highest EDI (ng/kg b.w./day) occurred in Denmark (1.91), followed by Sweden (1.87), Netherlands (1.79), Italy (1.65), and France (1.61). Slightly lower EDI value was identified in South Korea (is 0.96±0.46) as compared with these WE countries (**Fig. 2a**). The similarity in EDI

spatial distribution between "Trade" results (**Fig. 1a**) and "NO-Trade" results (**Fig. 2a**) was not unexpected because there were high fish PCB-153 concentrations in coastal waters of Europe (**Supplementary Fig. 9**), and high fish consumption in these countries (**Supplementary Fig. 13**). To see more clearly the contribution that global fish trade makes, we provide in **Supplementary Fig. 16** the difference between "Trade" and "NO-Trade" results (defined as $\Delta EDI = EDI_1 - EDI_2 = EDI_{GT}$). In countries proximate to major PCB emission sources and with greater EDI values of PCB-153 via fish consumption, the EDI_{GT} values are negative and small. This implies that the fish consumers in these countries would benefit from the global fish trade through increasing consumption of imported marine fish from cleaner marine environments and decreasing consumption of local fish caught near PCB-153 sources, in line with the findings reported by previous studies[12,26]. In contrast, the EDI_{GT} values of PCB-153 in most countries engaged in the global fish trade are positive (**Fig. 2b**), indicating increasing exposure from PCB-153. The percent contributions to EDI through consumption of fish traded globally (**Fig. 2c**) show large reductions for Nordic Europe, Middle Eastern and Northeast Asian countries: -214% in Belgium, -210% in United Arab Emirates, -137%, Kuwait -112% in France, -88% in Sweden, -83% in Italy, and -54% in South Korea. For the rest of the world, globally traded fish increase the EDI (**Fig. 2b**). The largest percent increase occurs in landlocked countries (e.g., Central and North African countries, Austria, Czech Republic, Chad, Niger) that have no marine fish fisheries. Large percent EDI increases (90-100%) can also be found in African countries that import a substantial percentage of the fish consumed (Seychelles (90%),

Mauritania (52%), Mauritius (60%), Benin (42%), Cameroon (53%)) (**Fig. 2c**). Greenland, Australia, China, and several countries in Africa, Latin America, and central Europe have a large EDI_{GT} owing to, according to the UN Comtrade reported data, imported fish with higher PCB-153 concentrations.

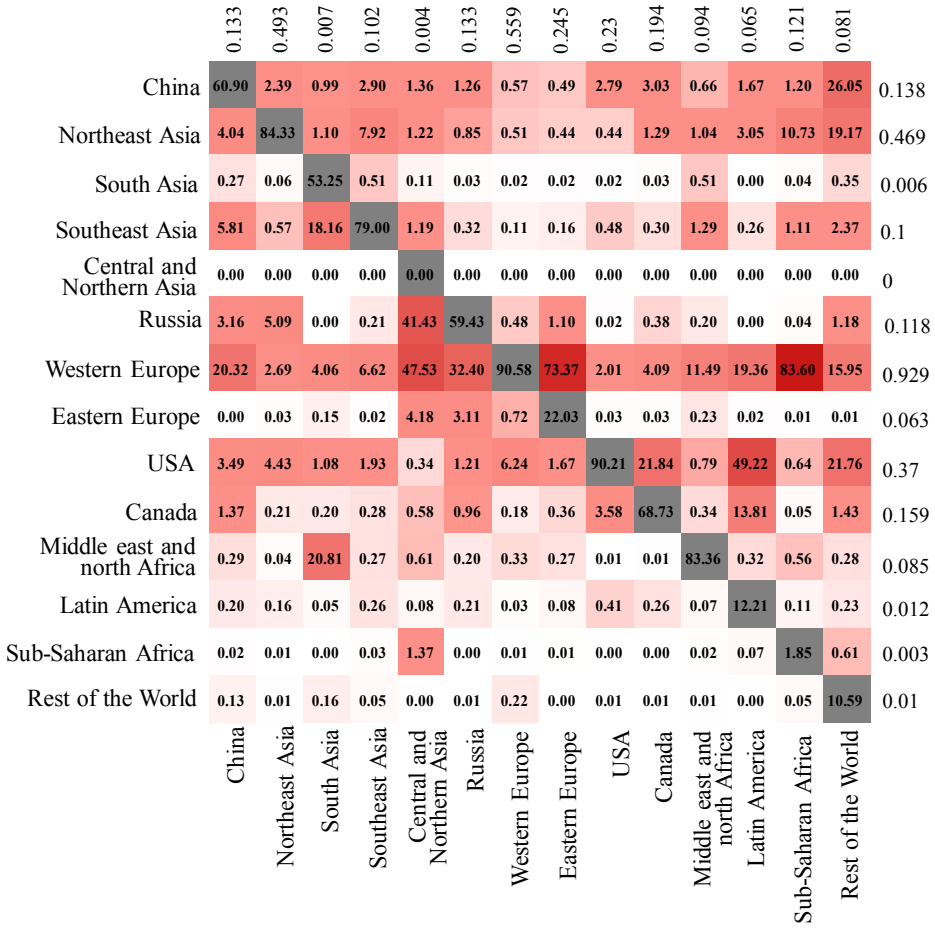

Fig. 3 Transfer of the EDI of PCB-153 embodied in global marine fish trade among the fourteen regions in 2012. Each cell in the column of matrix shows percentage of EDI (%) due to fish consumption from 14 regions (**Supplementary Fig. 11**). The diagonal, containing grey cells, highlights the percent EDI in each region due to local marine fish consumption (marine fish caught in the same region). The simulated TFC EDI for each region via total fish ingestion (local and imported) is shown at the top of the matrix and ingestion of fish caught in the same region and consumed by all regions

236 on the right of the matrix.

237

238 The model results (**Figs. 1&2**) can also be displayed as EDI embodied in inter-
239 regional import/export of marine fish species (**Fig. 3** and **Supplementary Fig. 12**)
240 estimated by reference to the 2012 global fish trade data matrix from UN Comtrade.
241 **Figure 3** shows the percentage of the EDI via fish intake for the year 2012 that derived
242 from the consumption of fish imported from elsewhere for any given region. Examining
243 the first column in **Fig. 3**, we see that China got 60.9% of its PCB-153 EDI by
244 consuming locally-caught fish. Fish imported from WE supplied 20.3% and the other
245 12 regions together supplied the remaining 18.8%. For Sub-Saharan Africa, we found
246 the greatest percent impact from imported fish: 84% of the EDI came from the fish
247 imported from Western and Nordic Europe compared to <2% from local fish. In return,
248 WE got a miniscule percent (0.01%) of its EDI from fish imported from Sub-Saharan
249 Africa. **Supplementary Fig. 12a** further shows that WE resulted in the biggest EDI at
250 0.42 ng/kg b.w./day induced by fish export to other regions, followed by the USA (0.16),
251 China (0.06), and Northeast Asia (0.05). The EDI via fish export and intake from these
252 four regions accounted for 87% of global TFC EDI in traded fish in 2012. The marine
253 fish captured in these regions contributed greater EDI of PCB-153 to other regions. For
254 example, as the largest fish export region, WE contributed 73.4% to the TFC EDI
255 embodied in PCB-153 contaminated fish intake in Eastern Europe, 47.5% to Central
256 and Northern Asia, and 32% to Russia (**Fig. 3**). Likewise, the USA contributed 49% to
257 TFC EDI in Latin America, 22% to Canada, and 22% to rest of the World. China and

Northeastern Asia also posed 26% and 19% of TFC EDI to rest of the World.

In 2012, Western and Nordic Europe, China, Russia, Latin America, and the USA were the major exporters of marine fish, and China and Africa were the major importers (**Supplementary Fig. 15**). Accordingly, WE, the USA, and China were also net exporters of marine fish through global fish trade, yielding net EDI of 0.37, 0.14, and 0.006 ng/kg b.w./day to those countries importing marine fish from these three countries, respectively (**Fig. 4a**). Other regions as net fish importers provided sinks for marine fish and got EDI embodied in imported marine fish. Similar to the $\%EDI_{GT}$ displayed by country in **Fig. 2b**, the regional $\%EDI_{GT}$ values for Northeast Asia (-61%), the USA (-43%), and WE (-37%) show that populations in these countries have reduced exposure to PCB-153 due to the export of locally caught fish and the import of fish from countries located far from the major historical PCB emission sources. In contrast, the fish import/export balance resulted in an increased exposure to fish consumers in Central and Northern Asia (100%), Sub-Saharan Africa (89%), Australia and Greenland (87%), Latin America (84%), and South Asia (47%). WE, as a large exporter of marine fish (**Supplementary Fig. 15**) caught regionally in waters subject to relatively large PCB-153 deposition, also contributed to the largest EDI (**Fig. 4a**): 0.18 ng/kg b.w./day to Eastern Europe, 0.1 ng/kg b.w./day to Sub-Saharan Africa, 0.04 ng/kg b.w./day to Russia, and 0.03 ng/kg b.w./day to China. Through its wide export of marine fish, the USA contributed EDI of 0.04 ng/kg b.w./day to Canada, 0.03 ng/kg b.w./day to WE, and 0.03 ng/kg b.w./day to Latin America. Although China was the biggest importer of marine fish from the USA among those countries importing marine fish from the USA,

the EDI in China was little impacted owing to relatively lower PCB-153 concentrations in the seawater near the USA as compared to that in European coastal waters (**Supplementary Fig. 9**) and lower quantity of imported fish from the USA than from the Europe (**Supplementary Figs. 15 and 17**). **Figure 4** also shows that WE and the USA were two major contributors to EDI embodied in global fish trade when all targeted marine fish species were accounted for. The EDI induced by other fish trade in the rest of world is less than 0.1 and 0.001 for selected six fish species trade. Due to lower PCBs contamination in the Southern Hemisphere's oceans, Latin America, Sub-Saharan Africa, and rest of the World got only 12%, 2%, and 11%, respectively, of their PCB-153 EDI by consuming locally-caught fish. Overall, the global fish trade induced EDI from Western and Nordic Europe increased the exposure to PCB-153 in the importing countries (**Figs. 3** and **4a**). In particular, the summed mean EDI via fish consumption in China and the other 13 regions from the fish caught in China is 0.14 ng/kg b.w./day (**Fig. 3** right hand column) compared to 0.93 ng/kg b.w./day for WE.

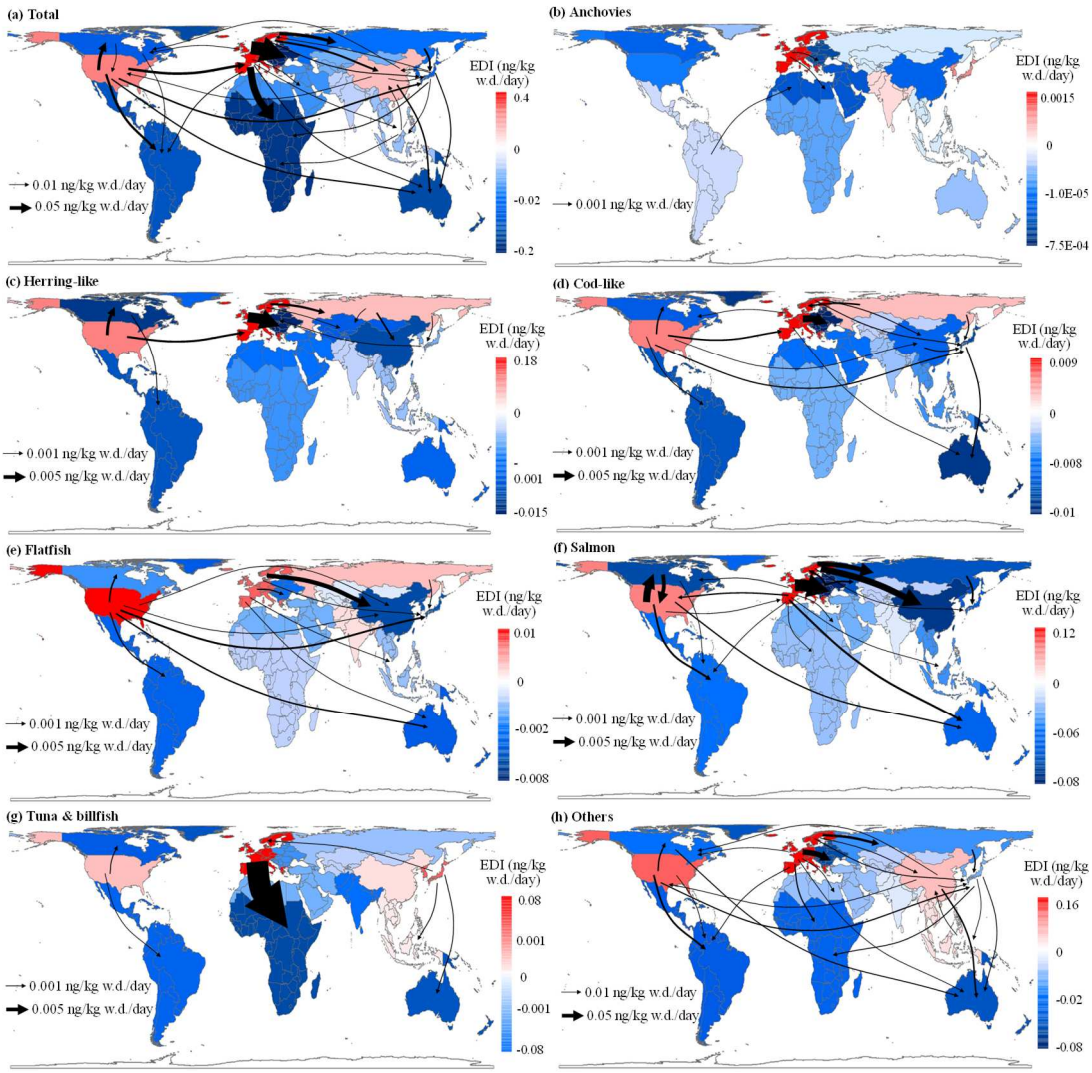

Fig. 4 EDI embodied in PCB-153 via international fish trade between 14 regions (ng/kg b.w./day) during 2012. The 14 regions (**Supplementary Fig. 11**) highlighted in the figure were chosen based on similarity in EDI and geographical proximity. Red indicates regions of net EDI via fish export, blue of net EDI via fish import through global trade. Arrows indicate EDI≥0.001ng/kg b.w./ day for anchovies, herring-likes, cod-likes, flatfish, salmon, and tuna & billfish, and ≥0.01ng/kg b.w./ day for other fish and total fish.

Temporal Change in fish trade, PCB-153 level, and exposure

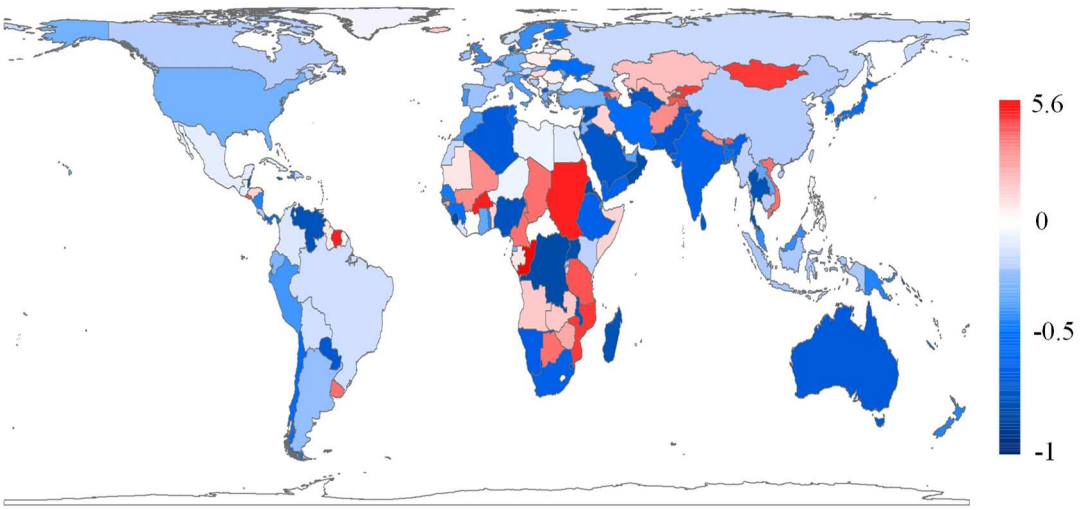

Fig. 5 Normalized EDI (Estimated Daily Intake) fraction for PCB-153 via marine fish consumption between 2003 and 2012, defined by EDI = (EDI_{2012} – EDI_{2003})/EDI_{2003}, where EDI_{2012} and EDI_{2003} are the simulated EDIs for PCB-153 ingestion via marine fish consumption in 2012 and 2003.

Modeled PCB-153 concentrations in air and seawater, which declined between 2003 and 2012, reflect the general post phase-out decline of PCB concentrations globally[27]. We would, therefore, expect a similar decline in exposure from PCB-153 transferred in the fish trade. We calculated the normalized EDI fraction for the annual mean PCB-153 concentration averaged over all selected marine fish species between 2003 and 2012, defined as (EDI_{2012} – EDI_{2003})/EDI_{2003}. As shown in **Fig. 5**, for many regions, especially those close to historical sources of PCBs (e.g., Europe, USA, Canada, Australia, northeast Asia), the normalized fraction is negative, indicating declining exposure from PCB-153 between 2003 and 2012. In contrast, for many African countries, Central Asia and Mongolia, and Brazil, positive EDI fractions manifest increasing human exposure from PCB-153 via marine fish consumption which

runs counter to the declining trends of PCB-153 in the environment. Some of these countries have increased EDI by over factor of 5.6 between 2003 and 2012. This finding, however, mirrors the increasing reliance on imported marine fish by these countries during this time interval (**Supplementary Fig. 18a**). In a few countries like China, India, and Russia, enhanced marine food imports are accompanied by positive EDI fraction. This apparent contradiction likely arises from increasing fish exports during the same period, which resulted in a net fish-trade surplus (**Supplementary Fig. 18b**).

Exposure to PCB-153 from farmed fish in global trade

Global aquaculture production has grown substantially during the last decades[28]. Having significantly higher lipid content than wild fish, farmed salmon farmed salmon also tend to carry markedly higher burdens of PCBs than the wild ones[29]. Given that farmed fish are becoming increasingly important sources of seafood, accounting for almost 50% of the world seafood intake in 2010[30], a comprehensive assessment of human exposure to PCBs embodied in global fish trade should also consider the farmed fish pathway. Human exposure to these farmed fish species cannot be estimated using the marine food web model but can be calculated considering feeding strategies used by fish farms. Among farmed fish, salmonid aquaculture grew from 12,000 tonnes in 1980 to 2.4 million tonnes in 2011[31], which accounted for 70% of the farmed fish market in the world[32]. More than 92% of salmonid aquaculture was farmed Atlantic salmon in 2013[33]. Norway was the world's largest producer of salmonids in 2012 accounting for 60% of world total production, followed by Chile (19%), UK (8%), and

343 Canada (5%). The remaining 8% was provided by rest of the world[34] (**Supplementary**
344 **Fig. 19**). In contrast, the proportion of global wild salmon production decreased from
345 98% in 1980[32] to about 30% in 2012 in total salmon production[30]. In the past decades,
346 the wild catch of salmonid fish species varied between 0.7 and 1 million tonnes[32], and
347 most wild salmonids were caught by North American, Japanese, and Russian fisheries[35].
348 Accounting for 69% of global total salmon production (wild + farmed) in 2012[32],
349 Atlantic salmon was selected to assess human exposure to PCB-153 embodied in global
350 salmon trade. To do so, we designated and performed three model scenarios, namely,
351 wild salmon, farmed salmon fed by traditional feed made using marine ingredients such
352 as fish oil and meal produced from pelagic feral fish, and farmed salmon fed by the
353 alternative feed (the feed with lower marine ingredients), respectively. **Figure 6** shows
354 the modeled EDIs for PCB-153 via salmon ingestion (ng/kg bw/day) in those countries
355 importing Atlantic salmon from Norway, Chile, UK, and Canada. As a largest exporter
356 of Atlantic salmon (**Fig. 6, Supplementary Fig. 20**), Norway also contributed the
357 largest EDIs via ingestion of salmon fed by the alternative feeding in 2012 to importers:
358 0.92 ± 0.53 (mean ± SD, ng/kg b.w./day) in Sweden, 0.43 ± 0.25 in Denmark,
359 0.23±0.13 in Finland, and 0.11±0.06 in Poland. As the second biggest exporter of
360 Atlantic salmon (**Fig. 6, Supplementary Fig. 20**), however, Chile only contributed 0.02
361 ±0.007 ng/kg b.w./day of EDIs to Japan, 0.007±0.004 to Brazil, and 0.005±0.002 to
362 the USA, the three major importers of Atlantic salmon from Chile. The lower exposure
363 in Atlantic salmon from Chile could be attributed to fish meals and oil originated from
364 the cleaner marine environment around Chile and Peru. The highest exposure occurred

in Atlantic salmon from the UK. Although only accounting for 5% of the world total Atlantic salmon export (**Supplementary Fig. 20**), the UK contributed 0.05 ± 0.04 ng/kg b.w./day EDI to Ireland, 0.02 ± 0.01 to France, and 0.02 ± 0.01 to Denmark, respectively, owing to higher PCB-153 levels in meal and oil used in Scottish salmon feeding (**Supplementary Table 5-7**). With more than 95% of Atlantic salmon exported to the USA, Canada contributed the EDI at 0.007 ± 0.01 ng/kg b.w./day to the USA.

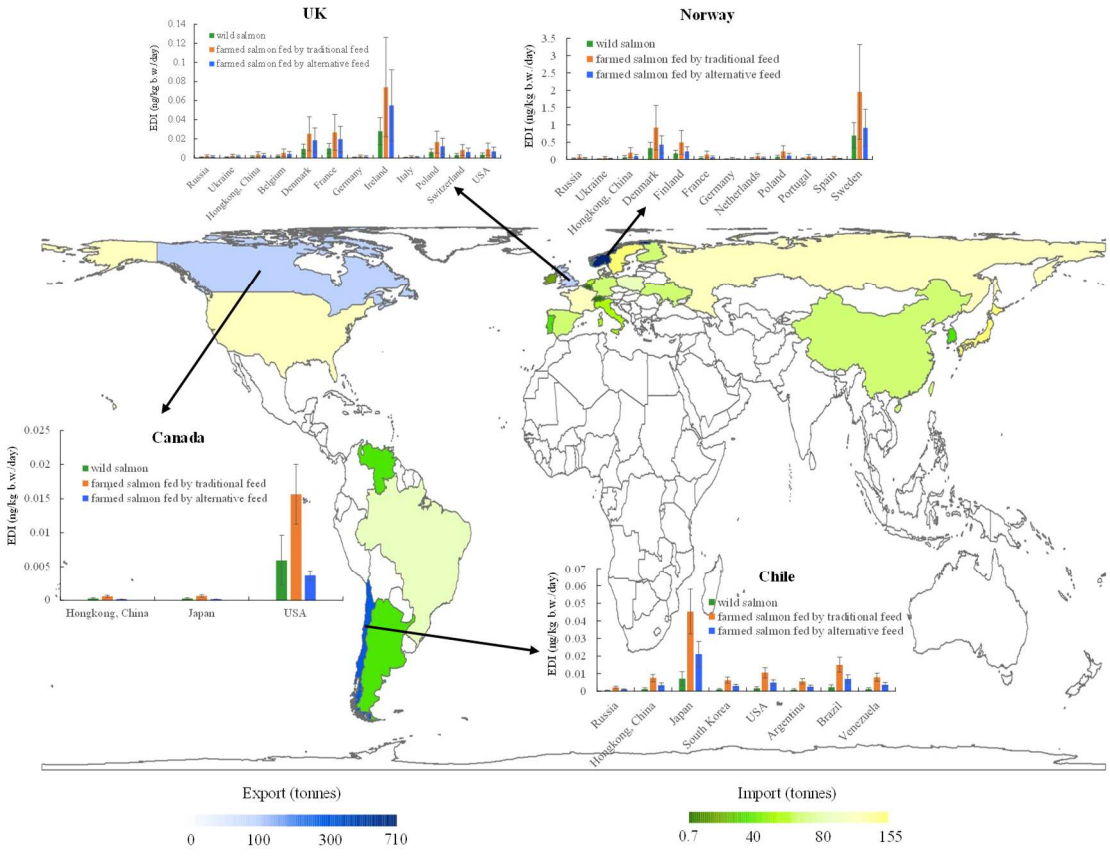

Fig. 6 Modeled EDI for PCB-153 through salmon intake embodied in international Atlantic salmon trade (ng/kg b.w./day) in 2012. The map shows major countries exporting and importing Atlantic salmon (tonnes). The quantity of salmon export is scaled using the shallow to deep blue color bar on the bottom left and import is scaled using the deep green to shallow yellow color bar on the bottom right of the figure. Bar charts denote the estimated EDIs ≥0.001 ng/kg b.w./day of PCB-153 via salmon intake

in those countries as major importers of Atlantic salmon fish from Norway, Chile, the UK, and Canada as major salmon exporters, simulated from the sensitivity model run.

To examine the sensitivities of human exposure via intake of wild and farmed salmon, we firstly assumed that all Atlantic salmon were wild. **Figure 6** shows that the modeled EDIs of farmed salmon fed by the traditional feed were considerably higher than those of wild salmon due to higher PCB-153 levels in the former (ng g^{-1} wet weight, **Supplementary Table 8**). The PCB-153 concentrations in farmed salmon from the 4 countries in lipid weight (ng g^{-1} lipid weight) are provided in **Supplementary Table 9**. In particular, the EDIs of Chilean farmed salmon fed by traditional feed was 6.4-fold higher than Chilean wild salmon. It should be noted that PCB-153 levels in wild salmon in the present study were simulated using the marine food web model cascading the dietary structure of Atlantic salmon (see **Supplementary Data 1**). In contrast, farmed salmon were fed by fishmeal comprised of smaller feed-fish, such as mackerel, which were rich in fish oil and therefore prone to bioaccumulation of lipophilic contaminants like the PCBs[36]. Previous studies also have shown that farmed salmon have much higher concentrations of contaminants than wild salmon[29,37,38]. Hites et al. examined the levels of PCBs and organochlorine pesticides in over 2 metric tons farmed and wild salmon collected from all over the world and found that concentrations of these contaminants in farmed fish were eight times higher than that in wild salmon, particularly in Europe where contaminant loads were markedly higher than those in North and South America[29]. It has been shownthat traditional salmon feeds are the main source of POPs in farmed Atlantic salmon fillets[39]. Due to scarcity of fish meal and fish

oil, the use of these two marine raw materials in feed production has been reduced and replaced by vegetable ingredients, reducing levels of dioxins and dioxin-like PCBs[39,40]. **Figure 6** also shows that EDIs of PCB-153 through the consumption of salmon fed by alternative feed decreased markedly compared to that of salmon fed by traditional feed. In particular, the EDIs by taking in PCB-153 contaminated Scottish salmon fed by alternative feed were lower than that of wild salmon. As a potential source of organic chemicals, oily fish was also an important source of health promoting nutrients such as the very long chain omega-3 (VLC-n3) fatty acids[41,42]. The overall health effects of consumption of oily fish such as Atlantic salmon is, therefore, a trade-off between beneficial nutrients and potentially harmful compounds[42]. To reduce the contaminants level in fish meal and oil, several decontamination technologies were used in salmon feed production, such as activated carbon adsorption, steam deodorization, and short-path distillation[43,44]. It is expected that global PCBs levels in both wild and farmed salmon will continue to decline in coming years along with declining PCBs in the environment and increasing reliance on vegetable ingredients and application of decontamination technologies.

Discussion

The global trade of marine fish contaminated by PCBs and other persistent toxic chemicals carries with it a human exposure risk. On the other hand, the fish trade benefits developed and developing countries by providing cheaper and off-season foods and by promoting the development of agricultural economies. The food-trade network,

422 which has significantly altered global food supply during the past two decades, is
423 complex due to processing of multiple food ingredients with components imported
424 from many regions and countries. The rapidly expanding global food trade challenges
425 food safety, a prominent example being potential contamination by pesticides and
426 industrial chemicals that have been broadcast to the environment[45,46]. Concerns about
427 residues of these toxic chemicals in food products undergoing global trade have resulted
428 in high standards for food safety[47,48]. Here we have addressed the particular exposure
429 associated with the trade of marine fish. Marine fish contamination takes place at origin
430 because environmental compartments, including the ocean, contain legacy
431 contaminants and these together with new and emerging contaminants continue to enter
432 the ocean due to modern use and recycling. This contamination is biomagnified such
433 that predatory fish tend to accumulate the highest concentrations among fish species;
434 therefore food web structure and position in the food web structure become critical
435 components of fish contamination. This set of circumstances makes regulation and
436 monitoring for POPs residues difficult, and requires recourse to models incorporating
437 environmental transport, exchange, phase partitioning, and food webs. Here, we have
438 made a first attempt to quantify the human exposure from POPs carried within the
439 global food trade, using an example PCB-153, and the year 2012. We have developed
440 models to project the environmental aspects of PCB uptake in the ocean's food webs,
441 the human-related aspects of trading fish and the significance to humans by translating
442 the results into estimated daily intakes of PCB-153 by humans. The models showed that
443 mean EDI from PCB-153 via marine fish consumption was decreased by 61%, 43%

444 and 37% respectively in Northeast Asia, the USA, and WE (**Fig. 2b**), which are
445 proximate to the major PCB-153 emission sources, because these countries consumeed
446 imported marine fish from distant regions less contaminated by PCB-153. In contrast,
447 other regions distant from PCB sources have increased EDIs due to the import of fish
448 from the more contaminated regions. The largest enhancement of exposure occurred in
449 Central and Northern Asia where the EDI values were derived completely from the
450 import of marine fish. In addition, the EDI in Sub-Saharan Africa, Australia and
451 Greenland, and Latin America increased by 8.2, 6.97, and 5.28 fold respectively due to
452 reliance on global trade compared with the EDI values that would result from just local
453 fish consumption. As a result, these regions obtained, respectively, 98.2%, 89.4%, and
454 87.8% of their EDIs from consumption of imported marine fishes from more
455 contaminated regions. Leading among the exporting regions, WE contributed 83.6% to
456 the EDI in Sub-Saharan Africa via consumption of PCB-153 contaminated marine
457 fishes, 73.4% to Eastern Europe, 47.5% to Central and North Asia, and 32% to Russia.
458 The approach and rationale developed here could be extended to other toxic
459 chemicals (e.g., Hg, DDT, PBDEs) and other human food items (e.g., meat and poultry,
460 domestic animal feed, and vegetable crops). Transparency in food safety is essential in
461 food trade. Regular mandated food safety inspections, randomly conducted on a
462 relatively small number of samples, are expensive even in developed countries[48]. In
463 many developing countries, the international food safety standards and regulations are
464 seldom enforced and sometimes revoked[49]. Based on past increases in trade volume and
465 complexity, and an evolving industry bringing into use of new chemicals, the challenges

of regulation will only get worse. The model developed here provides a useful tool to determine the origin of toxic chemicals in traded food, and to scale the level of exposure inherent in specific trade pathways. Quantifying these pathways informs stakeholders and trade agencies about the large-scale risks in food trade and thereby informs a more efficient food inspection process[50]. We emphasize that the present study paints a picture of the exposure from a single compound, PCB-153, traded among countries via commercial fish. Unlike the traditional long-range transport routes through the atmosphere and oceans, this pathway is aimed directly at human consumption. Given the lack of domestic trade data, particularly in developing countries, simulation of toxic chemicals transported domestically is presently not practicable. More precise prediction of the food trade related exposure could be significantly improved by implementation of combined domestic and international food trade into our model. Such a dataset could also provide a more robust basis to validate the model assessment.

Methods

Analytical framework

The model applied here includes three major components (**Supplementary Fig. 1**). First, a modified version of the CanMETOP (Canadian Model for Environmental Transport of Organochlorine Pesticides)[51,52] together with a high-resolution emission inventory map[18] was used to produce an estimate of the spatial distribution of PCB-153 in the atmosphere, soil, sea water, sediment, and phytoplankton. Second, we calculated PCB-153 concentration in marine fish using a marine food web model. Third, the redistribution of PCB-153 via the international marine fish trade was estimated, which was then used to project the exposure to humans through consumption via this pathway. The model framework yielded "gridded" PCB-153 concentrations in air, seawater, soil, and aquatic sediment on a 1°×1° latitude/longitude resolution. The gridded concentrations in water and sediment across the global oceans were then implemented into the marine food web model with the same spatial resolution to predict PCB-153 levels in the targeted marine fish. The various fish

493 catch data for different countries on a 0.5º×0.5º latitude/longitude resolution were provided by Sea
494 Around Us which were subsequently extrapolate into the 1º×1º latitude/longitude resolution. Given
495 that salmon is a major farmed and commercial fish widely consumed in many countries, human
496 exposure to PCB-153 via the intake of traded farmed salmon as compared to traded wild salmon
497 was simulated. PCB-153 loading to coastal waters via tributary runoff and its contribution to the
498 total PCB loadings were also investigated.

499 **Modified CanMETOP model**

500 The CanMETOP is a three-dimensional atmospheric transport model coupled with a dynamic
501 fugacity-based soil-air exchange model, and a water-air exchange model based on the two-thin film
502 theory[51]. The model was originally developed for application to regional scale atmospheric transport
503 and has been extended to the global scale to investigate the intercontinental long-range transport of
504 POPs with the spatial resolution of 1° latitude by 1° longitude[52]. The model has been applied
505 extensively to simulate atmospheric transport and deposition, as well as the multi-phase exchange
506 of POPs among different environmental compartments[53]. Here, we have upgraded and improved the
507 water-sediment-phytoplankton exchange modules in the CanMETOP. In marine ecosystems,
508 phytoplankton is often considered as the bottom trophic level into which organic chemicals in the
509 water must be exchanged before they can be passed up the food web to fish[54]. We coupled the water-
510 sediment-phytoplankton modules based on a fugacity approach[55] using CanMETOP. The model was
511 integrated from 2002 to 2012 to permit the accumulation of PCB-153 in the global marine
512 environment. Details are presented in **Supplementary text 1**.

513 **Marine food web model**

514 For trophic levels higher than phytoplankton, organic chemicals accumulate in lipid tissue
515 mostly from dietary uptake and secondarily from an exchange with the water[56]. Therefore, predator–
516 prey relationships are crucial to characterize contamination patterns scaled from individual prey
517 items to the ecosystem level and to predict bioaccumulation and biomagnification within ecological
518 networks[57]. Marine food webs can be extraordinarily complex, with thousands of species ranging
519 from single-celled organisms to fishes and whales connected by an intricate web of predator–prey
520 interactions. Given large knowledge gaps, it was impossible to include all species and feeding
521 relationships in the food web model. In this work, we applied a model with simplified and practical
522 trophic structure and feeding relationships which took into consideration the toxicokinetics of
523 chemical uptake, elimination, and bioaccumulation in individual organisms and trophic dynamics
524 of the aquatic food web[58]. First, the concentration of PCB-153 in zooplankton and benthic
525 invertebrates was calculated by assuming equilibrium partitioning between water and zooplankton
526 or sediment pore water and benthos[58]. Then, based on the feeding relationships, PCB-153 in 38
527 marine fishes was estimated. Input into the food web model included PCB-153 concentrations in
528 water, sediment, and phytoplankton, obtained from the water-air, sediment-water, and
529 phytoplankton-water exchange modules in the CanMETOP (details are presented in
530 **Supplementary text 2**).

531 **PCBs entering coastal waters via runoff**

Atmospheric deposition and riverine runoff have been regarded as the main pathways and sources of PCBs in marine basins[59,60]. In a review article, Preston reported that the atmosphere input 80% ΣPCB to the world oceans since PCBs were mostly released in the atmosphere[61]. Extensive investigations into pathways of PCBs to the North American Great Lakes identified that atmospheric deposition was the dominant loading pathway for PCBs[62]. Here we modeled tributary runoff in a typical case to examine the relative significance of the individual PCB loading pathway (particle and diffusive gas phase deposition, and runoff) to coastal waters of Shanghai, a coastal megacity of China. The results reveal that tributaries runoff contributed <5% of PCB loading to offshore water (**Supplementary text 3, Supplementary Figs. 2** and **3**).

PCB-153 concentration in marine fish species in countries

The coupled CanMETOP and marine food web models predicted global PCB-153 concentrations in 38 marine fish species on a grid resolution of 1° latitude × 1° longitude. The Sea Around Us provided the spatial fish production data for the 7 fish categories including anchovies, herring-like, cod-like, flatfish, salmon, tuna & billfish, and the other fish for different country on a grid resolution of 30-min for different country (http://www.seaaroundus.org). Based on feeding behavior and spatial production data from the Sea Around Us, 38 fish species were categorized into 7 groups, with each group comprising several fish species (see **Supplementary Data 1**). We then added up the gridded catch data of 38 fish species in their corresponding fish categories (7 groups) to obtain the catch of the 7 fish categories for different countries on a resolution of 1°× 1° lat/long (**Supplementary Fig. 14**). Finally, we calculated PCB-153 concentration in 7 fish categories for each country as follows:

$$P_{j,p,q} = \frac{1}{m}\sum_{i=1}^{m} P_{i,j,p,q} \quad (1)$$

$$P_{j,q} = \sum_{p=1}^{n} P_{j,p,q} \quad (2)$$

where P is production of marine fish (tonnes). i is 38 fish species, j is 7 fish categories. The subscript p is a cell with a resolution of 1° latitude × 1° longitude, and q is country or region. m is number of fish species for each fish category (see **Supplementary Data 1**) and n is number of cells for country or region q.

The global spatial distribution of PCB-153 level in the 7 fish categories with a spatial resolution of 1° latitude × 1° longitude is shown in **Supplementary Fig. 10**.

Potential health exposure embodied in global marine fish trade

The estimated daily intakes (EDI, ng/kg b.w./d) of PCB-153 via fish consumption can be calculated by

$$EDI_i = C_i I_i / W \quad (3)$$

where C_i is PCB-153 level in a marine fish category i (ng g^{-1}), I_i is daily per capita consumption of i*th* marine fish i (g d^{-1}), and W is the mean adult body mass, taken as 65 kg in the present study.

The TFC EDI of PCB-153 induced by marine fish consumption is the sum of EDI_i for 7 fish categories. The daily consumption of anchovies, herring-like, cod-like, flatfish, and tuna & billfish

in each country in 2012 is obtained from global trade data in UN Comtrade (https://comtrade.un.org) and FAO (http://www.fao.org/fishery/statistics/software/fishstatj/en). Given that farmed salmon accounted for approximately 70% of total salmon production and landed values (wild + farmed) in the world in 2011, the daily salmon consumption in each country was validated by salmon production and trade values from FAO (http://www.fao.org/fishery/statistics/software/fishstatj/en). The per-capita daily consumption of the "other fish" category in each country was obtained by the per capita daily total consumption of seven marine fish categories (FAO, http://www.fao.org/faostat/en/#data/CL) minus the six marine fish categories. Per capita consumption of 7 marine fish species is shown in **Supplementary Fig. 13**. To discriminate the impact of the fish trade on exposure, we performed two model scenario simulations. Scenario 1 (S1,) incorporated international trade, referred to as "Trade" simulation, whereas Scenario 2 (S2) neglected fish trade but instead assumed that all marine fish were harvested and consumed locally for coastal countries and were not involved in (zero) fish trade for land-locked countries, referred to as "NO Trade" simulation. Based on the UN Comtrade global fish trade matrix, almost all commercial marine fish species were involved in the global trade.

Model evaluation and uncertainty

To establish the level of confidence in the present model investigation, we have carried out extensive model performance evaluations and validations via statistical error analysis for modeled and sampled PCB-153 concentration data in air, seawater, sediment, and fish. Overall, the results show good agreements between modeled and measured data. Details are presented in **Supplementary Text 4, Supplementary Figs. 4-7,** and **Supplementary Tables 7** and **8**.

Our model results were subject to uncertainties from various input variables, including global PCB-153 emission inventory, the simulation of three model combining environmental fate, marine food web, and human exposure assessment. The simulation of the environmental fate model was subject to errors in inputs of emission and physicochemical properties of chemicals according to previous studies[63]. We assigned an uncertainty of factor 10 to PCB-153 emissions proposed by Breivik et al.[64] and Wöhrnschimmel et al.[65]. The coefficient of variation (*CV*) of physicochemical properties ranged from 4.8% to 34.7% (**Supplementary Table 1**). By sensitivity analysis, the uncertainty of the marine food web model, and human exposure assessment were mainly derived from weight, lipid content, diet compositions of various fish species, lipid content in fish diets used in the marine food web model, and per capita marine fish consumption by country (see **Supplementary Data 1**). Since Monte Carlo and other sensitivity models are computational prohibitive, we used a first-order error propagation approach to calculate the model uncertainties in terms of the method presented in Huang et al.[66]. Based on the aggregation of the uncertainties above, we estimate an overall uncertainty of EDI with factors of 9.3-12.1 for different regions in 2012. In addition, the statistical data used in our study, including spatial production of different fish, and global fish trade matrix by different fish can also produce uncertainties for our model results. These uncertainties were not considered in the present study due to data unavailability. Further details of

uncertainty analysis are presented in **Supplementary Text 5** and **Supplementary Fig. 8**.

References

1. Rostami, I. & Juhasz, A. Assessment of Persistent Organic Pollutant (POP) Bioavailability and Bioaccessibility for Human Health Exposure Assessment: A Critical Review. *Crit. Rev. Env. Sci. Tec.* **41**, 623–656 (2011).
2. Batt, A. L., Wathen, J. B., Lazorchak, J. M., Olsen, A. R. & Kincaid, T. M. Statistical survey of persistent organic pollutants: risk estimations to humans and wildlife through consumption of fish from US Rivers. *Environ. Sci. Technol.* **51**, 3021–3031 (2017).
3. Batool, S. *et al.*, Geographical distribution of persistent organic pollutants in the environment: A review. *J. Environ. Biol.* **37**, 1125–1134 (2016).
4. Domingo, J. Concentrations of environmental organic contaminants in meat and meat products and human dietary exposure: A review. *Food Chem. Toxicol.* **107**, 20-26 (2017).
5. Guo, W., Pan, B., Sakkiah, S., Yavas, G., Ge, W., Zou, W. & Tong, W. & Hong, H. Persistent Organic Pollutants in food: contamination sources, health effects and detection methods. *Int. J. Environ. Res. Public Health*. 16, 4316 (2019)..
6. Committee on Nutrient Relationships in Seafood. *Seafood Choices: Balancing Benefits and Risks*. Edited by Nesheim, M and Yaktine, A. The National Academies Press, available at http://nap.edu/11762 (2007).
7. Gascón, M. *et al.*, Effects of persistent organic pollutants on the developing respiratory and immune systems: a systematic review. *Environ. Int.* **52**, 51–65 (2013).
8. AMAP, 2016. *AMAP Assessment 2015: Temporal Trends in Persistent Organic Pollutants in the Arctic*. Arctic Monitoring and Assessment Programme (AMAP), Oslo, Norway. vi+71pp
9. AMAP, 2018. AMAP Assessment 2018: *Biological Effects of Contaminants on Arctic Wildlife and Fish*. Arctic Monitoring and Assessment Programme (AMAP), Oslo, Norway. vii+84pp
10. Ng, C. A. & Goetz, N. V. The Global food system as a transport pathway for hazardous chemicals: the missing link between emissions and exposure. *Environ. Health Persp.* **125**, 1–7 (2017).
11. Breivik, K., Czub, G., McLachlan, M. S. & Wania, F. Towards an understanding of the link between environmental emissions and human body burdens of PCBs using CoZMoMAN. *Environ. Int.* **36**, 85–91 (2010).
12. Undeman, E., Brown, T. N., McLachlan, M. S. & Wania, F. Who in the world is most exposed to polychlorinated biphenyls? Using models to identify highly exposed populations. *Environ. Res. Lett.* **13,** 064036 (2018).
13. Gobas, F. A. Assessing Bioaccumulation Factors of Persistent Organic Pollutants in Aquatic Food-Chains. In Persistent Organic Pollutants: Environmental Behaviour and Pathways of Human Exposure, edit by S. Harrad, Springer Science+Business Media New York (2011).
14. Mackay, D., Shiu, W. Y., Ma, K. C. & Lee,S. C. Handbook of physical-chemical

properties and environmental fate for organic chemicals. CRC Press, Boca Raton (2006).
15. Sethajintanin, D., Johnson, E. R., Loper, B. R. & Anderson, K. A. Bioaccumulation profiles of chemical contamination in fish from the lower Willamette River, Portland Harbour, Oregon. *Environ. Contam. Toxicol.* **46**, 114–123 (2004).
16. McLachlan, M. S., Undeman, E., Zhao, F. & MacLeod, M. Predicting global scale exposure of humans to PCB 153 from historical emissions. *Environ. Sci. Proc. Imp.* **20,** 747–756 (2018)
17. Faroon, O. & Ruiz, P. Polychlorinated biphenyls: New evidence from the last decade. *Toxi. Indus. Health*, **32**, 1825–1847 (2016)
18. Breivik, K., Armitage, J. M., Wania, F., Sweetman, A. & Jones, K. C. Tracking the global distribution of persistent organic pollutants accounting for E-waste exports to developing regions. *Environ. Sci. Technol.* 50, 798-805 (2016).
19. Gioia, R. *et al.*, Polychlorinated Biphenyls (PCBs) in air and seawater of the Atlantic Ocean: Sources, trends and processes. *Environ. Sci. Technol.* **42**, 1416–1422 (2008).
20. Gómez-Lavín, S., Gorri, D. & Irabien, A. Assessment of PCDD/Fs and PCBs in Sediments from the Spanish Northern Atlantic Coast. *Water Air Soil Pollut.* **221**, 287–299 (2011).
21. Froescheis, O., Looser, R., Cailliet, G. M., Jarman, W. M. & Ballschmiter, K. The deep-sea as a final global sink of semivolatile persistent organic pollutants? Part I: PCBs in surface and deep-sea dwelling fish of the North and South Atlantic and the Monterey Bay Canyon (California). *Chemosphere.* **40**, 651–660 (2000).
22. Devin, Ben. Gentamicin therapy. *Drug Intell. Clin. Pharm.* **8**, 650-655 (1974).
23 Breivik, K., Sweetman, A., Pacyna, J. M. K. & Jones, C. Towards a global historical emission inventory for selected PCB congeners — a mass balance approach 1. Global production and consumption. *Sci. Total Environ.* **290**, 181–198 (2002).
24. Breivik, K., Sweetman, A., Pacyna, J. M. K. & Jones, C. Towards a global historical emission inventory for selected PCB congeners — A mass balance approach: 3. An update. *Sci. Total Environ.* **377**, 296–307 (2007)
25. McLachlan, M. S., Undeman, E., Zhao, F. & MacLeod, M. Predicting global scale exposure of humans to PCB 153 from historical emissions. *Environ. Sci. Proc. Imp.* **20,** 747–756 (2018)
26. Undeman, E., Brown, T. N., Wania, F. & McLachlan, M. S. Susceptibility of human populations to environmental exposure to organic contaminants. *Environ. Sci. Technol.* **44**, 6249–6255 (2010).
27. Kong, D., MacLeod, M., Hung, H. & Cousins, I. T. Statistical analysis of long-term monitoring data for persistent organic pollutants in the atmosphere at 20 monitoring stations broadly indicates declining concentrations. *Environ. Sci. Technol.* **48**, 12492–12499 (2014).
28. FAO. The state of world fisheries and aquaculture. Food and Agriculture Organization of the United Nations. Available at http://www.northernharvestseafarm.com/images/AGR-Thought-Piece-Salmon.pdf.
29. Hites, R. A. *et al.*, Global assessment of organic contaminants in farmed salmon.

Science **303,** 226-229 (2004).
30. Nøstbakken, O., Hove, H., Duinker, A., Lundebye, A., Berntssen, M. & Hannisdal, R. Contaminant levels in Norwegian farmed Atlantic salmon (Salmo salar) in the 13-year period from 1999 to 2011. *Environ. Int.* **74,** 274-280 (2015).
31. Asche, F., Roll, K. H., Sandold, H. N., Dengjun, A. S. & Zhang D. Salmon aquaculture: Large companies and increased production. *Aquacult. Econ. Manag.* **17,** 322–339 (2013).
32. Marine Harvest ASA, Salmon Farming Industry Handbook 2018. Available at http://hugin.info/209/R/2200061/853178.pdf.
33. The Authority on seafood. Seafish, Responsible Sourcing Guide: Farmed Atlantic salmon. 2015. Available at https://www.seafish.org/media/1403303/_2_atlantic_salmon_rsg_-_cocker_04-15kg.pdf.
34. FAO. Globefish Highlights 2014. Food and Agriculture Organization of the United Nations. Available at http://www.fao.org/3/a-bc008e.pdf.
35. Knapp, G., Roheim, C. A. & Anderson, J. L. The Great Salmon Run: Competition Between Wild and Farmed Salmon. TRAFFIC North America, Washington DC. Available at https://www.traffic.org/site/assets/files/3637/great-salmon-run.pdf.
36. Carlson, D. L. & Hites, R. A. Polychlorinated Biphenyls in Salmon and Salmon Feed: Global Differences and Bioaccumulation. *Environ. Sci. Technol.* **39,** 7389-7395 (2005).
37. Hite, R.A. *et al.*, Global assessment of polybrominated diphenyl ethers in farmed and wild salmon. *Environ. Sci. Technol.* **38,** 4945-4949. (2004).
38. Shaw, U. *et al.*, PCBs, PCDD/Fs, and organochlorine pesticides in farmed Atlantic salmon from Maine, Eastern Canada, and Norway, and wild salmon from Alaska. *Environ. Sci. Technol.* **40,** 5347–5354 (2006).
39. Bell, J. G. *et al.*, Complete replacement of fish oil with a blend of vegetable oils affects dioxin, dioxin-like polychlorinated biphenyls (PCBs) and polybrominated diphenyl ethers (PBDEs) in 3 Atlantic salmon (Salmo salar) families differing in flesh adiposity. *Aquaculture* 2012, **324–325,** 118–126.
40. Berntssen, M. H. G., Lundebye, A. & Torstensen, B. E. Reducing the levels of dioxins and dioxin-like PCBs in farmed Atlantic salmon by substitution of fish oil with vegetable oil in the feed. *Aquacult. Nutr.* **11,** 219–231 (2005).
41. Berntssen, M. H. G. *et al.*, Reducing persistent organic pollutants while maintaining long chain omega-3 fatty acid in farmed Atlantic salmon using decontaminated fish oils for an entire production cycle. *Chemosphere* 2010, **81,** 242–252.
42. Lundebye, A. K. *et al.*, Lower levels of Persistent Organic Pollutants, metals and the marine omega 3-fatty acid DHA in farmed compared to wild Atlantic salmon (Salmo salar). *Environ. Res.* 2017, **155,** 49–59.
43. Oterhals, Å., Solvang, M., Nortvedt, R. & Berntssen, M. H. G. Optimization of activated carbon-based decontamination of fish oil by response surface methodology. *Eur. J. Lipid Sci. Technol.* 2007, **109,** 691-705.
44. Oterhals, Å. & Berntssen, M. H. G. Effects of Refining and Removal of Persistent Organic Pollutants by Short-Path Distillation on Nutritional Quality and Oxidative

741 Stability of Fish Oil. *J. Agric. Food Chem.* 2010, **58,** 12250–12259.
742 45. Buzby, J. C. International Trade and Food Safety: Economic Theory and Case
743 Studies. (US Department of Agriculture, 2003). Available at
744 http://citeseerx.ist.psu.edu/viewdoc/download?doi=10.1.1.201.8435&rep=rep1&ty
745 pe=pdf.
746 46. World Health Organization (WHO). Pesticide residues in food – Fact sheet. (WHO,
747 2018). Available at http://www.who.int/mediacentre/factsheets/pesticide-residues-
748 food/en/.
749 47. International Federation of Organic Agriculture Movements European Regional
750 Group (IFOAM EU Group). Guideline for Pesticide Residue Contamination for
751 International Trade in Organic. (2012). Available at http://www.ifoam-
752 eu.org/sites/default/files/page/files/ifoameu_reg_pesticide__
753 residue_cont_guideline_201203.pdf.
754 48. World Trade Organization (WHO). Workshop on Pesticide Maximum Residue
755 Levels (MRLS): Recommendation for Endorsement by SPS Committee. Available
756 at
757 https://docs.wto.org/dol2fe/Pages/SS/directdoc.aspx?filename=q:/G/SPS/W292R2.
758 pdf.
759 49. Montory, M. & Barra, R. Preliminary data on polybrominated diphenyl ethers
760 (PBDEs) in farmed fish tissues (Salmo salar) and fish feed in Southern Chile.
761 Chemosphere, 63, 1252–1260 (2006).
762 50. NRC (National Research Council). Exposure Science in the 21st Century: A Vision
763 and a Strategy. National Academies Press, Washington (2012).
764 51. Ma, J., Daggupaty, S., Harner, T. & Li, Y. Impacts of lindane usage in the Canadian
765 prairies on the Great Lakes ecosystem. 1. Coupled atmospheric transport model and
766 modeled concentrations in air and soil. *Environ. Sci. Technol.* **37**, 3774–3781 (2003).
767 52. Zhang, L., Ma, J., Venkatesh, S., Li, Y. & Cheung, P. Modeling evidence of episodic
768 intercontinental long-rang Mackay e transport of lindane. *Environ. Sci. Technol.* **42**,
769 8791–8797 (2008).
770 53. Ma, J., Daggupaty, S. M., Harner, T., Pierrette, P. & Waite, D. Impacts of lindane
771 usage in the Canadian prairies on the Great Lakes ecosystem - 2: Modeled dry, wet
772 depositions and net gas exchange fluxes, and loadings to the Great Lakes. *Environ.*
773 *Sci. Technol.* **38**, 984-990 (2004).
774 54. Wallberg, P. & Andersson, A. Transfer of carbon and a polychlorinated biphenyl
775 through the pelagic microbial food web in a coastal ecosystem. *Environ. Toxicol.*
776 *Chem.* **19**, 827–835 (2000).
777 55. Mackay, D. Multimedia environmental models: The fugacity approach. 2nd Edition,
778 CRC Press, Boca Raton (2001).
779 56. Vermeulen, N. P. Fish bioaccumulation and biomarkers in environmental risk
780 assessment: a review. *Environ. Toxicol. Phar.* **13**, 57–149 (2003).
781 57. Taffi, M., Paoletti, N., Liò, P., Pucciarelli, S. & Marini, M. Bioaccumulation
782 modelling and sensitivity analysis for discovering key players in contaminated food
783 webs: The case study of PCBs in the Adriatic Sea. *Ecol. Model.* **306**, 205–215 (2015).
784 58. Gobas, F. A. P. C. J. & Arnot, A. Food web bioaccumulation model for

polychlorinated biphenyls in San Francisco Bay, California, USA. *Environ. Toxicol. Chem.* **29**, 1385-1395 (2010).
59. Tolosa, I. *et al.*, PCBs in the western Mediterranean. Temporal trends and mass balance assessment. *Deep-Sea Res.* II, **44,** 907-928 (1997).
60. Boesch et al. Marine Pollution in the United State. Available at https://www.pewtrusts.org/en/research-and-analysis/reports/2001/02/12/marine-pollution-in-the-united-states.
61. Preston, M. R. The interchange of pollutants between the atmosphere and oceans. *Mar. Pollut. Bull.* **24,** 477-483 (1992).
62. Melymuk, L. *et al.*, From the city to the lake: Loadings of PCBs, PBDEs, PAHs and PCMs from Toronto to Lake Ontario. *Environ. Sci. Technol.* **48,** 3732-3741 (2014).
63. Breivik, K., Sweetman, A., Pacyna, J. M. & Jones, K. C. Towards a global historical emission inventory for selected PCB congeners — a mass balance approach 2. Emission. *Sci. Total Environ.* **290**, 199–224 (2002).
64. Wöhrnschimmel, H., Macleod, M. & Hungerbuhler, K. Emissions, Fate and Transport of Persistent Organic Pollutants to the Arctic in a Changing Global Climate. *Environ. Sci. Technol.* **47**, 2323–2330 (2013).
65. Huang, T. *et al.*, Jiang, W., Ling, Z., Zhao, Y., Gao, H., Ma, J. Trend of cancer risk of Chinese inhabitants to dioxins due to changes in dietary patterns: 1980–2009. *Sci. Rep.* **6,** 21997 (2016).

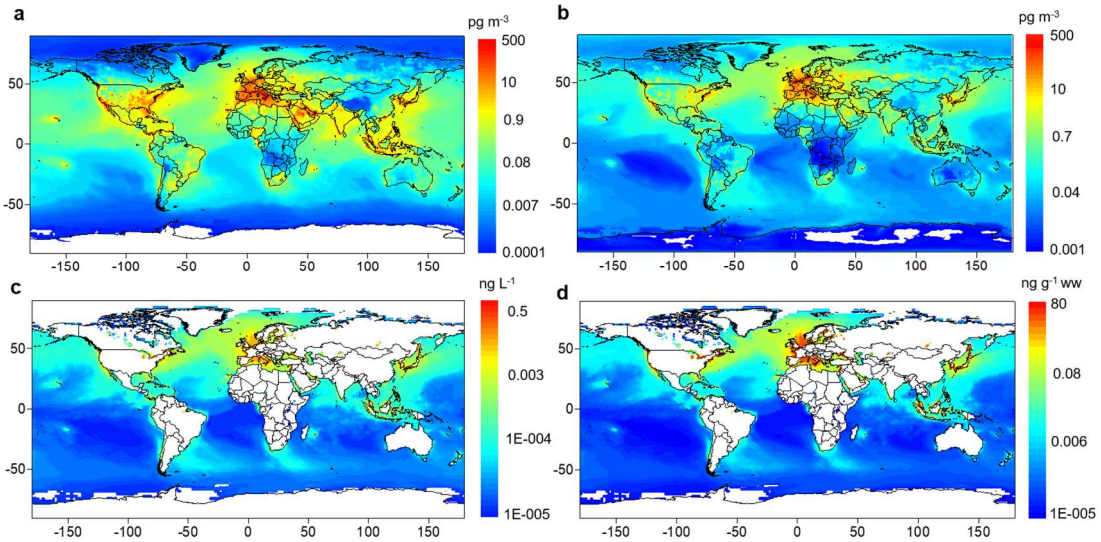

Extended Data Fig. 1 | Modeled concentrations (for 2012) of PCB-153. **a**, Atmospheric gas (pg m^{-3}), **b**, atmospheric particle phase (pg m^{-3}), **c**, water (ng L^{-1}), and **d**, sediment (ng g^{-1} ww).

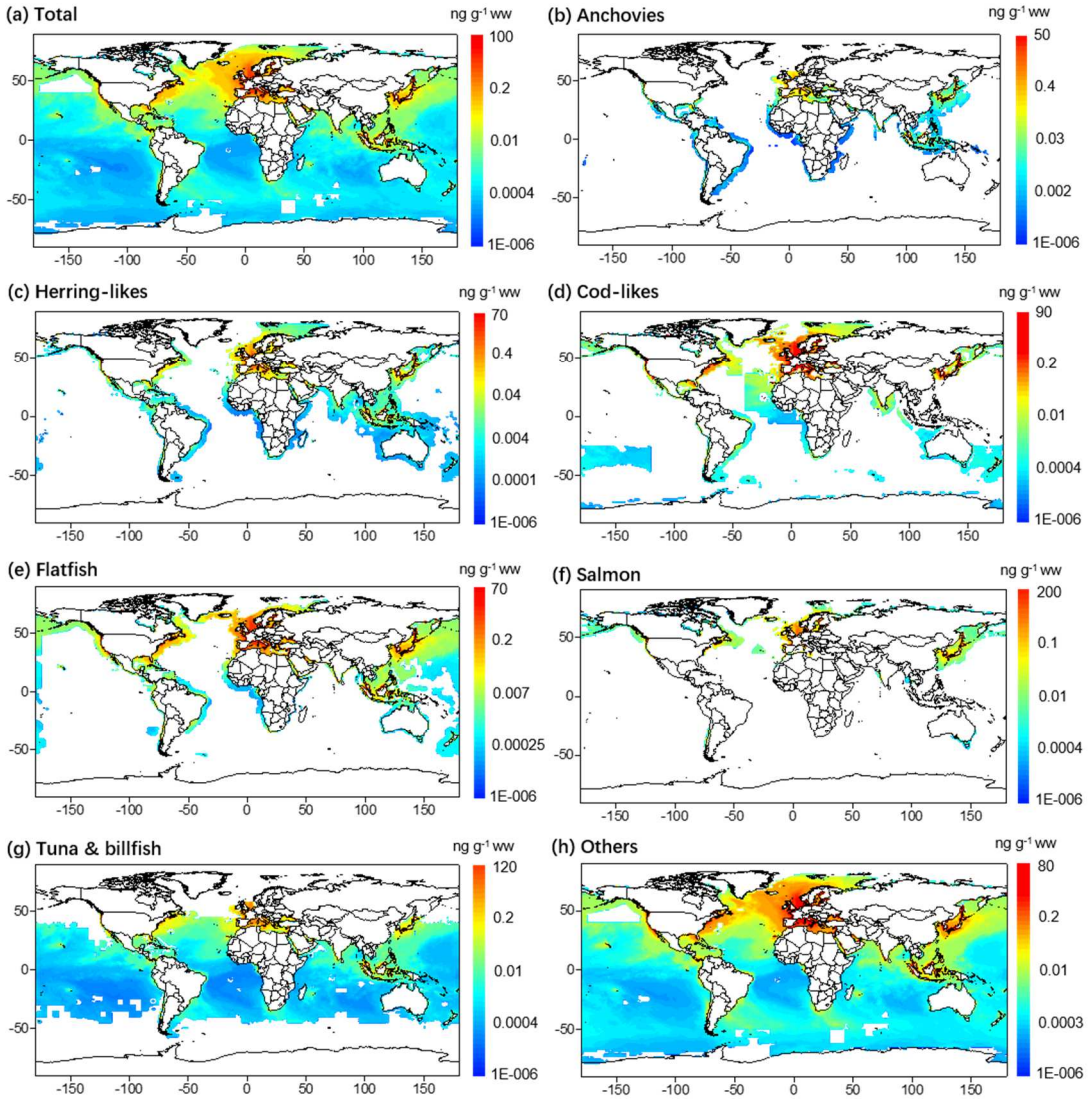

Extended Data Fig. 2 | Modeled PCB-153 concentrations in marine fish (ng g^{-1} ww) for various categories. **a**, Total fish, **b**, anchovies, **c**, herring-likes, **d**, cod-likes, **e**, flatfish, **f**, salmon, **g**, tuna & billfish, and **h**, other fishes.

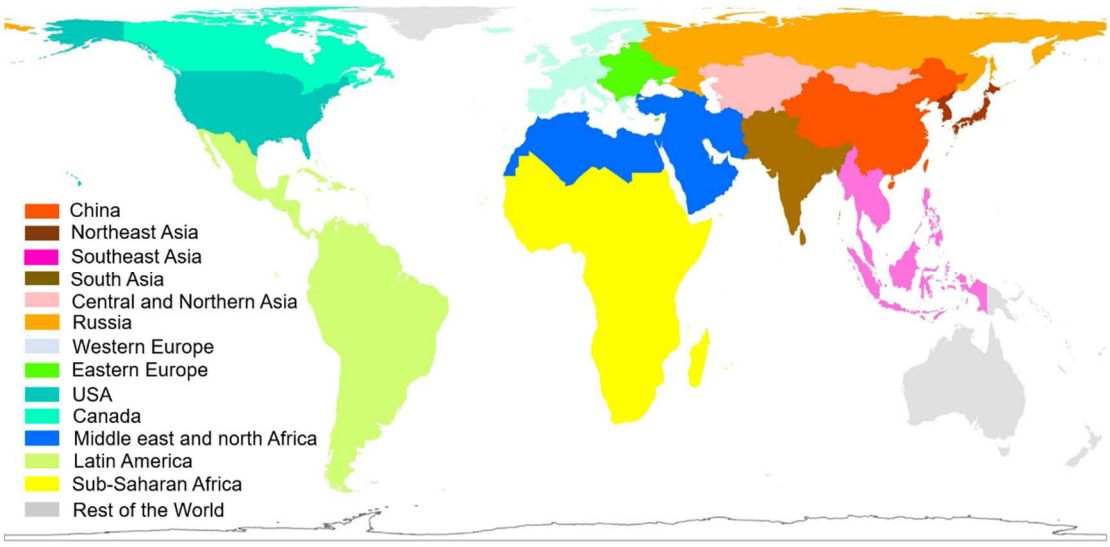

Extended Data Fig. 3 | The map of 14 regions regrouped from countries involved in the global fish trade. The map provides a key to the color scheme.

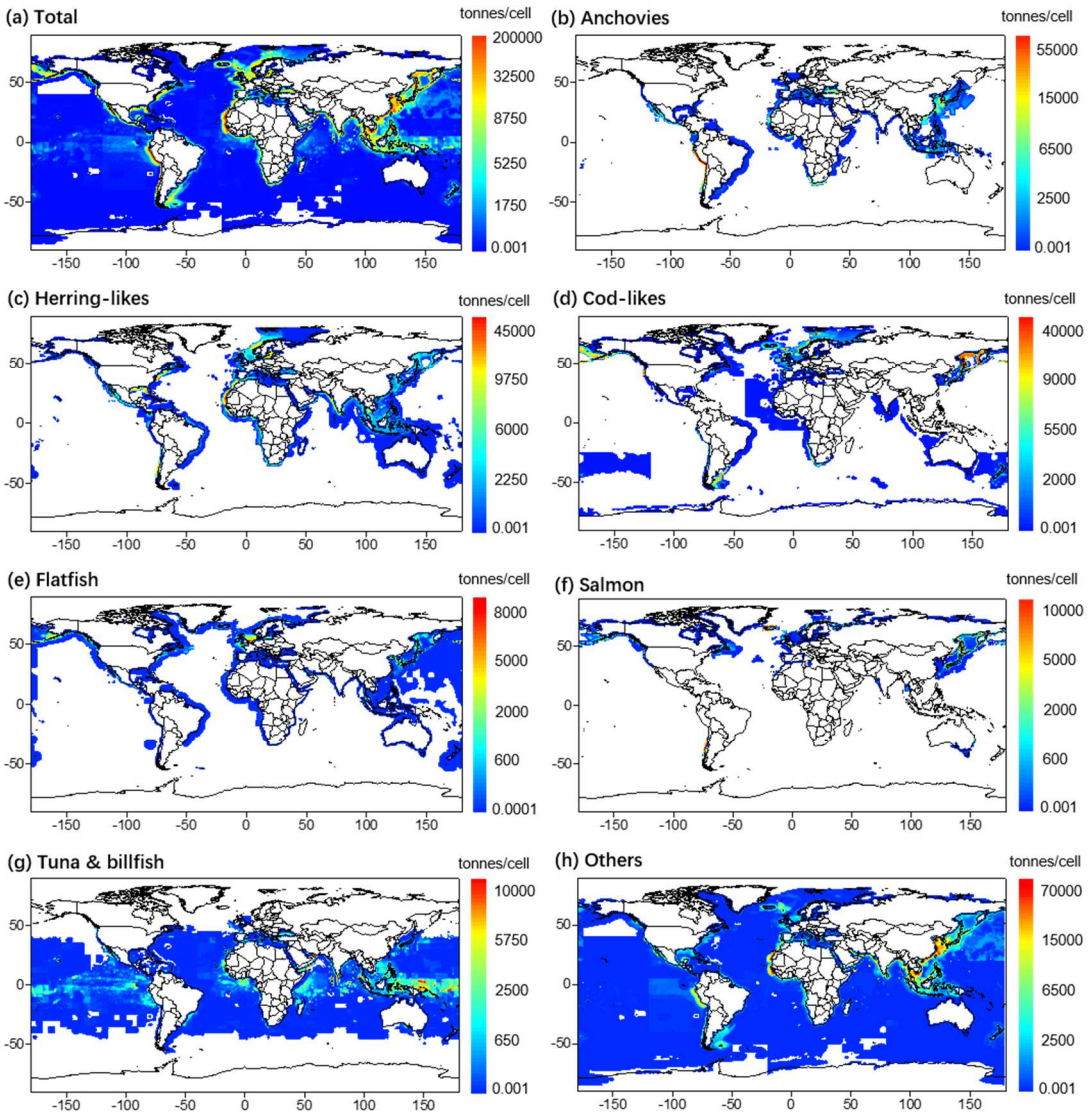

Extended Data Fig. 4 | Global production (tonnes/cell) for selected marine fish at a 1° longitude by 1° latitude resolution in 2012. **a**, Total fish. **b**, Anchovies. **c**, Herring-like fish. **d**, Cod-like fish. **e**, Flatfish. **f**, Salmon. **g**, Tuna and billfish. **h**, Other fishes.

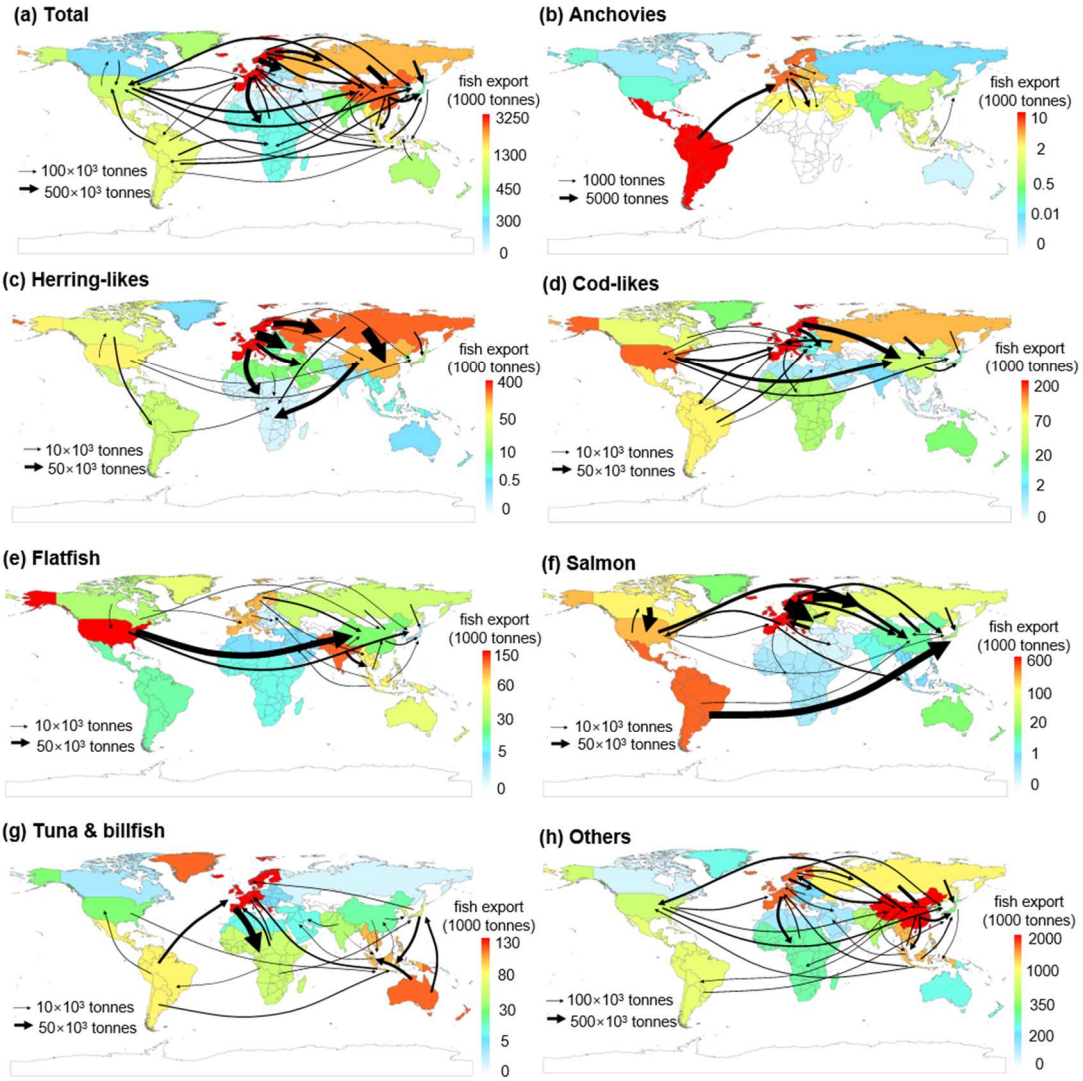

Extended Data Fig. 5 | Exports of various marine fish categories (1000 tonnes) through global trade in 2012. The color shading in each region indicates the total export of marine fish. The width of the arrows represents the relative marine fish exports ≥ 1000 tonnes for anchovies (b), ≥ 10,000 tons for herring-like (c), cod-like (d), flatfish (e), salmon (f), and tuna & billfish (g), and ≥ 100,000 tons for total fishes (a) and other fishes (h) in 2012.

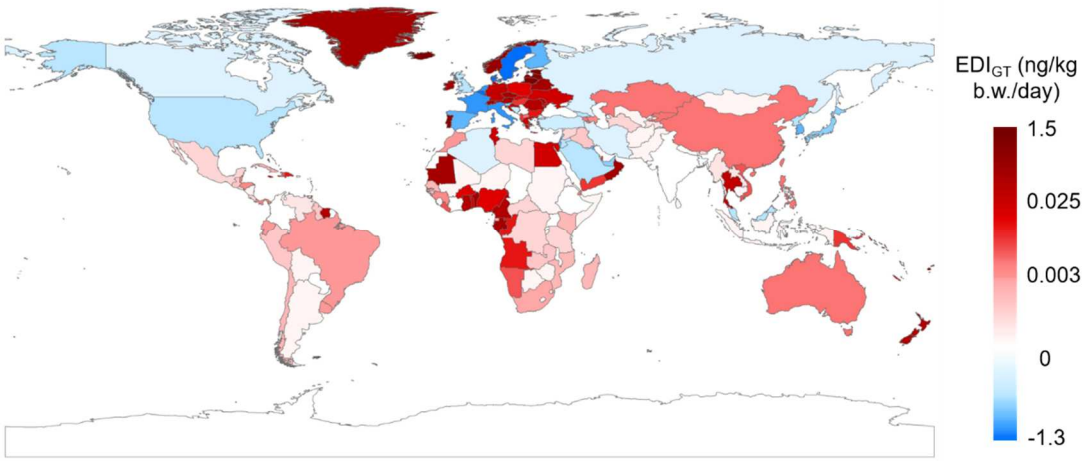

Extended Data Fig. 6 | Difference of EDI between Trade and NO-Trade model runs. The difference is estimated by EDIDF = EDIT-EDINT, referred to as Trade and NO-Trade simulated EDI, which is equivalent to the intake due to consumption of fish acquired through global trade.

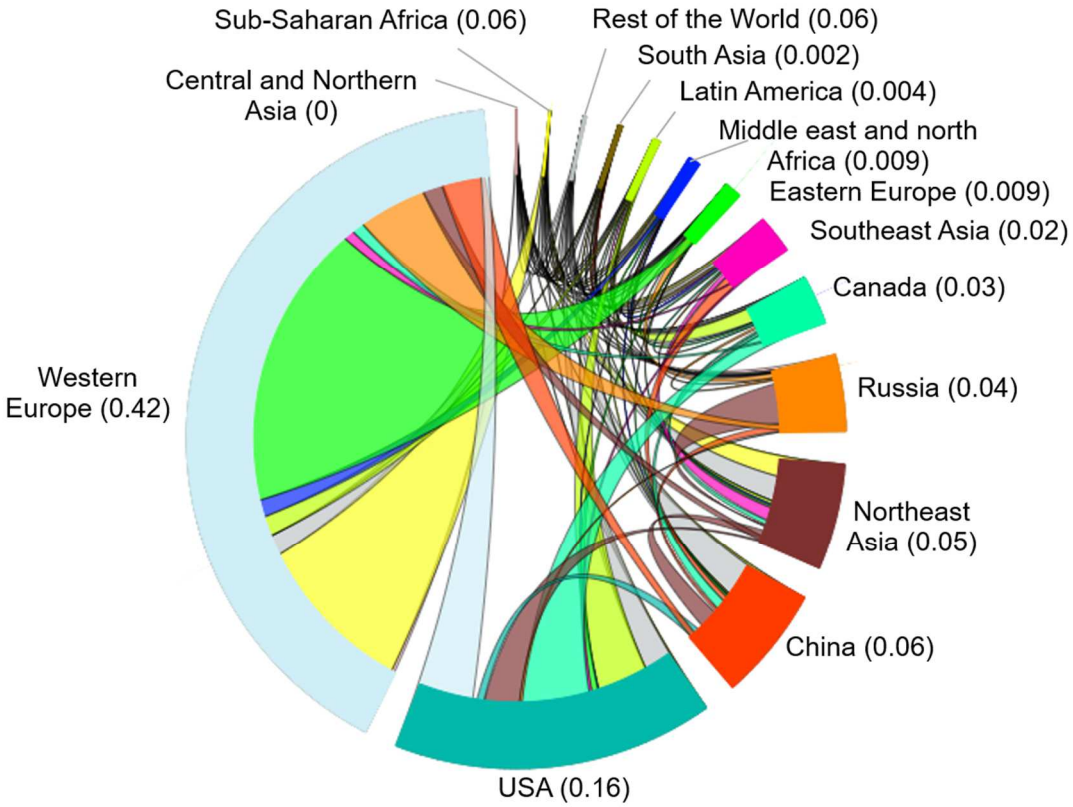

Extended Data Fig. 7 | Interregional EDI transfers embodied in the global marine fish trade illustrated as a Circos type graph. Numbers in brackets indicate EDIs of PCB-153 in each region (Extended Data Fig. 3). The width of each band represents the magnitude of EDI and the band color represents the net inflow of EDI. The colors of outer circular rings correspond to the regions marked.

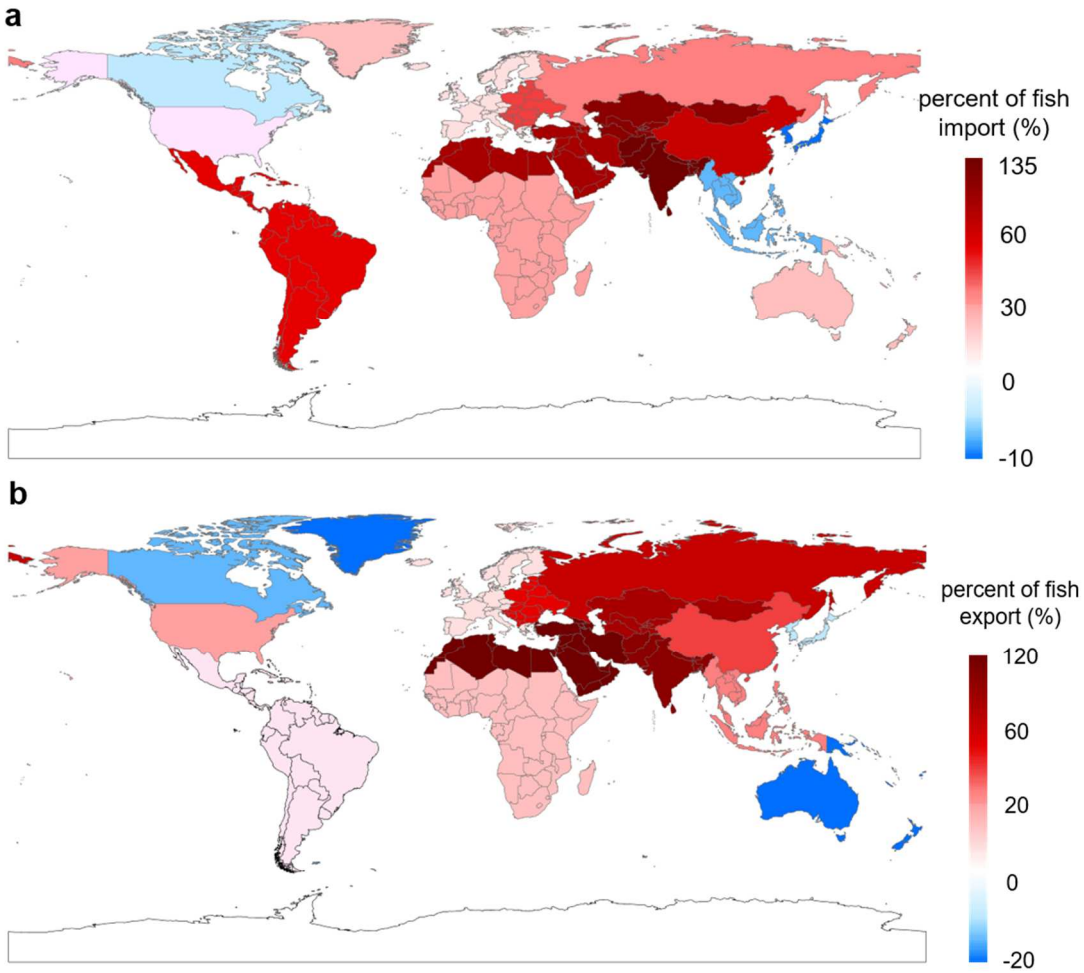

844

845 **Extended Data Fig. 8 |** Percent change between 2003 and 2012. **a**, Marine fish imported and **b**,
846 marine fish exported for various countries and regions. Percent was calculated as (I2012 –
847 I2003)/I2003×100, where I2012 and I2003 are marine fish imported or exported in 2012 and
848 2003.

849

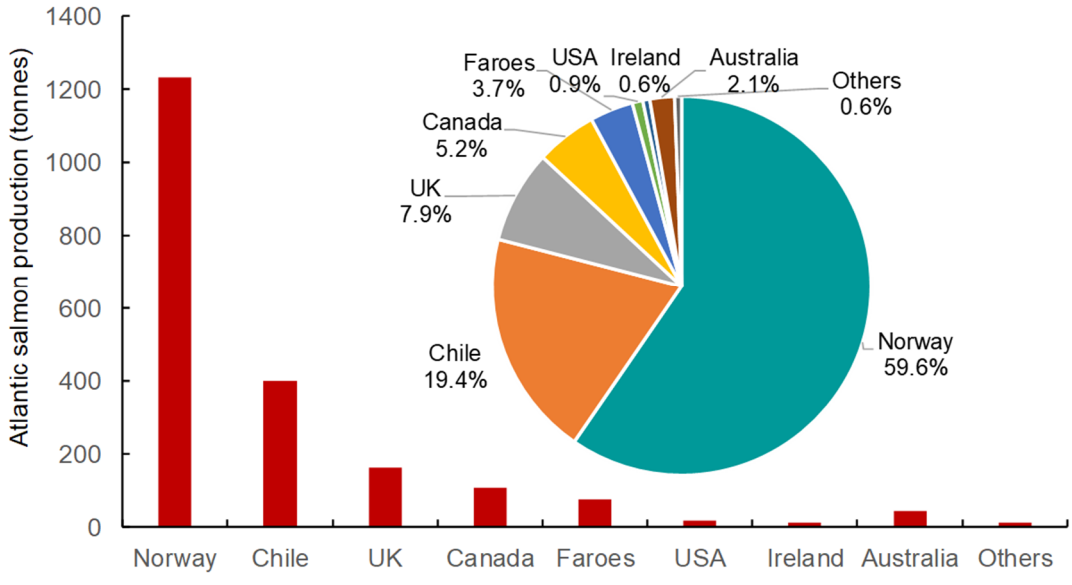

850

Extended Data Fig. 9 | Production (tonnes, bars) and percentage (pie chart) of farmed Atlantic salmon by countries. Farmed Atlantic salmon production in 2012 from 9 countries (red bars) and their respective contribution to global total farmed salmon production (%, pie chart).

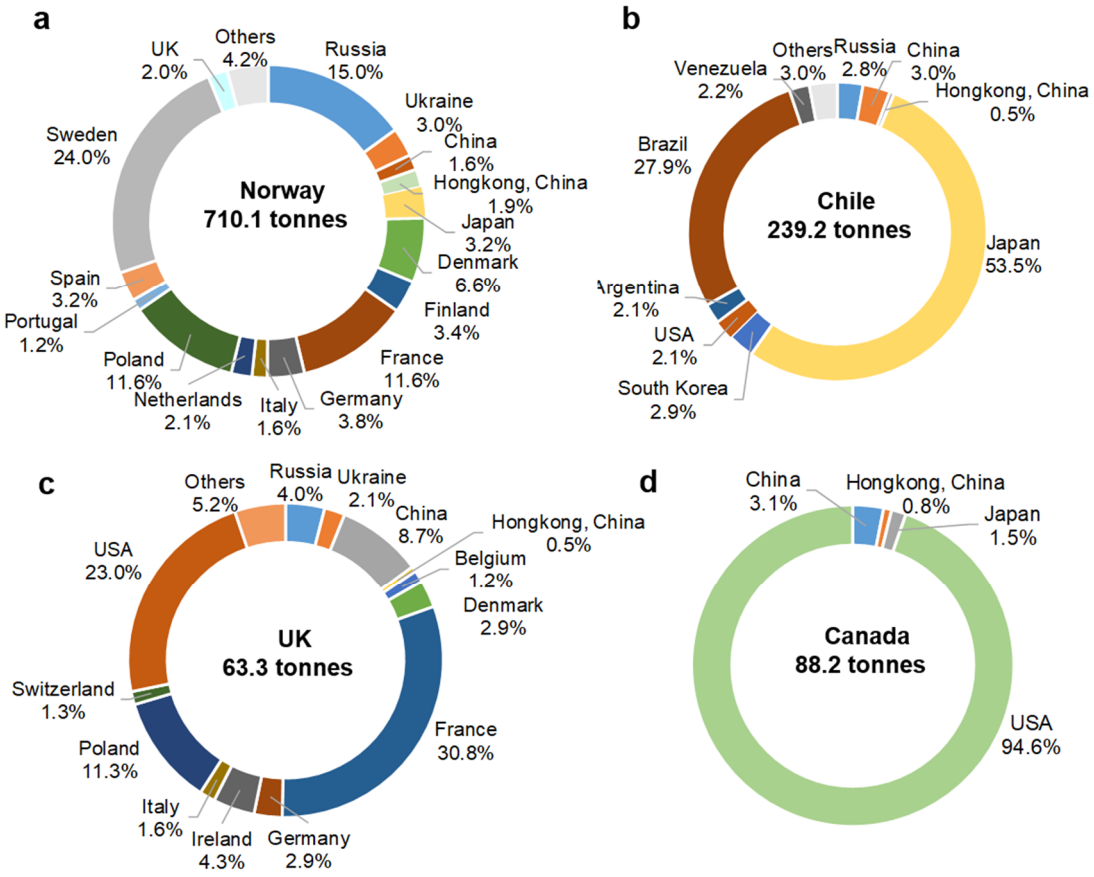

Extended Data Fig. 10 | Export of Atlantic salmon from major countries with salmonid aquaculture (tonnes). **a**, Norway, **b**, Chile, **c**, UK, and **d**, Canada. The colors in the ring chart represent the percentage of Atlantic salmon produced and exported from these 4 countries to those countries importing Atlantic salmon.

Supplementary Information for

Human exposure to polychlorinated biphenyls embodied in global fish trade

Tao Huang[1*], Zaili Ling[1], Robie W. Macdonald[3,4], Hong Gao[1], Shu Tao[2], Chongguo Tian[5], Shijie Song[1], Wanyanhan Jiang[1], Lulu Chen[1], Kaijie Chen[2], Zhiyong Xie[6], Yuan Zhao[2], Liuyuan Zhao[1], Chen Gu[1], Xiaoxuan Mao[1], Jianmin Ma[2,1*]

[1] Key Laboratory for Environmental Pollution Prediction and Control, Gansu Province; College of Earth and Environmental Sciences, Lanzhou University, Lanzhou 730000, P. R. China

[2] Laboratory for Earth Surface Processes, College of Urban and Environmental Sciences, Peking University, Beijing 100871, P. R. China

[3] Department of Environment and Geography, Centre for Earth Observation Science, University of Manitoba, Manitoba R3T 2N2, Canada

[4] Fisheries and Oceans Canada, Institute of Ocean Sciences, Sidney, British Columbia V8L 4B2, Canada

[5] Key Laboratory of Coastal Zone Environmental Processes and Ecological Remediation, Yantai Institute of Coastal Zone Research, Chinese Academy of Sciences, Yantai 264003, P. R. China

[6] Helmholtz-Zentrum Geesthacht, Centre for Materials and Coastal Research GmbH, Institute of Coastal Research, Max-Planck Straße 1, DE-21502 Geesthacht, Germany

This file includes:

Other Supporting Information for this manuscript include the following:

Supplementary Data 1 to 2 (Excel)

Supplementary Note 1. PCB-153 concentrations in environmental media

Model simulations for 2012 show higher PCB-153 concentrations in air and higher deposition (**Extended Data 1**) in Western Europe (WE) and the eastern seaboard of the USA, in line with higher emissions of this PCB congener from these two regions[1]. Higher average PCB-153 concentrations were simulated for water and sediment off the west and east coasts of the North Atlantic Ocean compared with the coasts of North Pacific and Indian Oceans, agreeing with observations[2-4]. PCB-153 entering oceans via surface runoff is discussed in Methods of main text and **Supplementary Note 6**. As a result of the higher water and sediment concentrations, the simulated concentration of PCB-153 averaged in all selected fish species was considerably higher for European coastal waters (Atlantic and Mediterranean) than for the rest of the global ocean (**Extended Data 2**). Therefore, fish from European coastal waters exported in global trade presented the greatest burdens of PCB-153.

Supplementary Note 2. PCB-153 exposure in traded fish-other details

The "Trade" simulations (**Fig. 1a**) show higher EDIs (ng/kg b.w./day) in WE and Northeast Asia, with the highest ranked countries being Malta (1.52, 95% confidence interval (95% CI): 0.13-17.21), Estonia (1.28, 95% CI: 0.13-12.25), Denmark (1.26, 95% CI: 0.12-13.65), Netherlands (1.17, 95% CI: 0.1-14.18), Lithuania (1.17, 95% CI: 0.11-12.03), and Italy (0.9, 95% CI: 0.09-8.8). These high EDIs directly reflect the higher PCB-153 concentrations in the fish consumed (**Extended Data 2**) and the high fish consumption in these countries (**Extended Data 10**). According to Breivik et al.[5, 6], the total global production of PCBs (1.324 million tonnes between 1930 and 1993), occurred mostly in WE, followed by the USA, Japan, and the former Soviet Union. Accordingly, WE emitted the largest amount of PCBs, followed by the USA, Eastern Europe, Japan, South Korea, and other countries[1], which can be identified by high levels of PCB-153 measured near the coasts of these countries (**Extended Data 1**). The residents of WE tended to consume more marine fish than others, leading to higher EDI values (**Fig. 1a**).

When global trade was not accounted for in the model, WE countries and South Korea had the greatest exposure to PCB-153 via fish consumption, caused by its high levels (**Extended Data 2**) in fish and high population densities. The similarity in EDI spatial distribution between "Trade" results (Fig. 1a) and "NO-Trade" results (**Fig. 2a**) was not unexpected because there were high fish PCB-153 concentrations in coastal waters of

Europe (**Extended Data 1**), and high fish consumption in these countries (**Extended Data 10**).

The model results (**Figs. 1&2**) can also be displayed as EDI embodied in inter-regional import/export of marine fish species (**Fig. 3** and **Extended Data 6**) estimated by reference to the 2012 global fish trade data matrix from UN Comtrade. In 2012, Western and Nordic Europe, China, Russia, Latin America, and the USA were the major exporters of marine fish, and China and Africa were the major importers (**Extended Data 4** and **Supplementary Fig. 3**). Accordingly, WE, the USA, and China were also net exporters of marine fish through global fish trade, yielding net EDI of 0.37 (95% CI: 0.04-3.82), 0.14 (95% CI: 0.01-1.64), and 0.006 (95% CI: 0.001-0.072) ng/kg b.w./day to those countries importing marine fish from these three countries, respectively (**Fig. 4a**). Other regions as net fish importers provided sinks for marine fish and got EDI embodied in imported marine fish. Similar to the $\%EDI_{GT}$ displayed by country in **Fig. 2b**, the regional $\%EDI_{GT}$ values for Northeast Asia (-61%), the USA (-43%), and WE (-37%) show that populations in these countries have reduced exposure to PCB-153 due to the export of locally caught fish and the import of fish from countries located far from the major historical PCB emission sources. Although China was the biggest importer of marine fish from the USA among those countries importing marine fish from the USA, the EDI in China was little impacted owing to relatively lower PCB-153 concentrations in the seawater near the USA as compared to that in European coastal waters (**Extended Data 1**) and lower quantity of imported fish from the USA than from the Europe (**Supplementary Fig. 3** and **Extended Data 4**). **Figure 4** also shows that WE and the USA were two major contributors to EDI embodied in global fish trade when all targeted marine fish species were accounted for. The EDI induced by other fish trade in the rest of world is less than 0.1 and 0.001 for selected six fish species trade. Overall, the global fish trade induced EDI from Western and Nordic Europe increased the exposure to PCB-153 in the importing countries (**Figs. 3** and **4a**). In particular, the summed mean EDI via fish consumption in China and the other 13 regions from the fish caught in China is 0.14 (95% CI: 0.01-1.65) ng/kg b.w./day (**Fig. 3** right hand column) compared to 0.93 (95% CI: 0.09-9.5) ng/kg b.w./day for WE.

Supplementary Note 3. Human exposure to PCB-153 via farmed Atlantic salmon trade

3.1 Production and export of farmed Atlantic salmon

The export of Atlantic salmon from Norway, Chile, UK, and Canada is collected from the Seafood Research Report published by Pareto Securities in 2016[7]. The Atlantic salmon export from Chile and UK to various countries is collected from Globefish Highlights published by FAO in 2015[8]. The Atlantic salmon exported from Norway and Canada to various countries is collected from the UN Comtrade (https://comtrade.un.org), which is verified with total export data reported in Seafood Research Report[7]. **Extended Data 9** presents the export of Atlantic salmon from Norway, Chile, UK, and Canada, respectively, to various countries.

3.2 PCB-153 level in farmed Atlantic salmon

With a congener-specific uptake and elimination rate constant at a certain feeding rate and dietary concentration (C_{feed}), the concentration of a chemical in a farmed fish (C_{fish}) at a given time can be calculated as[9,10]

$$C_{fish}(t) = \frac{\alpha F t}{k+\gamma} C_{feed}\left(1 - e^{-(k+\gamma)t}\right) + C_{fish0} e^{-(k+\gamma)t} \quad \text{(S36)}$$

where C_{fish} is the chemical level in farmed salmon (ng g^{-1} wet weight); C_{feed} is the chemical level in salmon feed (ng g^{-1} wet weight); F is feeding rate (g feed g^{-1} fish d^{-1}); a is the uptake rate of chemical (%); C_{fish0} is initial chemical concentration in salmon (ng g^{-1} wet weight); k is the elimination constant (k^{-1}); and γ is the growth rate (d^{-1}). Compared with sampled data, this model yields more accurate PCB-153 levels in farmed salmon fish than the food web model presented above because farmed salmon fish fed by feed ingredients do not follow the marine food bioaccumulation mechanism.

In the kinetic model simulating the feed-to-fillet transfer of dioxins and PCBs in feeds to farmed Atlantic salmon, the PCBs level in farmed salmon through feed intake at a steady state is given by[11,12]

$$C_{fish} = \delta F t C_{feed} \quad \text{(S37)}$$

where δ is the accumulation efficiency (%), or the net effect of dietary absorption and elimination for salmon. If the feed composition and PCB concentrations are known, eq. (S37) can be rewritten as

$$C_{fish} = \sum_{i=1}^{n} \delta F_{total} f_i C_{feed,i} \quad \text{(S38)}$$

where F_{total} is a total feed intake rate for farmed salmon (kg feed kg^{-1} fish); f_i is feed composition (%); and $C_{feed,\,i}$ is the PCB-153concentration level in feed ingredient i (ng g^{-1} wet weigh).

Since the health risk of a chemical occurs by ingesting edible part of salmon contaminated by the chemical, the accumulation efficiency for feed-to-fillet transfer is used to estimate PCB-153 level in salmon fillets. Compared to the whole fish, lipophilic organic contaminant concentrations in salmon fillets are lower due to the high contamination of adipose fat in the viscera[13,14]. In eq (S38), δ for the feed-to-fillet transfer of PCB-153 is 0.47 ± 0.014[9], F_{total} is the feed conversion ratio (FCR), which is the amount of feed (in kilograms) required to produce 1 kg of farmed animal[15-17]. Since global salmon feed ingredients in the 1990 were dominated by traditional feed, we assumed a FCR of 1.7[18]. In 2012, this value dropped to 1.3 due to the changes in feed ingredients from traditional to alternative feed[19]. To investigate the impact of feed composition (f_i) on the PCB-153 level in farmed salmon, two feed compositions, traditional feed and alternative feed, were modeled and compared. For traditional feed of Atlantic salmon, global average salmon feed ingredients composed of 59% fish meal, 24% fish oil, and 17% vegetable oil[20] were used in the calculation of PCB-153 contamination. The alternative feed composition for Atlantic farmed salmon in Norway, Chile, UK, and Canada in 2012 are presented in **Supplementary Table 1**. Fish oil and fish meal are the main sources for POPs in salmon feeds and farmed salmon[23-26]; therefore, seasonal changes in these sources affect POPs loads in farmed salmon[27] as does the geographical locations from which the feed derives[11,14]. The origin of fish meal and fish oil used in salmon feed in these four countries is listed in **Supplementary Table 2**. The PCB-153 concentrations in fish meal and fish oil used in salmon feed in Norway, Chile, UK, and Canada were collected from the literature and are listed in **Supplementary Table 3**. As seen, fish meal and oil produced from pelagic fish species from the Nordic region have higher concentrations than those from the Southern Hemisphere. Due to the absence of sufficient data on the origin of fish meal and fish oil for salmon producing and exporting countries, the fish meal and fish oil produced in Northern countries and the Southern Hemisphere were used as upper and lower bounds of farmed salmon feeds to calculate PCB-153 level in farmed salmon for Norway and the UK. Given that PCB-153 concentrations in plant matter (vegetable products such as vegetable oil, protein, and meal) used to produce farmed salmon feeds are considerably lower than those in fish meal and fish oil, and that plant matter is provided by many countries[15,21,33-35], PCB-153 levels in plant products used to feed Atlantic salmon in Norway were also used in the remaining three countries. With these hypotheses, we performed model simulations. The modeled PCB-153 levels in salmon fillets in Norway,

Chile, UK, and Canada are presented in **Supplementary Tables 4** and **5**, which also lists sampled data. The results show that the modeled PCB-153 concentration in farmed salmon is comparable to measured data.

Supplementary Note 4. Modified CanMETOP model

4.1. Model description and input parameters

The CanMETOP is a three-dimensional atmospheric transport model coupled with a dynamic 4D fugacity-based soil-air exchange model, and a water-air exchange model based on the two-thin film theory[36]. The horizontal spatial resolution of the modified CanMETOP on the global scale is 1°×1° latitude/longitude with 14 vertical layers at 0, 1.5, 3.9, 10, 100, 350, 700, 1200, 2000, 3000, 5000, 7000, 9000, and 11000 m. Three-dimensional atmospheric advection, eddy diffusion, and dry/wet deposition processes are included in the model, as are the exchange at the interfacial boundaries of air-water, air-soil, and air-snow/ice, and degradation in air, soil, and water. The soil compartment also accounts for organic chemical diffusion and leaching processes. The model, originally developed for modeling environmental fate and atmospheric transport of POPs on a regional scale, was subsequently extended to a global scale to investigate the intercontinental long-range transport of POPs with a spatial resolution of 1° latitude by 1° longitude[37]. The model has previously been applied extensively to simulate atmospheric transport and deposition, source-receptor relationships, as well as the multi-environmental compartment (air, soil, water, snow/ice, vegetation) exchange of POPs[38]. In a marine ecosystem, phytoplankton is often regarded as the bottom trophic level into which organic chemicals in the water must be exchanged before they can be passed up the food web to fish[39]. We couple the water-sediment-phytoplankton modules based on a fugacity approach[40] using CanMETOP. The model is integrated from 2002 to 2012 to permit the accumulation of PCB-153 in the global marine environment. It is noted that the water compartment in CanMETOP is described by a mass balance approach, which does not include stratification in surface ocean and deeper ocean water in the model. Hence, the model is not able to trace the exchange and diffusion of a chemical within oceans. Nevertheless, compared with deep oceans, a large body of evidence has shown considerably higher levels of PCBs in coastal waters where the majority of fishery activities (90%) take place.

Meteorological data (including winds, atmospheric pressure, temperature, precipitation) were obtained from the National Center for Environmental Prediction

(NCEP) reanalysis (6-hourly objectively analyzed data) with a spatial resolution of 1°×1° latitude/longitude (https://www.esrl.noaa.gov/psd/data/gridded/reanalysis). These data were interpolated to time steps of 20 min. The coarse resolution NCEP winds, and temperature data in the surface boundary layer (≤100m) interpolated to the high-resolution CanMETOP model grids were adjusted using the Monin-Obukhov similarity theory in the constant flux layer. Terra in height and surface roughness length, obtained from the CMC (Canadian Meteorological Centre) were also interpolated into each model grid. A global PCB-153 emission inventory (https://projects.nilu.no/globalpcb) accounting for e-waste exports and imports from 2002 to 2012 with a spatial resolution of 1°×1° latitude/longitude recently developed by Breivik et al.[1] and the physicochemical properties of PCB-153 (**Supplementary Table 6**) were used as input to CanMETOP.

4.2. Updated modules in CanMETOP

To obtain PCB-153 concentrations in aquatic sediment and phytoplankton, water-sediment and water-phytoplankton exchange modules were coupled with the air-water exchange module in CanMETOP using a fugacity approach. The mass balance equations for water, sediment and phytoplankton modules are formulated as follows[44]:

$$V_a Z_a \frac{df_a}{d_t} = D_{aw}(f_w - f_a) - f_a \phi A_w (U_q Q + U_p) Z_q \quad \text{(S1)}$$

$$V_w Z_w \frac{df_w}{dt} = D_{aw}(f_a - f_w) + D_{sw}(f_s - f_w) + D_{pw}(f_p - f_w) + f_s U_r A_s Z_s - f_w U_d A_s Z_w \quad \text{(S2)}$$

$$V_s Z_s \frac{df_s}{dt} = D_{sw}(f_w - f_s) + f_w U_d A_s Z_w - f_s U_r A_s Z_s \quad \text{(S3)}$$

$$V_p Z_p \frac{df_p}{dt} = D_{pw}(f_w - f_p) - f_p \rho_p Z_p (\mu \frac{N}{N+k} P) \quad \text{(S4)}$$

where:

$$D_{aw} = k_v A_w Z_w \quad \text{(S5)}$$

$$D_{sw} = k_t A_s Z_w \quad \text{(S6)}$$

$$D_{pw} = k_{pd} \rho_p P Z_p \quad \text{(S7)}$$

$$\rho_p = \xi_p \gamma_p V_w \quad \text{(S8)}$$

where f_i is the fugacity of an organic chemical in *ith* phase (Pa). V_i is the volume of *ith* phase (m^3). Z_i is the fugacity capacity of the organic chemical in in *ith* phase (mol m^{-3} Pa^{-1}). D values describe transport and transformation between phases (mol Pa^{-1} d^{-1}). Except

for diffusion and transport between phases, the growth dilution of phytoplankton for organic chemical, $f_p\rho_p Z_p(\mu\frac{N}{N+k}P)$, is also taken into consideration. The other parameters and variables in equations (S1) - (S8) are defined in **Supplementary Table 7**. Based on the fugacity capacity (mol m^{-3} Pa^{-1}) of a phase, Z_i, estimated using equations (S1) - (S4), PCB-153 concentrations (C_i, mol m^{-3}) in an environmental compartment, i, can be calculated by

$$C_i = Z_i f_i. \quad \text{(S9)}$$

Supplementary Note 5. Marine food web model

5.1. PCB-153 in zooplankton

The uptake and bioaccumulation of PCB-153 in zooplankton occurs mainly through the exchange between organisms and seawater[51,52]. Equilibrium partitioning of PCB-153 into zooplankton can be derived as:

$$C_z = K_{ow} \times L_z \times C_{WD} \quad \text{(S10)}$$

where C_z (ng kg^{-1}) is PCB-153 concentration in zooplankton, C_{WD} is the truly dissolved phase PCB-153 concentration in water (ng L^{-1}), and L_z is the lipid fraction of zooplankton[53].

C_{WD} can be calculated as follows[54]:

$$C_{WD} = C_W \times BSF \quad \text{(S11)}$$

$$BSF = 1/(1 + K_{ow} \times [OM]/d_{OM}) \quad \text{(S12)}$$

where C_W is total PCB-153 concentration in water (ng L^{-1}) obtained from CanMETOP simulation. BSF is the bioavailable solute fraction for chemical in water. $[OM]$ is the concentration (kg L^{-1}) of organic matter in the water. d_{OM} is the density of the organic matter (kg L^{-1}).

5.2. PCB-153 in benthic invertebrates

PCB-153 concentrations in benthic invertebrates are accumulated via the equilibrium partitioning of PCB-153 between lipids within the organism, the organic carbon fraction (OC) of sediments, and the interstitial water[55,56]. Assuming a partition equilibrium, PCB concentration in benthic invertebrates can be defined by:

$$C_b \times d_l/L_b = C_s \times d_{oc}/OC \quad \text{(S13)}$$

where C_b and C_s is PCB-153 concentrations in benthic invertebrates (ng g^{-1}) and sediments (ng g^{-1}), respectively. d_l is the density of lipids in benthos (=0.9 kg L^{-1})[53], L_b is the lipid fraction in benthos (=0.2 kg lipid/kg organism)[53], d_{oc} is the density of the organic carbon fraction of the sediments, which is approximately the same with d_l[54], and OC is the organic

carbon fraction in sediments (=0.02 kg OC/kg sediment)[46].

5.3. PCB-153 in fish

In the present study we have segregated 38 commercially important global marine fish species into seven categories: anchovies, herring-like, cod-like, flatfish, salmon, tuna & billfish, and the other fish. Whereas each group included several species, PCB-153 concentrations in all 38 species were modeled separately. Detailed lipid contents and weights of these marine fish species are provided in **Supplementary Data 1**.

The uptake of PCB-153 by fish occurs predominantly from the water via gills, within the gastrointestinal tract (GIT) through food consumption, and via chemical absorption through the skin. PCB-153 elimination by fish includes loss via the gills, execretion with fecal matter, and metabolic transformation[57-59]. It should be noted, however, fish have no notable capability to degrade PCB-153. In addition, PCB concentration within the fish may be reduced by growth dilution. A food web model for fish that accounts for these various factors can then be defined as[53,60];

$$\frac{dC_f}{dt} = k_1 C_w + k_d \sum(P_i C_{d,i}) - (k_2 + k_e + k_m + k_g) C_f \quad \text{(S14)}$$

where C_w is the concentration of PCB-153 in water (ng L^{-1}), $C_{d,i}$ is the concentration in prey item i (ng kg^{-1}), C_f is the concentration in fish (ng kg^{-1}), k_1 is the rate constant for uptake from water via gills (L $kg^{-1}day^{-1}$), k_d is the rate constant for chemical uptake from food (kg food/kg fish/day), P_i is the fraction of the diet consisting of prey item i (see **Supplementary Data 1**), k_2 is the rate constant for the elimination via gills to water (d^{-1}), k_e is the rate constant for the elimination by fecal ingestion (d^{-1}), k_m is the rate constant for metabolic transformation of chemicals (d^{-1}), and k_g is the rate constant for growth dilution (d^{-1}). The lipid content of a fish's diet was used to calculate the concentration of a chemical in prey item i ($C_{d,i}$, ng kg^{-1}), as presented in **Supplementary Data 1**.

The fish uptake of chemicals can be also estimated using the steady-state form of Eq. 14, defined as[61]

$$C_f = \frac{(k_1 C_w + k_d \sum(P_i C_{d,i}))}{k_2 + k_e + k_m + k_g} \quad \text{(S15)}$$

The gill uptake rate constant, k_1, is associated with the gill ventilation rate G_v (L d^{-1}) and uptake efficiency of the targeted chemical across the gill surface[60];

$$k_1 = (E_w G_v)/W \quad \text{(S16)}$$

where W is the wet weight of the whole fish body (kg) (see **Supplementary Data 1)**. For fish, E_w can be expressed as a function of K_{ow}[61];

$$E_w = (1.85 + 155/K_{ow})^{-1} \quad \text{(S17)}$$

G_v in Eq. S15 can be approximately derived from an allometric relationship based on wet weight and dissolved oxygen concentration D_{ox} (mg O_2 L^{-1})[62].

$$G_v = (980 * W^{0.65})/D_{ox} \quad \text{(S18)}$$

The rate constant for chemical elimination via fish respiration is expressed as the gill elimination rate constant (d^{-1})[52,63], defined as;

$$k_2 = k_1/(L_b * K_{ow}) \quad \text{(S19)}$$

where L_b is whole fish body lipid fraction (%) (see **Supplementary Data 1**).

Measurements show that the fecal elimination rate constant, k_e (d^{-1}), is approximately 3 to 5[53,63]. Referring to Gobas et al.[53], we choose k_e to be a factor of 4 smaller than k_d;

$$k_e = 0.25 * k_d \quad \text{(S20)}$$

The rate at which the chemical is absorbed from the diet or the dietary uptake rate constant (kg kg^{-1} d^{-1}) is defined as[53].

$$k_d = F_d * E_d/W \quad \text{(S21)}$$

Although E_d varies considerably from 0 to 100% in various diets and between 0 to 90% in fish, it is approximately 50% for those chemicals with a log K_{ow} between 6 and 7[53,64-66]. Based on the lipid-water, two-phase resistance model, which hypothesizes that dietary transfer occurs as transport across aqueous and lipid (or membrane) phases, E_d is given by[54,60]

$$E_d = (5.1 * 10^{-8} * K_{ow} + 2)^{-1} \quad \text{(S22)}$$

For the feeding rate, F_d, we adopted a simple bioenergetics relationship recommended by Weininger[67], given by;

$$F_d = 0.022 * W^{0.85} * exp(0.06 * T_w) \quad \text{(S23)}$$

The growth dilution rate constant k_g is given by[68]

$$k_g = 0.0005 * W^{-0.2} \quad \text{for temperatures around 10ºC} \quad \text{(S24)}$$

$$k_g = 0.00251 * W^{-0.2} \quad \text{for temperatures around 25ºC} \quad \text{(S25)}$$

A metabolic transformation rate constant, k_m, can be used to measure metabolic elimination. Given that fish have an extremely limited capability to biotransform PCB-153, k_m can be assumed to be 0[62].

Supplementary Note 6. PCB-153 entering coastal waters via surface runoff

The major pathways of PCBs to the oceanic environment include atmospheric processes, tributary runoff, and final effluent discharge from wastewater treatment plants

(WWTPs). It has been reported that 60% PCBs can be removed by waste treatment processes[69,70]. With the application of secondary biofiltration, the 90% of PCB can be removed[71]. Melymuk et al. also found that WWTPs contributed <5% of PCBs loadings from the Toronto City to Lake Ontario. Tributary runoff of PCBs as another pathway contributed less than the 30% of PCB loading from the Toronto City to Lake Ontario[72]. Whereas, the tributary runoff of PCBs in rural areas to oceans is lower than that in urban area. As a case, we estimate PCB-153 loading from Shanghai, China, to the nearby coastal waters. We compare the contributions of modeled dry particle deposition, wet deposition, gas absorption, and tributary runoff to PCB-153 loading to the offshore water of Shanghai. **Supplementary Figure 4** illustrates the two model grid cells covering Shanghai, Suzhou, and the adjacent East China Sea (ECS), including the Huangpu River and the Yangtze River running to the ECS. The area selected here is relatively smaller than a field sampling study[73] but includes Shanghai city clusters as primary PCB emission sources[74]. The cell on the left (Shanghai city clusters) is the source region and the right cell covers the offshore region. **Supplementary Figure 5** shows modeled diffusive gas deposition, total (dry + wet) particle deposition, and tributary runoff of PCB-153 (kg/yr) to the coastal water (cell 2). The deposition fluxes are output directly from the CanMETOP simulated results. The tributary runoff from the Shanghai city clusters to coastal water is obtained using a runoff model which takes into consideration the PCB emission (usage) from Shanghai city cluster, and the rivers draining into the coastal waters (by multiplying measured concentration in river water[73] with the average water flow rate). A sensitivity model test is also carried out by assuming the area of all rivers in the grid cell 1 to be 1% and 10% of the total area of cell 1, respectively, thereby to examine the potential contribution of the riverine input of PCB-153 from cell 1 to its loading to the coastal water (the model grid cell 2) via tributary runoff. As seen from **Supplementary Fig. 5**, gas absorption made the largest contribution (84 and 80% in the two sensitivity model tests) to PCB-153 total loading to the coastal water (cell 2), followed by the total deposition (~10%), and the tributaries runoff at 1% and 5% in the two model sensitivity tests. Overall, our results show that the atmospheric loadings dominate PCB-153 entering into the coastal water in Shanghai, in line with the previous findings by Morris and Lester[71] and Melymuk et al.[72].

Supplementary Note 7. Model performance evaluation and validation

To establish the level of confidence in the present model investigation, we conducted extensive model validation and evaluation by comparing modeling results with measured data for PCB-153 concentrations in air, water, sediment, and fish. We collected sampled PCB-153 concentrations worldwide from literature and major PCB sampling programs. The scatter plot with the 1:1 correspondence line, together with the 1/n and n times lines, is used to display the comparison between simulated and measured PCB-153 concentrations. The fraction of prediction with a factor *n* (*FACn*)[75] as a count of the fraction of points within 1/n and n times of the measured data is also employed in our evaluation metrics. *FACn* is defined as:

$$1/n \leq FACn \leq n \quad \text{(S26)}$$

Two most commonly used metrics, the mean bias (*MB*), and the mean error (*ME*) are also used to quantify the departures of simulated concentrations from measured data. Mean bias and mean error are defined as:

$$\mathrm{MB} = 1/\mathrm{N} \sum_{i=1}^{N} M_i - O_i \quad \text{(S27)}$$

$$\mathrm{ME} = 1/\mathrm{N} \sum_{i=1}^{N} |M_i - O_i| \quad \text{(S28)}$$

where M_i is ith (i = 1, . . ., N, where N is the number of the simulated data) modelled concentration. O_i is ith (i = 1, . . ., N, where N is the number of the measured data) measured concentration.

To provide a measure of the relative differences between the model predictions and the observations, the normalized mean bias (NMB) and the normalized mean error (NME) are estimated. These two metrics are defined as:

$$\mathrm{NMB} = \frac{\sum_{i=1}^{N} M_i - O_i}{\sum_{i=1}^{N} O_i} \quad \text{(S29)}$$

$$\mathrm{NMB} = \frac{\sum_{i=1}^{N} |M_i - O_i|}{\sum_{i=1}^{N} O_i} \quad \text{(S30)}$$

To determine spatial patterns and investigate long-range transboundary transport, several international monitoring programs for POPs have been established since the 1990s under the umbralla of EMEP (Co-operative Programme for Monitoring and Evaluation of the long-range transmissions of air pollutantsin Europe), IADN (Integrated Atmospheric Deposition Network)[76], AMAP (Arctic Monitoring and Assessment Programme)[77], and GAPS (Global Atmospheric Passive Sampling). Among them, the EMEP and IADN programs provide most comprehensive and longest time series measurement data for POPs since the early 1990s. The daily air concentrations of PCB-153 were collected every 6 days or one month in the EMEP program and every 12 days in the IADN program. The daily

concentration time series in gas and particle phases of PCB-153 of these two programs from 2002 to 2012 were used in the evaluation of modeled atmospheric concentrations. The sampling locations are shown in **Supplementary Fig. 6a** and **Supplementary Table 8**. Detailed information of measured data for air is provided in **Supplementary Data 2**.

Supplementary Figure 6b shows that simulated air concentration of PCB-153 match reasonably well with the measured data at a correlation coefficient of r =0.62 ($p<0.001$) and normalized mean bias = 3.27%. **Supplementary Table 9** shows that FAC10 is 92.69, manifesting that 92.69% of the simulated air PCB-153 concentrations is within 0.1 and 10 times of measured concentrations. **Supplementary Figure 6c** illustrates the comparisons of simulated and measured site-specific changes in air concentrations of PCB-153. The result shows that simulated mean concentrations from 2002 to 2012 are 1.7, 3.0 and 1.9 times higher than the sampled data at Sleeping Bears Dunes (SBD), Burnt Island (BNT), and Pallas. The model reproduces well the measured concentrations with weekly or monthly time series at other IADN master sampling sites, expect for Sturgeon Point (STP), where the simulated mean concentration from 2002 to 2008 was 3.6 times lower than measured concentration. The model overestimates daily air concentrations of PCB-153 from 2002 to 2009 by about two orders of magnitude at Zeppelin monitoring station, but matches well with the measured time series from 2010 to 2012. **Supplementary Figure 6c** also shows that our model captures observed seasonal concentration cycle with a peak in summer months and a trough in the wintertime. **Supplementary Table 9** further shows that MB and NMB between simulated and measured PCB-153 air concentration with all samples (N=3475) is 0.045 ng m^{-3} and 3.27%, suggesting that, overall, the model slightly overestimated PCB-153 air concentrations at most sampling sites. Given the NMB of 3% and FAC2 of 40% (**Supplementary Table 9**), we could conclude that our model performance is good[75]. Friedman and Selin[78] have compared their modeled PCB-153 air concentration using Geos-Chem atmospheric chemistry model with monthly and seasonally average concentrations at the arctic Zeppelin site and the Great Lakes Burnt Island site. Their result shows a correlation coefficient of 0.73 and bias at -0.53. Comparing with their result, our modelling result evaluation against more sampling data yields lower mean bias.

Measured data for PCB-153 concentrations in seawater, sediment, and marine fish are collected from the International Council for the Exploration of the Sea (ICES) and literature (sampling locations are marked in **Supplementary Fig. 7a** for water, **Supplementary Fig.**

8a for sediment, **Supplementary Fig. 9a** for fish, and **Supplementary Table 8**). Detailed information of measured data for water, sediment, and fish is provided in **Supplementary Data 2**. As shown, modeled concentrations match reasonably well with the measured data at a correlation coefficient of r =0.74 ($p<0.001$) for water (**Supplementary Fig. 7b**), r =0.52 ($p<0.001$) for sediment (**Supplementary Fig. 8b**), and r =0.53 ($p<0.001$) for fish (**Supplementary Fig. 9b**). **Supplementary Figure 7c** and **Supplementary Figure 8c** show that the model reproduces well the measured concentrations at five water monitoring sites and four sediment sampling sites for PCB-153. The model overestimated PCB-153 mean water concentration at the W6 site from 2010 to 2012, but within the same order of magnitude. The model also reproduces the decline in measured concentrations in water and sediment. **Supplementary Table 9** shows that 87.6% and 81.4% of simulated PCB-153 concentrations in water and sediment are within 0.1 and 10 times of measured concentrations, respectively. The MB and NMB between simulated and measured PCB-153 concentration in water for all sample size (N=210) is 0.23 pg L^{-1} and 11.14%, again suggesting the good model performance[75]. The model appeared to underestimate PCB-153 concentration in sediment at most sampling sites characterized by negative MB (-0.16 ng g^{-1} ww) and NMB (-28.4%).

Supplementary Figure 9c shows the comparisons between the modeled and measured concentrations of PCB-153 in twelve marine fish species. Results show that the modeled concentrations are associated well with the measured concentrations for almost all fish species ($p < 0.01$ for herring, perch, sole, and cod, $p < 0.05$ for flounder, and salmon, and $p < 0.5$ for other fish species, except for plaice), suggesting that the model is able to predict nicely the trend of measured PCB-153 concentrations in fish, though on average, the modeled concentrations were slightly higher than measured concentrations in cod, flounder, perch, plaice, and sole, and lower than measured concentrations in eel, mackerel, tuna, and anchovy. **Supplementary Figure 9d** shows that the model reproduces reasonably well the annual variation in PCB-153 concentrations in fish from 2002 to 2012. As seen, PCB-153 levels increased from 2002 to 2006, and decreased thereafter. **Supplementary Table 9** shows that 91.2% of simulated PCB-153 concentrations in fish are within 0.1 and 10 times of the measured data. MB and NMB values between measured and sampled PCB-153 concentrations in fish are -0.34 ng g^{-1} ww and -11.54%, respectively, indicating that the model underestimate somewhat the PCB-153 concentrations in fish, but overall the simulated concentrations match reasonably well in terms of the air quality model evaluation

criteria[41].

It is important to note that most of the measured data were collected from coastal waters where both atmospheric deposition and runoff from land may contribute to PCB-153 concentration. Since tributary runoff made insignificant contribution to total PCB-153 loadings (**Supplementary Fig. 5**), we examine only modeled atmospheric concentration and gaseous diffusive deposition[35,79]. The differences between modeled and sampled results could also be resulted from a spatial mismatch between sampling sites and the model grid with the area of 1°×1° latitude/longitude. This size of a model grid cell in many cases covers both coastal land and water, leading to a deviation depending on where within the grid a sampling site was located. Detailed information of measured data for air, water, sediment, and fish are provided in **Supplementary Data 2**.

Supplementary Note 8. Uncertainties and limitations

Monte Carlo analysis, a method often used to quantify uncertainties in health and environmental risk assessments[80], requires parameterization of the degree of uncertainty and the shape of input distributions associated with each input parameter. Here, we combined the CanMETOP model, marine food web model, and health risk assessment models. The global CanMETOP model, by itself, includes complex dynamical and physical processes, such as deposition and precipitation scavenging, horizontal and vertical advection, turbulent diffusion, and exchange between environmental media. The model complexity and implementation of the CanMETOP model precludes an estimate of uncertainty using Monte Carlo analysis. Instead, we used a first-order error propagation approach[8] to calculate the uncertainties in modeled concentrations (Cf_{out}) in the various environmental compartments and within marine food web. Specifically, uncertainties were calculated by propagating input parameter (Cf_i) uncertainties using the formula;

$$Cf_{out} = \exp\sqrt{\sum_i (\ln Cf_i)^2 \times S_i^2} \quad \text{(S31)}$$

where Cf_{out} and Cf_i are the confidence factors that span the 95% confidence interval around the median of a log-normally distributed variable, and S_i is the relative sensitivity of the model output subject to changes in input parameter i.

Cf_{out} indicates to what extent X might deviate from the median (u)[42,81]:

$$probability\ \left\{\frac{u}{Cf_{out}} < X < u \cdot Cf_{out}\right\} \quad \text{(S32)}$$

The relationships between *Cf* and standard deviation (σ) of a log-normal distribution are[8]

$$Cf = e^{2\sigma} \quad \text{(S33)}$$

The coefficient of variation CV is given by

$$CV = \sqrt{e^{\sigma^2} - 1} \quad \text{(S34)}$$

which is also defined as the ratio of the standard deviation to the mean. Further details in the estimation of *CF* and *CV* are referred to references 8, 9, and 47.

The sensitivity, *S* is calculated by

$$S = \left(\Delta O / O\right) / \left(\Delta I / I\right) \quad \text{(S35)}$$

where ΔI and ΔO are the relative changes in input (I) and output (O) parameters of interest, respectively. The average sensitivity of increasing and decreasing an input parameter was calculated by varing each input parameter by ±10%.

Due to the large number of input parameters used in this study, only those significantly affecting modeling results were taken into consideration. The uncertainties in PCB-153 concentrations in environmental compartment simulated by the CanMETOP come predominantly from uncertainties in emission inventories, physicochemical properties, and the model representation of chemical and processes. A factor 10 of uncertainties was assigned for PCB-153 emission which was suggested in Breivik et al.[82] and Wöhrnschimmel et al.[43] For the uncertainties associated with physicochemical properties of PCB-153, *Cf* values recommended by Macleod et al.[42] and Wöhrnschimmel et al.[43] were used (**Supplementary Table 6)**. Uncertainties associated with weight and lipid content of various fish species, diet compositions, and lipid content in fish diets used in the marine food web model were estimated as follows. The *Cf* for the weight and lipid content of sixteen fish species, and the lipid content in the diet (prey items) of the 38 commercial marine fishes were collected from the literature (**Supplementary Data 1**). The *CV* for the diet composition of the selected fish was neglected in this study. However, to reduce the error and uncertainty in the aquatic food web model associated with diet composition, 2-4 different diets for sixteen fish species were included (**Supplementary Data 1**). Due to the lack of uncertainty information for marine fish consumption by country, we assumed a 15% *CV* for this parameter. This choice was partly based on a reported annual per capita seafood consumption of 20-25 kg in Ghana[83], and 12-16 kg in New Zealand[84]. **Supplementary Figure 10** illustrates the total uncertainty of globally averaged EDI from NO-TRADE

simulation was a factor of 10.4, and the EDI in 14 regions are within factors of 9.3−12.1. The PCB-153 emission yields the largest uncertainty to EDI, contributing more than 85% to total uncertainty of EDI. The lipid contents of fish diets also contributed approximately 10% to the total uncertainty of EDI. Other parameters contributed less than 2% to the uncertainty of EDI.

Supplementary Figures

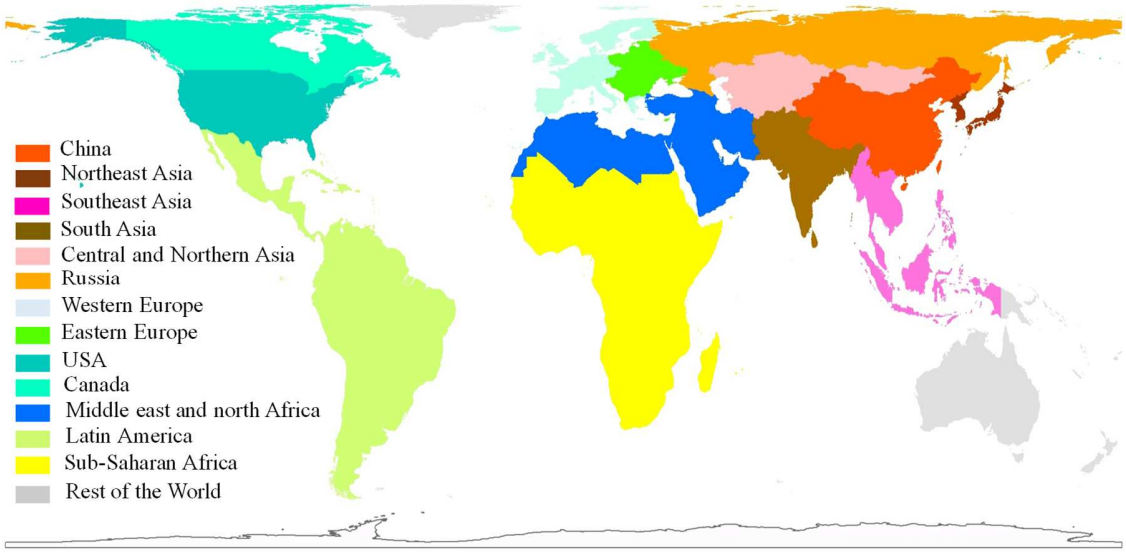

Supplementary Figure 1. The map of 14 regions regrouped from countries involved in the global fish trade. The map provides a key to the color scheme.

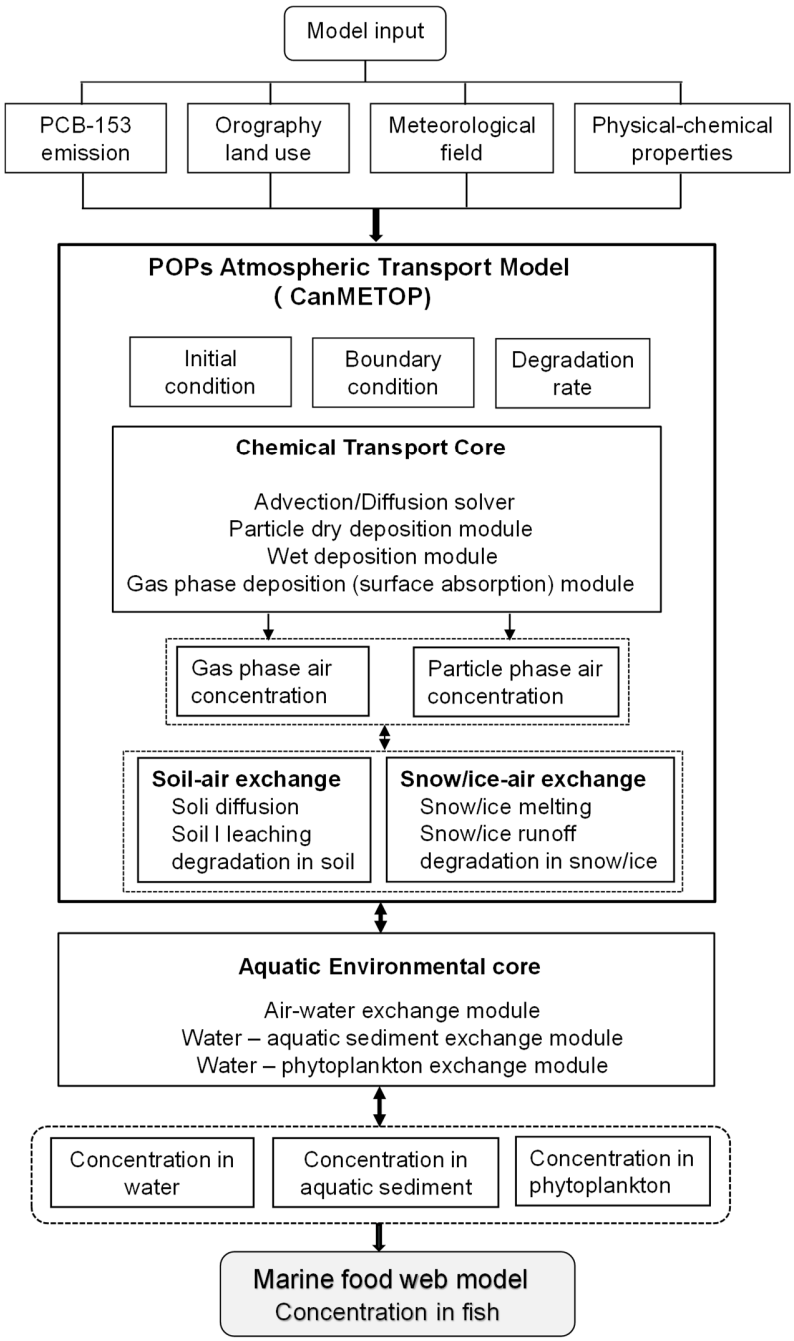

Supplementary Figure 2. A schematic diagram showing the model components for atmospheric transport, phase partitioning between the various environmental media, and the marine food web developed for the present study.

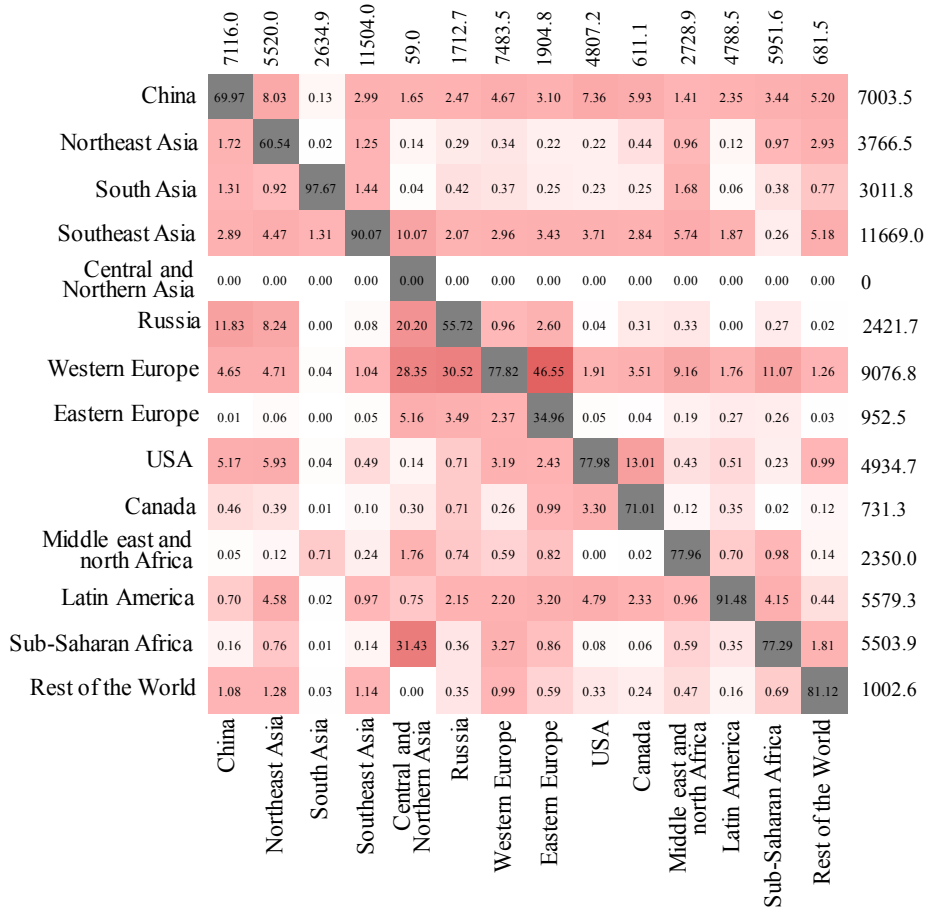

Supplementary Figure 3. Matrix for percent of commercially caught marine fish for each of 14 regions (**Supplementary Fig. 1**) caught locally (diagonal grey squares) or imported from other regions (diagonal, white - red squares) in 2012. The quantity of consumed marine fish (1000 tons) for each region caught locally and imported from other regions is shown at the top of the matrix. The quantity of marine fish caught locally for each region and consumed or exported to other regions is shown on the right of the matrix.

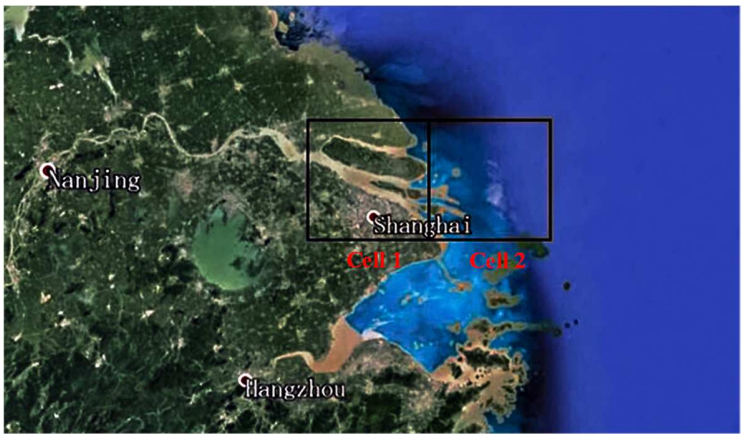

Supplementary Figure 4. Selected two cells covering Shanghai City (Cell 1) and adjacent costal water (Cell 2) of the Eastern China Sea. The photo is downloaded from the Google Map without copyright requested.

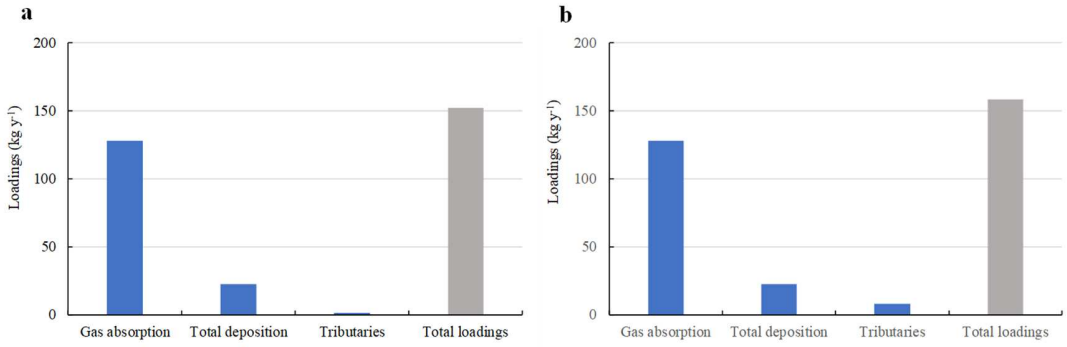

Supplementary Figure 5. Estimated loadings of PCB-153 (kg/yr) to cell 2 via total deposition, diffusive gaseous deposition, and tributary runoff. (**a**) The area of all rivers in the grid cell 1 is 1% of the total area of the cell 1; (**b**) the area of all rivers in the grid cell 1 is 5% of the total area of the cell 1.

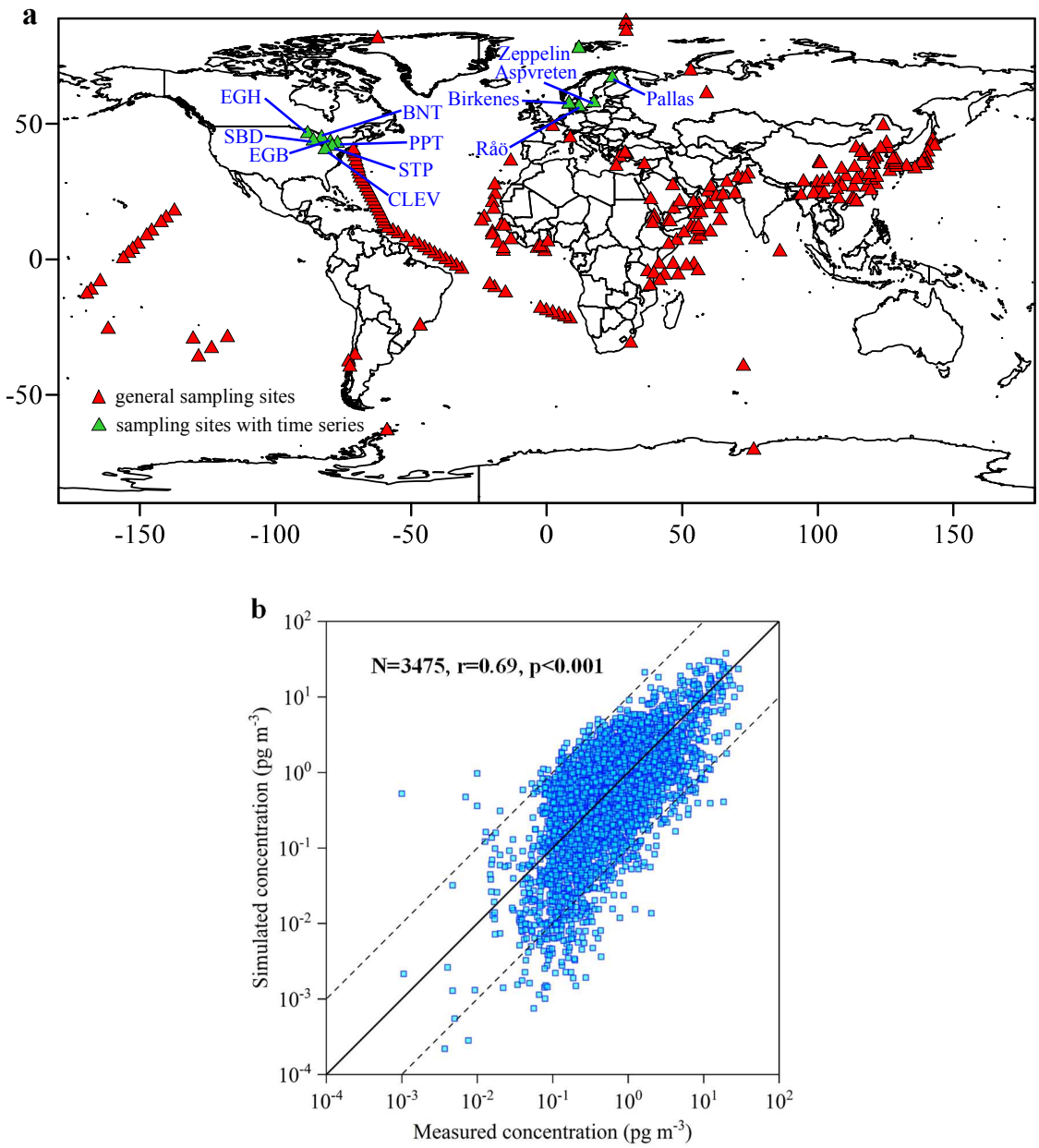
a
Zeppelin
Aspvreten
Birkenes
Pallas
EGH
BNT
SBD
PPT
EGB
Råö
STP
CLEV
general sampling sites
sampling sites with time series
50
0
-50
-150
-100
-50
0
50
100
150
b
N=3475, r=0.69, p<0.001
Simulated concentration (pg m-3)
Measured concentration (pg m-3)
10-4
10-3
10-2
10-1
100
101
102

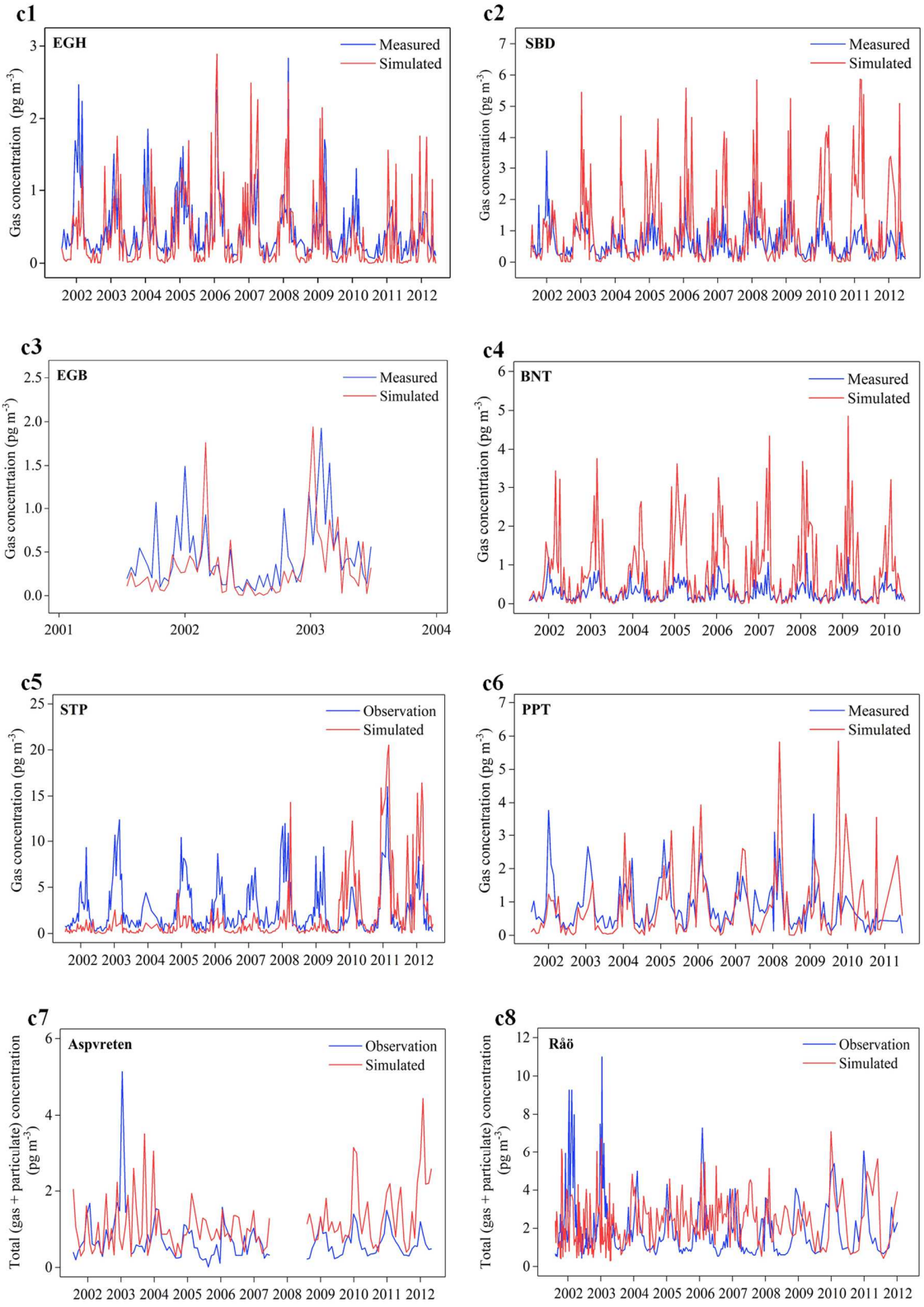
c1
EGH
Measured
Simulated
Gas concentration (pg m-3)
2002 2003 2004 2005 2006 2007 2008 2009 2010 2011 2012
c2
SBD
Measured
Simulated
Gas concentration (pg m-3)
2002 2003 2004 2005 2006 2007 2008 2009 2010 2011 2012
c3
EGB
Measured
Simulated
Gas concentrtaion (pg m-3)
2001 2002 2003 2004
c4
BNT
Measured
Simulated
Gas concentrtaion (pg m-3)
2002 2003 2004 2005 2006 2007 2008 2009 2010
c5
STP
Observation
Simulated
Gas concentration (pg m-3)
2002 2003 2004 2005 2006 2007 2008 2009 2010 2011 2012
c6
PPT
Measured
Simulated
Gas concentration (pg m-3)
2002 2003 2004 2005 2006 2007 2008 2009 2010 2011
c7
Aspvreten
Observation
Simulated
Total (gas + particulate) concentration (pg m-3)
2002 2003 2004 2005 2006 2007 2008 2009 2010 2011 2012
c8
Råö
Observation
Simulated
Total (gas + particulate) concentration (pg m-3)
2002 2003 2004 2005 2006 2007 2008 2009 2010 2011 2012

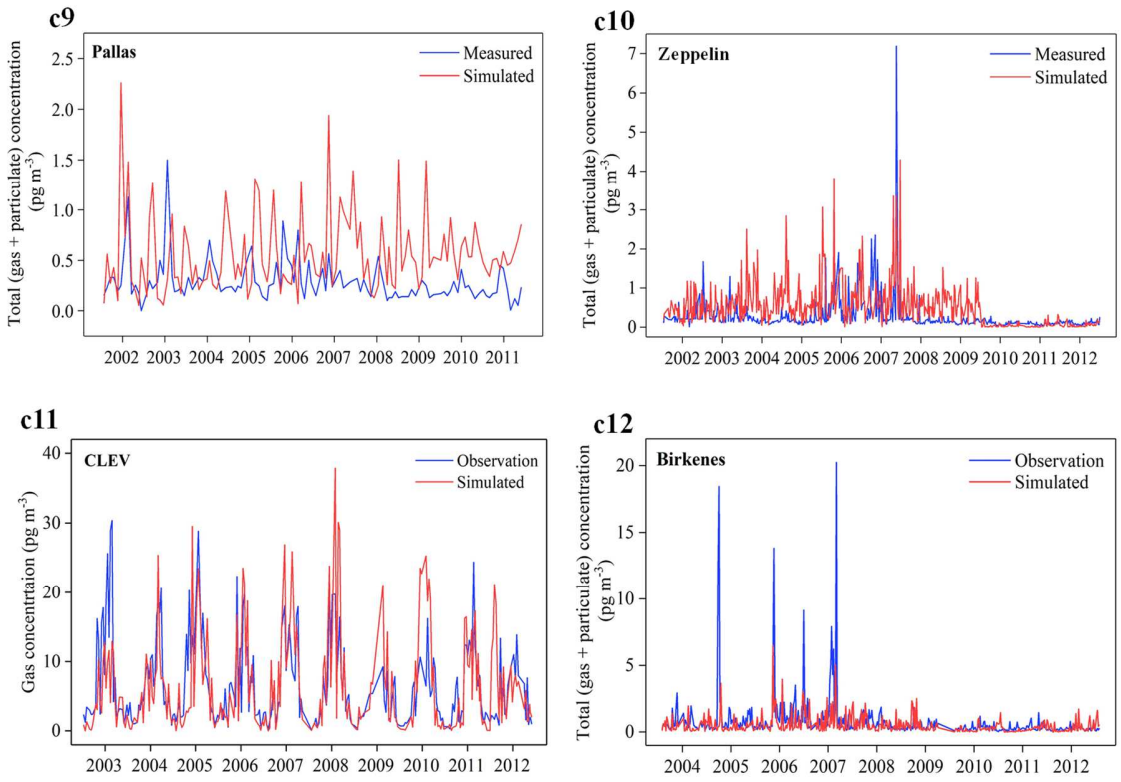

Supplementary Figure 6. Comparison between modeled and measured air concentrations of PCB-153. **(a)** Sampling sites assembled from various field campaigns by different research groups and from literature. **(b)** Scatter plot of modeled and measured air concentrations of PCB-153. The solid black line represents a 1:1 relationship, and the dashed black lines denote the boundaries where simulated concentrations are 0.1 and 10 times of measured concentrations. The data are presented in log-scale. **(c)** Comparisons between modeled and measured air concentrations of PCB-153 at twelve sites, as marked with green triangle in **Supplementary Fig. 6a** from 2002 to 2012, where sampled time series data are available. The information of the ten sampling sites is listed in **Supplementary Table 8**. All measured air concentrations of PCB-153 are presented in **Supplementary Data 2**.

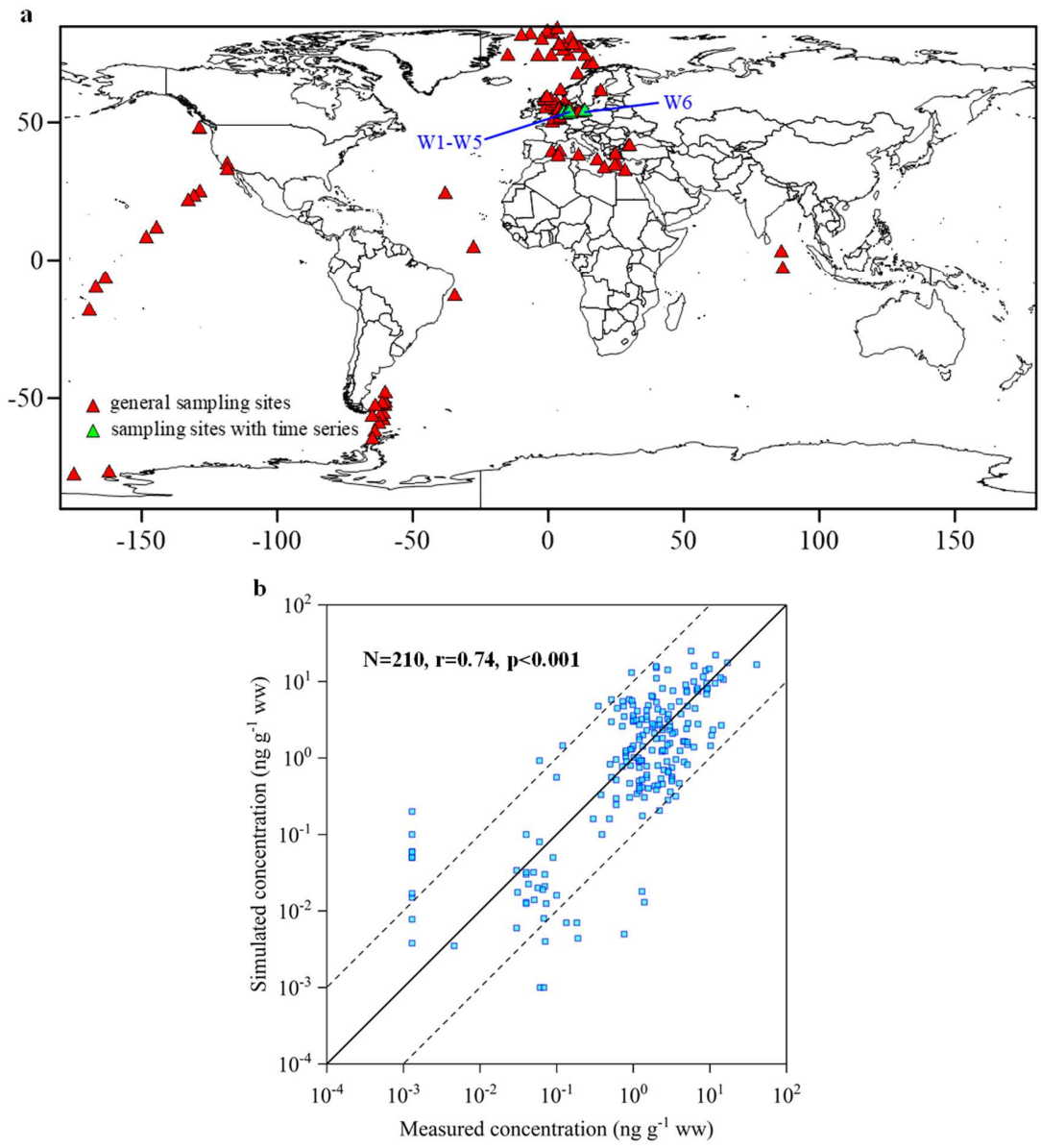
a
W6
W1-W5
general sampling sites
sampling sites with time series
50
0
-50
-150
-100
-50
0
50
100
150
b
N=210, r=0.74, p<0.001
Simulated concentration (ng g-1 ww)
Measured concentration (ng g-1 ww)
10-4
10-3
10-2
10-1
100
101
102

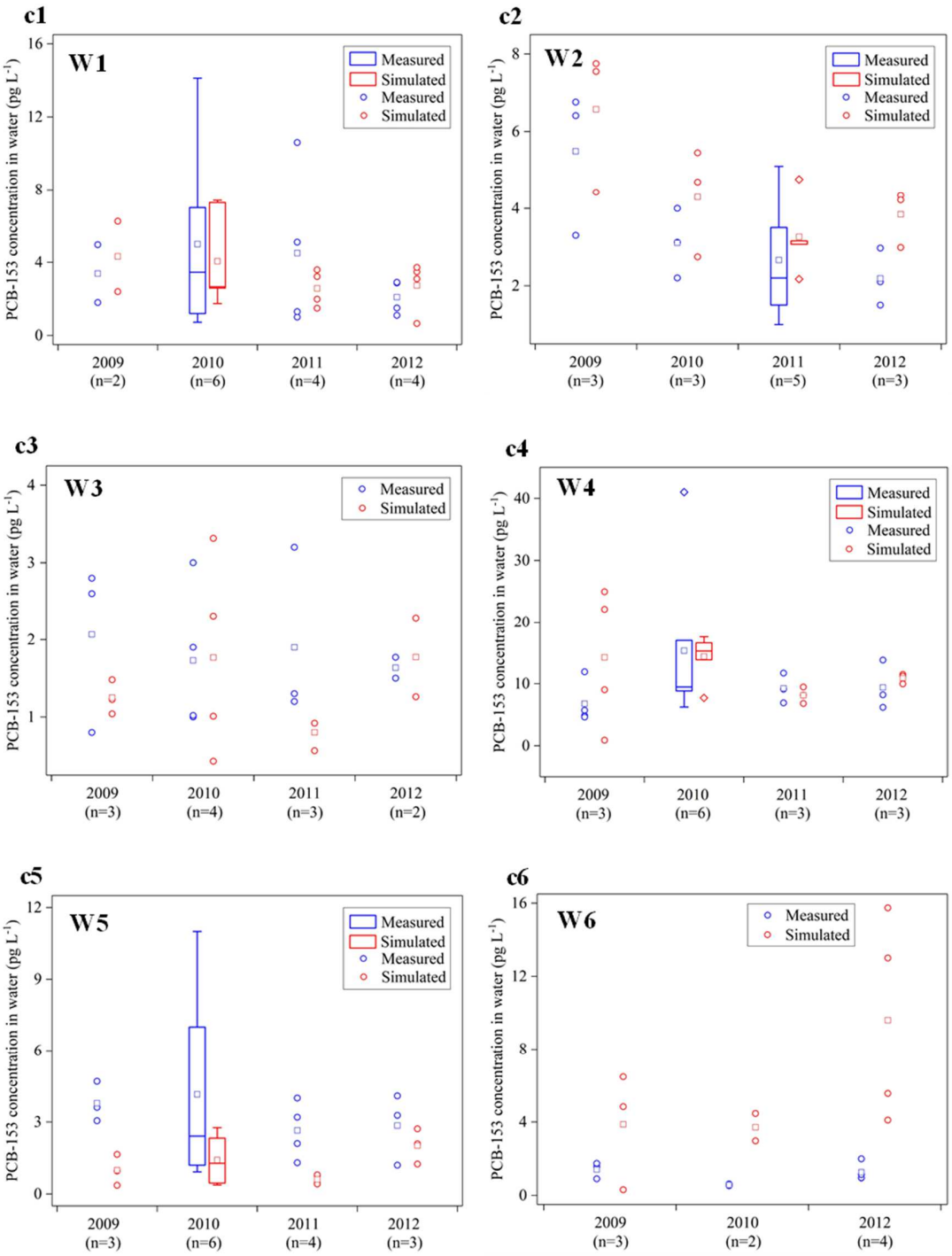

Supplementary Figure 7. (**a**) and (**b**), same as **Supplementary Fig. 6** but for comparison between modeled and measured concentrations of PCB-153 in water. **(c)** Comparisons between modeled and measured concentrations of PCB-153 at six sampling sites as marked with green triangle in **Supplementary Fig. 7a** from 2009 to 2012. The box limits represent the 25th and 75th percentiles. The open square denotes arithmetic mean value, the solid

line stands for the group median, the whiskers extend to the 5th and 95th percentiles, and the diamonds represent outliers. Data marked by circles are shown as individual points because of small sample size (n≤4). Information of six sampling sites with time series data of PCB-153 is listed in **Supplementary Table 8**. All measured concentrations of PCB-153 in water are listed in **Supplementary Data 2**.

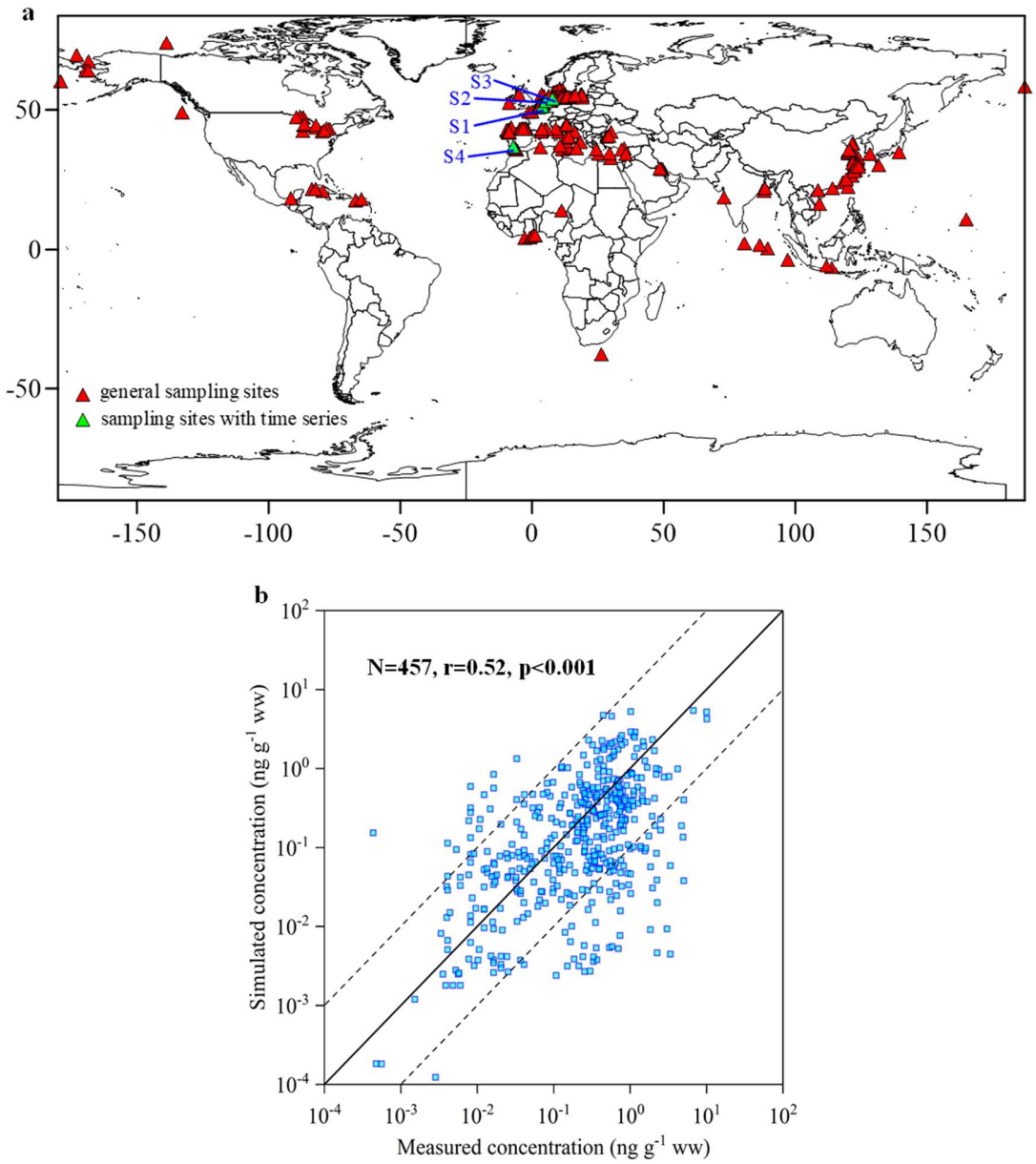

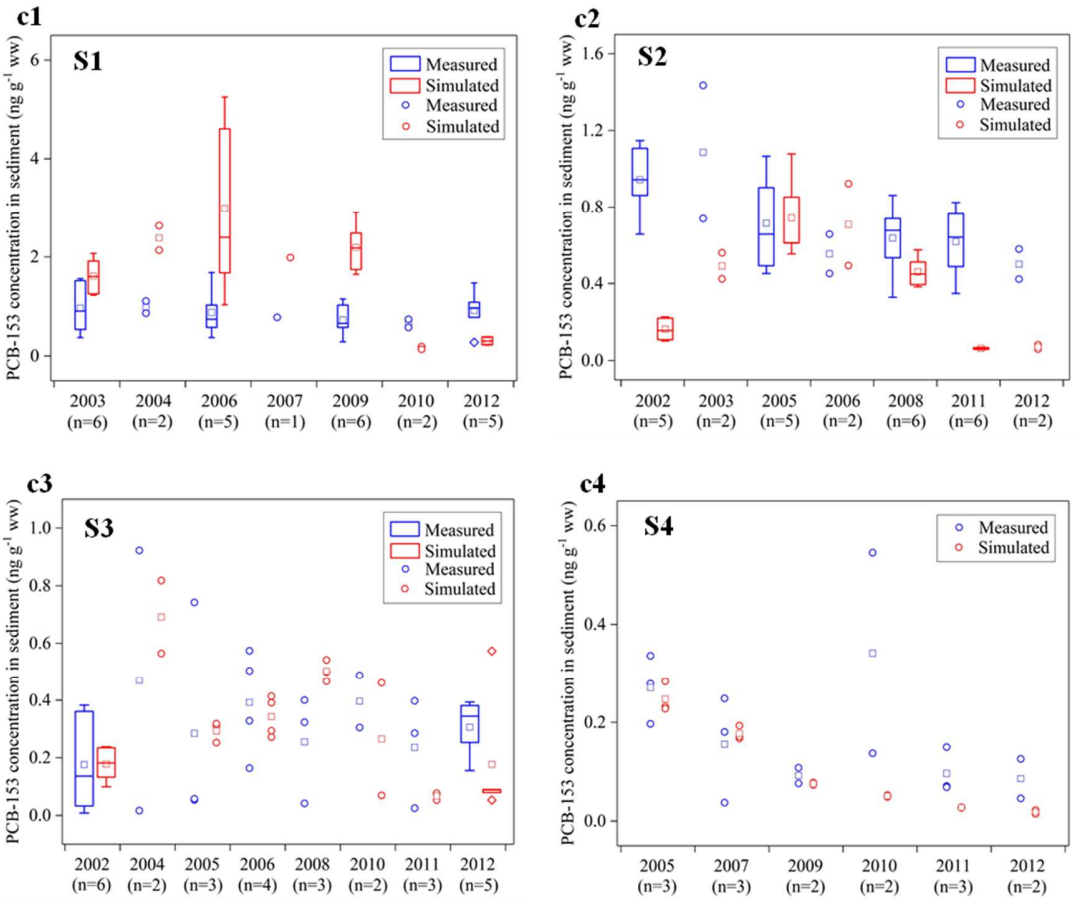

Supplementary Figure 8. (**a**) and (**b**), same as **Supplementary Fig. 6** but for comparison between modeled and measured concentrations of PCB-153 in sediment. **(c)** Same as **Supplementary Fig. 7c** but for sediment at four sampling sites marked by the green triangle in **Supplementary Fig. 8a**. The information of four sampling sites with time series is listed in **Supplementary Table 8**. All measured concentrations of PCB-153 in sediment are listed in **Supplementary Data 2**.

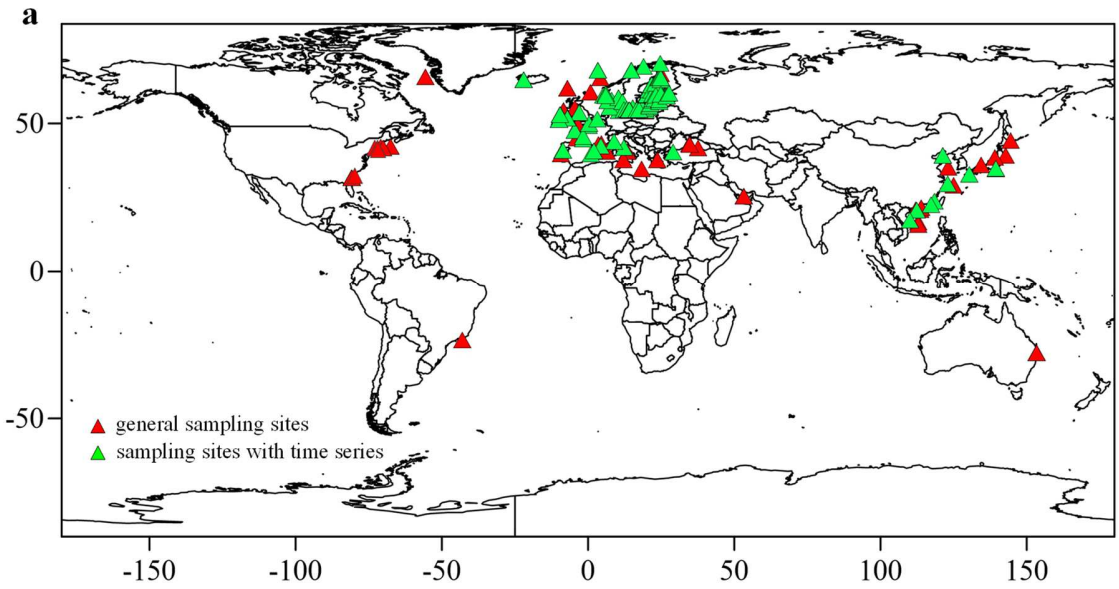
a
50
0
-50
general sampling sites
sampling sites with time series
-150
-100
-50
0
50
100
150

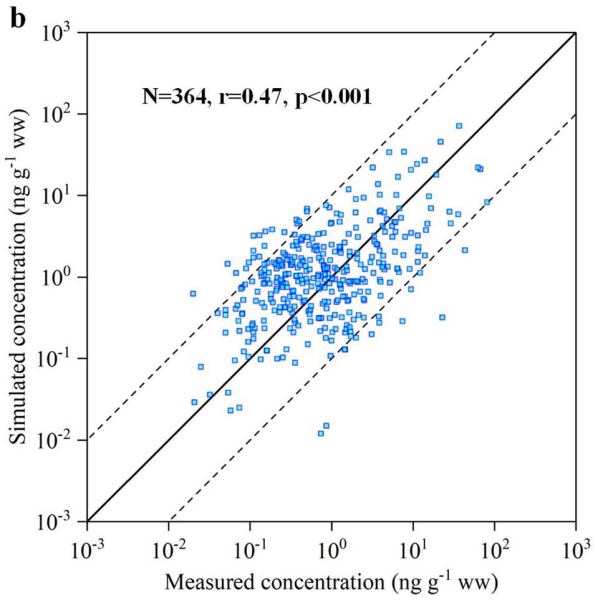
b
N=364, r=0.47, p<0.001
Simulated concentration (ng g-1 ww)
Measured concentration (ng g-1 ww)
10-3
10-2
10-1
100
101
102
103

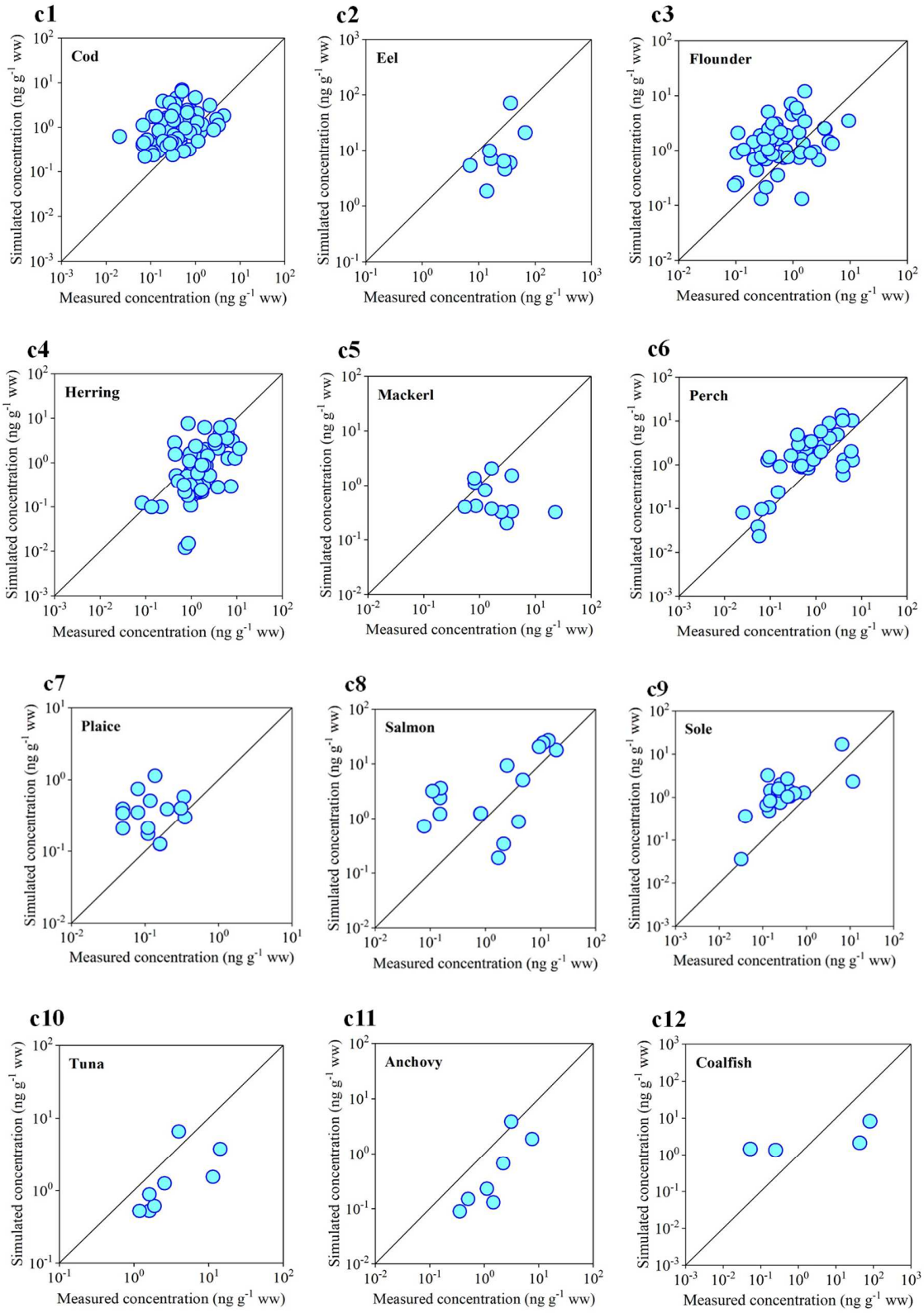
c1
Cod
c2
Eel
c3
Flounder
c4
Herring
c5
Mackerl
c6
Perch
c7
Plaice
c8
Salmon
c9
Sole
c10
Tuna
c11
Anchovy
c12
Coalfish
Simulated concentration (ng g-1 ww)
Measured concentration (ng g-1 ww)

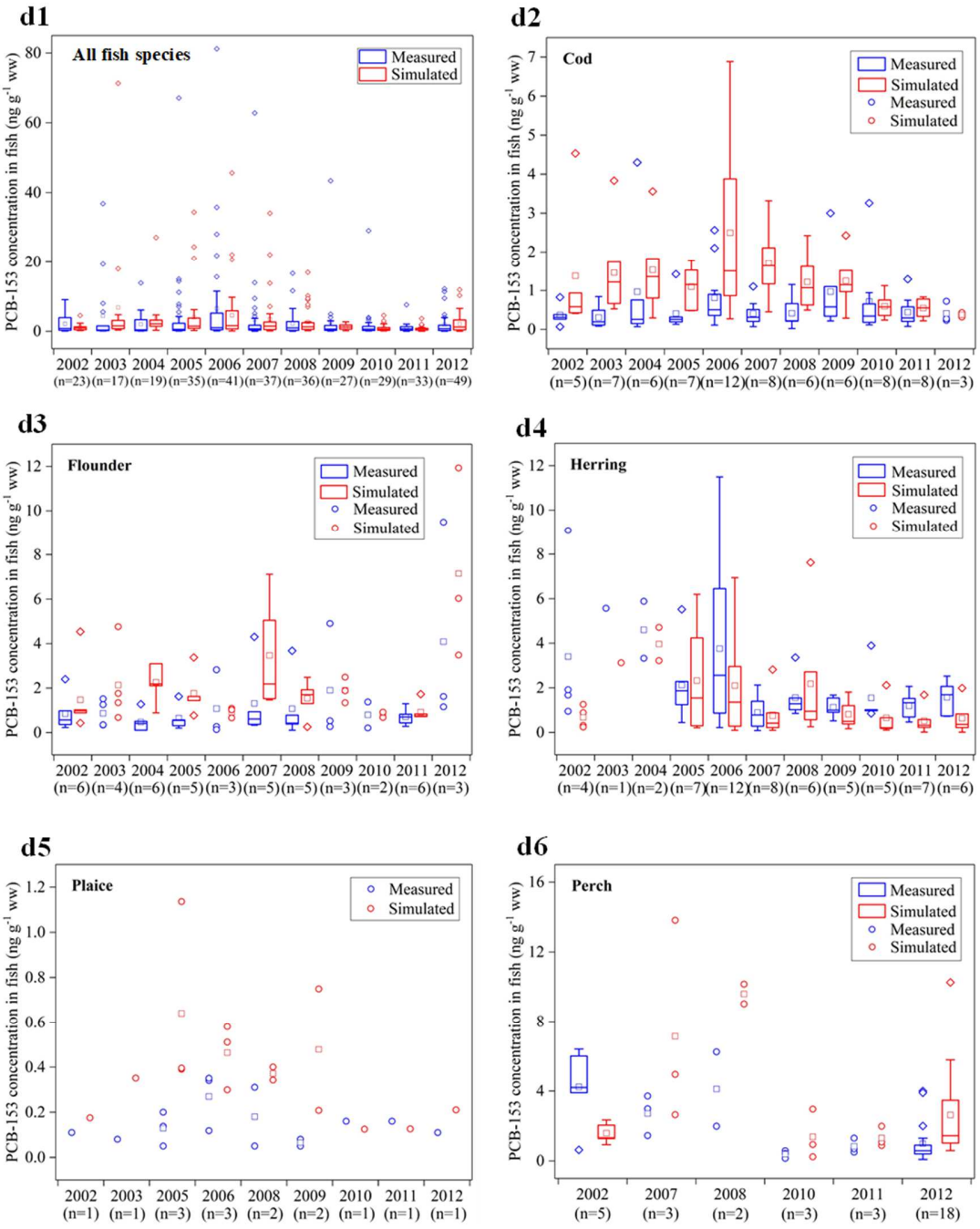
d1
All fish species
Measured
Simulated
PCB-153 concentration in fish (ng g-1 ww)
2002 2003 2004 2005 2006 2007 2008 2009 2010 2011 2012
(n=23)(n=17)(n=19)(n=35)(n=41)(n=37)(n=36)(n=27)(n=29)(n=33)(n=49)
d2
Cod
Measured
Simulated
Measured
Simulated
PCB-153 concentration in fish (ng g-1 ww)
2002 2003 2004 2005 2006 2007 2008 2009 2010 2011 2012
(n=5)(n=7)(n=6)(n=7)(n=12)(n=8)(n=6)(n=6)(n=8)(n=8)(n=3)
d3
Flounder
Measured
Simulated
Measured
Simulated
PCB-153 concentration in fish (ng g-1 ww)
2002 2003 2004 2005 2006 2007 2008 2009 2010 2011 2012
(n=6)(n=4)(n=6)(n=5)(n=3)(n=5)(n=5)(n=3)(n=2)(n=6)(n=3)
d4
Herring
Measured
Simulated
Measured
Simulated
PCB-153 concentration in fish (ng g-1 ww)
2002 2003 2004 2005 2006 2007 2008 2009 2010 2011 2012
(n=4)(n=1)(n=2)(n=7)(n=12)(n=8)(n=6)(n=5)(n=5)(n=7)(n=6)
d5
Plaice
Measured
Simulated
PCB-153 concentration in fish (ng g-1 ww)
2002 2003 2005 2006 2008 2009 2010 2011 2012
(n=1) (n=1) (n=3) (n=3) (n=2) (n=2) (n=1) (n=1) (n=1)
d6
Perch
Measured
Simulated
Measured
Simulated
PCB-153 concentration in fish (ng g-1 ww)
2002 2007 2008 2010 2011 2012
(n=5) (n=3) (n=2) (n=3) (n=3) (n=18)

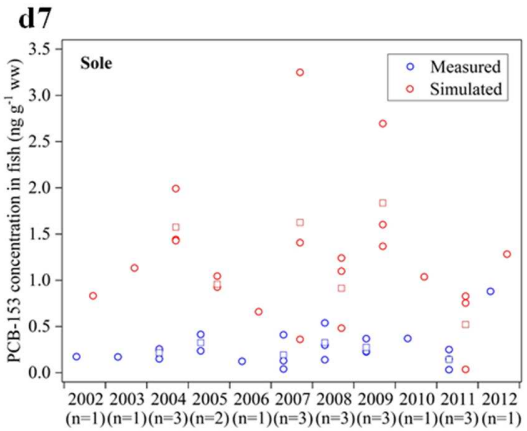

Supplementary Figure 9. Comparison between modeled and measured concentrations of PCB-153 in marine fish. **(a)** and **(b),** Same as **Supplementary Fig. 6a** and **Supplementary Fig. 6b** but for marine fish, respectively. **(c)** Comparison between the modeled and measured concentrations of PCB-153 in twelve marine fish species. The data are presented in log-scale. **(d)** Same as **Supplementary Fig. 8c** but for different marine fish species. **Supplementary Fig. 9d1** shows comparisons between modeled and sampled concentrations of PCB-153 in six fish species, and **Supplementary Figs. 9d2-d7** present comparison between modeled and sampled concentration of PCB-153 in each fish species. All measured concentrations of PCB-153 in marine fish species are listed in **Supplementary Data 2**.

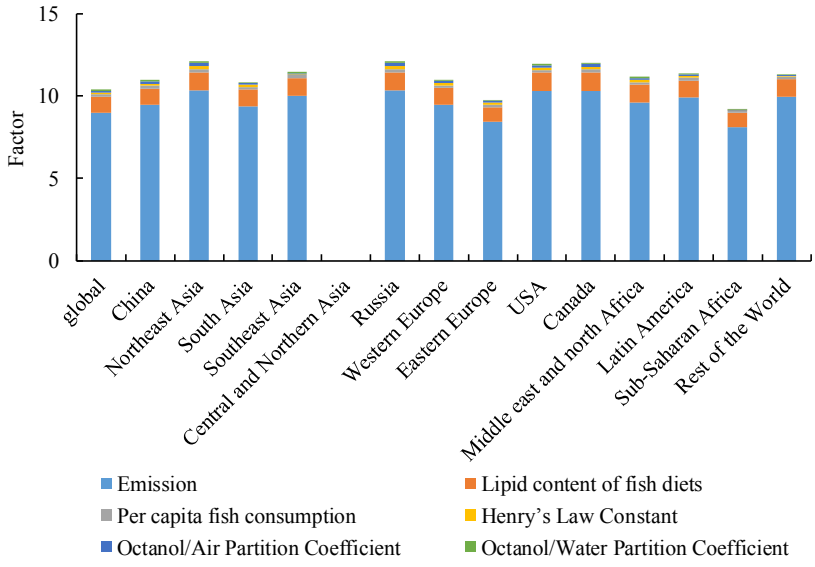

Supplementary Figure 10. Confidence factors that span the 95% confidence interval of EDI from No-trade simulation in different regions and the contribution (%) of the uncertainty from each input parameter given on the bottom of **Supplementary Fig. 10** to the total uncertainty of EDI. Shown is the parameters that exceed 1% contribution to total uncertainty.

Supplementary Tables

Supplementary Table 1. Atlantic salmon feed composition in different country

Country	Feed composition	Year	Source	In this study
Norway	13% fish meal, 9% fish oil, 21% veg oil, 49% veg meal, 8% other raw materials	2017	20	20% fish meal, 12% fish oil, 18% plant oil, 37% plant meal, 13% other materials
	20% fish meal, 12% fish oil, 68% vegetal raw materials	2012	21	
	20% fish meal, 11% fish oil, 37% plant protein, 18% plant oil, 11% starch, 3% micro ingredients	2012	25	
	26-30% fish meal, 17-19% fish oil, 11-13% rapeseed/canola oil, 8-12% meat and bone meal, 10-14% wheat, 3-4% wheat gluten meal, 7-9% sunflower seed meal	2008	19	
	25% fish meal, 15% fish oil, 15% rapeseed/canola oil, 12% soybean meal, 12% wheat, 20% other plant protein sources	2010	19	
Chile	9% fish meal, 7% fish oil, 20% Avian meal, 18% veg oil, 30% veg meal, 16% other raw materials	2017	20	20% fish meal, 10% fish oil, 18% animal by-products, 25% plant meal, 16% veg oil, 11% other materials
	25% fish meal, 12% fish oil, 12% rapeseed/canola oil, 20% plant meal, 17% poultry by-products	2008	18	
	20-25% fish meal, 15% fish oil, 25% plant protein sources, 10-20% animal by-products	2010	19	
UK	25% fish meal, 15% fish oil, 60% other raw materials	2014	11	25% fish meal, 24% fish oil, 40% plant meal, 5% plant oil, 6% other materials
	25.9% fish meal, 22% fish oil, 44.8% vegetable proteins/fillers, 4.1% vegetable oils, 1.5% Vitamin and minerals	2014	22	
	25% fish meal, 27.5% fish oil, 7.7% wheat, 15% wheat gluten, 10% soybean meal, 6.56% soy protein concentrate, 5.72% corn gluten meal, 2.5% premixes	2009	19	
	35% fish meal, 25% fish oil, 5% rapeseed/canola oil, 10% soybean meal, 10% wheat, 5% sunflower seed meal, 5% rapeseed/canola meal, 3% field pea meal, 5% faba bean meal	2008	19	
	35% fish meal, 25% fish oil, 12% wheat, 28% other materials	2010	19	
Canada	25-35% fish meal, 15-25% fish oil, 3-10% soybean meal, 12-18% wheat, 10-40% corn gluten meal, 3-10% rapeseed/canola meal, 10-15% poultry oil, 15-25% poultry by-product meal, 5-12% hydrolyzed feather meal, 6-8% blood meal	2008	19	25% fish meal, 15% fish oil, 35% plant meal, 25% animal by-products

Supplementary Table 2. Origin and species used for fish meal and oil in farmed salmon feed

	Fish meal	Fish oil	References
Norway	Norway/Iceland/Peru	Norway/Iceland/Peru	8, 19, 28, 29
Chile	Chile/Peru	Chile/Peru	
UK	Peru/Norway/Denmark	Peru/Norway/Denmark	
Canada	Chile/Peru	Chile/Peru	

Supplementary Table 3. PCB-153 concentration in salmon feed ingredients (ng g^{-1}). The values in brackets are coefficient of variation (%).

	Concentration (ng g^{-1})	Year	source	References	Concentration (ng g^{-1})	Year	source	References
Fish meal	2.0	2008	Denmark	30	1.93	2008	Norway	30
	2.25	2007	Denmark		1.52	2007	Iceland	
	1.68	2008	Denmark		2.62	2002	Iceland	

	3.98	2008	Denmark		0.62	2002	Norway	
	2.62	2008	Portland		1.58	2002	Iceland	
	2.39	2008	Portland		2.1 (4)	2006	Norway	31
	2.12	2007	Portland		0.17 (16)	2006	Peru	32
	3.67	2007	German					
Fish oil	12.79	2008	Denmark	30	17.64	2002	Norway	30
	8.47	2008	Denmark		42 (6)	2006	Norway	32
	9.43	2002	Iceland		6.5 (19)	2006	southern hemisphere	31
Vegetable meal mixture	0.2 (13)	2006	Wheat (Norway), Wheat gluten (Denmark), Corn gluten (USA), Soybean meal (Norway)	30				
Vegetable oil mixture	2.2 (7)	2006	Linseed oil (Germany), Palm oil (Norway), Rapeseed oil (Denmark)	29				

Supplementary Table 4. PCB-153 level in Atlantic salmon in Norway, Chile, UK, and Canada (ng g^{-1} wet weight)

	Modeled			Measured		
	Wild	Traditional feed	Ingredient feed	Ingredient feed	Year	References
Norway	1.01±0.54	2.84±1.99	1.33±0.78	2.03	2007-2009	35
Chile	0.23±0.13	1.43±0.41	0.66±0.23			
UK	1.07±1.06	2.84±1.99	2.1±1.42	2.78	1999	24
Canada	0.55±0.34	1.43±0.41	0.66±0.12			

Supplementary Table 5. PCB-153 level in Atlantic salmon in Norway, Chile, UK, and Canada (ng g^{-1}, lipid weight)

	Modeled			Measured		
	Wild	Traditional feed	Ingredient feed	Ingredient feed	Year	References
Norway	12.55±6.71	17.32±12.13	11.64±6.82	15.74	2007-2009	35
Chile	3.57±2.02	10.14±2.91	5.12±1.78			
UK	17.83±9.17	24.27±17.01	19.81±13.4	29.9	1999	24
Canada	8.54±5.28	11.04±2.17	5.55±1.01			

Supplementary Table 6. Physicochemical properties of PCB-153 used in the modeling study[41]

Parameters	Value	*Cf*	Parameters	Value	*Cf*
Molecular mass (g/mol)	360.88	1	Liquid vapor pressure (Pa)	1.57×10^{-4}	1.5
Molar volume (cm^3/mol)	237.4	1	Water solubility (g/m^3)	0.0002	1.5
Melting point (°C)	103.5	1	Log K_{oa}	-6.02+4696/T (K)	1.5
Entropy of Fusion (J/mol K)	56.5	1	Log K_{ow} (298 K)	6.87	1.1
Degradation rate constant in air (s^{-1})	1.45×10^{-7}	2	Log K_{oc} (298 K)	6.2	1.5*
Degradation rate constant in soil ($^{-1}$)	1.17×10^{-9}	2	Log H* (Pa m^3/mol)	12.72-3407/T (K)	1.5*
Degradation rate constant in water(s-1)	1.57×10^{-9}	2	BCF (298 K)	4.84	1
Degradation rate constant in sediment (s-1)	1.17×10^{-9}	2			

K_{oa}, K_{ow}, and K_{oc} are octanol-air, octanol-water, and organic carbon sorption partition coefficient, respectively. H is Henry's law constant. BCF is the bioconcentration factors. *Cf* is confidence factor obtained from literature[42,43].

Supplementary Table 7. Summary of parameters, units, values, and their derivation where appropriate for the fugacity equations

Par	Parameter Description	Derivation	Value	Unite	Source
V_w	Volume of water	A_wD_w		m^3	
V_s	Volume of sediment	A_wD_s		m^3	
V_p	Phytoplankton volume at steady state	$\xi_p\gamma_pP * V_w$		m^3	
A_w*	Air-water interface area	The fraction of water area in a grid cell with 1° lat × 1° long		m^2	
A_s	Sediment-water interface area	Area of grid with 1° lat × 1° long		m^2	
D_w	Depth of ocean water exchanging POPs with air		100	m	44
D_s	Depth of sediment exchanging POPs with water		0.05	m	44
Z_a	Fugacity capacity for air	$1/RT_a$		mol m^{-3} Pa^{-1}	
Z_q	Fugacity capacity for aerosols	$K_pT_{sp}Z_a$		mol m^{-3} Pa^{-1}	
K_p	Particle-gas partition coefficient (m^3 μg^{-1})				from CanMETOP
T_{sp}	Total suspended particulate concentration (μg m^{-3})				from CanMETOP
ϕ	Volume fraction occupied by aerosols				from CanMETOP
U_q	Precipitation rate			m h^{-1}	see CanMETOP model description
U_p	Dry deposition velocity				from CanMETOP
Q	Aerosol scavenging ratio		5×10^5		45
R	Idea gas constant		8.314	$Jmol^{-1}K^{-1}$	
T_a	Air temperature			K	from CanMETOP
T	Ocean temperature			K	https://modis.gsfc.nasa.gov/data/dataprod/mod28.php
Z_w	Fugacity capacity for water	$1/H$		mol m^{-3} Pa^{-1}	

H	Henry's law constant			Pa m^3mol^{-1}	see Supplementary Table 6
Z_s	Fugacity capacity for sediment	$K_{oc}f_{oc}\rho_s/H$		mol m^{-3} Pa^{-1}	
K_{oc}	Organic carbon/water partition coefficient			-	see Supplementary Table 6
K_{ow}	Octanol/water partition coefficient			-	see Supplementary Table 6
f_{oc}	Fraction of organic carbon in sediment		0.02		46
ρ_s	Density of sediment		2.3	Kg L^{-1}	47
Z_p	Fugacity capacity for phytoplankton	$K_{ow}Z_w$		mol m^{-3} Pa^{-1}	
k_v	Air-water volatilization/sorption mass transfer coefficient		0.000117	m h^{-1}	44
k_t	Sediment-water diffusion mass transfer coefficient		0.0001	m h^{-1}	47
k_{pu}	Phytoplankton-water uptake rate constant		4.57	h^{-1}	48
k_{pd}	Phytoplankton-water depuration rate	$k_{pu}Z_w/Z_p$		h^{-1}	
U_r	Sediment resuspension rate		1.1×10^{-8}	m h^{-1}	40
U_d	Sediment deposition rate		4.6×10^{-8}	m h^{-1}	40
P	Phytoplankton concentration			mg m^{-3}	49
γ_p	Phytoplankton mass-volume conversion		5.33×10^{-8}	m^3 mg N^{-1}	44
ξ_p	Phytoplankton lipid proportion		0.1	-	44
N	Total concentration of nutrients		3.5	mg N m^{-3}	44
μ	Maximum phytoplankton growth rate		0.04125	h^{-1}	50
k	Phytoplankton nutrient half-saturation		19.1	mg N m^{-3}	44

*The fraction of water area in a grid cell is estimated using land/sea mask

Supplementary Table 8. Sampling sites where time series measurement for air, water, and sediment are available

Air	Sites	Eagle Harbor (EGH)	Sleeping Bears Dunes (SBD)	Sturgeon Point (STP)	Burnt Island (BNT)	Point Petre (PPT)	Egbert (EGB)
	Lat/Lon	47.46 N 88.15 W	44.76 N 86.06 W	42.69 N 79.05 W	45.83 N 82.95 W	43.84 N 77.15 W	44.23 N 79.78 W
	Sites	Zeppelin	Pallas	Aspvreten	Råö	Birkenes/ Birkenes II	Cleveland (CLEV)
	Lat/Lon	78.91 N 11.89 E	68.00 N 24.24 E	58.80 N 17.38 E	57.39 N 11.9 E	58.38N 8.25E 58.39N 8.25E	41.49N -81.68W
Water	Sites	W1	W2	W3	W4	W5	W6
	Lat/Lon	53.67～54.33 N 5.67～6.50 E	53.67～54.18 N 6.50～7.43 E	54.68～55.28 N 6.78～7.50 E	54.00～54.25 N 8.10～8.39 E	54.66～55.05N 7.50～8.20 E	54.63～54.93 N 13.50～14.28 E
Sediment	Sites	S1	S2	S3	S4		

	Lat/Lon	51.55～52.30 N 3.51～4.40 E	53.54～54.38 N 7.65～8.49 E	42.06～42.44 N 8.65～9.12 W	36.58～37.14 N 6.63～7.30W		

Supplementary Table 9. Correlation coefficient, FAC, bias, and error statistics for comparison between modeled and measured concentrations for air, water, sediment, and fish

	N	r	p	FAC2 (%)	FAC5 (%)	FAC10 (%)	MB[a]	ME[a]	NMB (%)	NME (%)
Air	3475	0.69	<0.001	40.04	80.06	92.69	0.045	1.017	3.27	74.74
Water	210	0.74	<0.001	40.95	74.76	87.62	0.227	2.074	8.41	76.9
Sediment	457	0.52	<0.001	32.60	67.40	81.40	-0.162	0.50	-28.4	87.3
Fish	346	0.47	<0.001	33.69	70.33	91.21	-0.343	2.862	-11.54	96.25

Note: [a] unit is pg m^{-3} for air, pg L^{-1} for water, and ng g^{-1} ww for sediment and fish.

Supplementary Data 1. Species name, lipid contents, weights, and diet compositions represented in global marine food web.

Supplementary Data 2. Comparisons between modeled and measured PCB-153 concentrations in air, water, sediment, and fish.

References

1. Breivik, K., Armitage, J. M., Wania, F., Sweetman, A. & Jones, K. C. Tracking the global distribution of persistent organic pollutants accounting for E-waste exports to developing regions. *Environ. Sci. Technol.* 50, 798-805 (2016).
2. Gioia, R. *et al.*, Polychlorinated Biphenyls (PCBs) in air and seawater of the Atlantic Ocean: Sources, trends and processes. *Environ. Sci. Technol.* **42**, 1416–1422 (2008).
3. Gómez-Lavín, S., Gorri, D. & Irabien, A. Assessment of PCDD/Fs and PCBs in Sediments from the Spanish Northern Atlantic Coast. *Water Air Soil Pollut.* **221**, 287–299 (2011).
4. Froescheis, O., Looser, R., Cailliet, G. M., Jarman, W. M. & Ballschmiter, K. The deep-sea as a final global sink of semivolatile persistent organic pollutants? Part I: PCBs in surface and deep-sea dwelling fish of the North and South Atlantic and the Monterey Bay Canyon (California). *Chemosphere.* **40**, 651–660 (2000).
5. Breivik, K., Sweetman, A., Pacyna, J. M. K. & Jones, C. Towards a global historical emission inventory for selected PCB congeners — a mass balance approach 1. Global production and consumption. *Sci. Total Environ.* **290**, 181–198 (2002).
6. Breivik, K., Sweetman, A., Pacyna, J. M. K. & Jones, C. Towards a global historical emission inventory for selected PCB congeners — A mass balance approach: 3. An update. *Sci. Total Environ.* **377**, 296–307 (2007)
7. Pareto Securities. Seafood Research Report. Norway. (2016).
8. FAO (Food and Agriculture Organization of United Nations). Globe fish Highlights: A quarterly update on the world seafood markets. FAO. (2015).
9. Berntssen, M. H. G., Maage, A., Julshamn, K., Oeye, B. E. & Lundebye, A. K. Carry-over of dietary organochlorine pesticides, PCDD/Fs, PCBs, and brominated flame retardants to Atlantic salmon (Salmo salar L.) fillets. *Chemosphere* **83,** 95–103 (2011). doi:10.1016/j.chemosphere.2011.01.017
10. Berntssen, M. G. H., Sanden, M., Hove, H. & Lie, Ø. Modelling scenarios on feed-to-fillet transfer of dioxins and dioxin-like PCBs in future feeds to farmed Atlantic salmon (*Salmo salar*). *Chemosphere* **163,** 413–421 (2016). doi:10.1016/j.chemosphere.2016.08.067
11. Isosaari, P., Kiviranta, H., Lie, Ø., undebye, A. K., Ritchie, L. G. & Vartiainen, T. Accumulation and distribution of polychlorinated dibenzo-p-dioxin, dibenzofuran, and polychlorinated biphenyl congeners in Atlantic salmon (*Salmo salar*). *Environ. Toxicol. Chem.* **23,** 1672–1679 (2004). doi:https://doi.org/10.1897/03-367
12. Berntssen, M. H. G., Giskegjerde, T. A., Rosenlund, G., Torstensen, B. E. & Lundebye, A. K. Predicting world health organization toxic equivalency factor dioxin and dioxin-like polychlorinated biphenyl levels in farmed Atlantic Salmon (*Salmon Sala*r) based on known levels in feed. *Environ. Toxicol. Chem.* **26,** 13–23 (2007). doi:10.1897/06-122R.1
13. Isosaari, P., Vartiainen, T., Hallikainen, A. & Ruohonen, K. Feeding trial on rainbow trout: comparison of dry fish feed and Baltic herring as a source of PCDD/Fs and PCBs. *Chemosphere* **48,** 795–804 (2002). doi:10.1016/S0045-6535(02)00128-5
14. Lundebye, A. K. *et al.* Vartiainen, Dietary uptake of dioxins (PCDD/PCDFs) and dioxin-like PCBs in Atlantic salmon (Salmo salar). *Aquac. Nutr.* **10,** 199–207 (2004).

111 doi:10.1111/j.1365-2095.2004.00299.x
112 15. Ytrestøyl, T., Aas, T. S. & Åsgård, T. Utilisation of feed resources in production of
113 Atlantic salmon (Salmo salar) in Norway. *Aquaculture* **448,** 365–374 (2015).
114 doi:10.1016/j.aquaculture.2015.06.023
115 16. Davidson, J., Barrows, F. T., Kenney, P. B., Good, C., Schroyer, K. & Summerfelt,
116 S. T. Effects of feeding a fishmeal-free versus a fishmeal-based diet onpost-smolt
117 Atlantic salmon Salmo salar performance, water quality,and waste production in
118 recirculation aquaculture systems. *Aquacult. Eng.* **74,** 38–51 (2016).
119 doi:10.1016/j.aquaeng.2016.05.004
120 17. Torstensen, B. E. *et al.* Novel production of Atlantic salmon (Salmo salar) protein
121 based on combined replacement of fish meal and fish oil with plant meal and
122 vegetable oil blends. *Aquaculture* **285,** 193–200 (2008).
123 doi:10.1016/j.aquaculture.2008.08.025
124 18. Tacon, A. G. J. State of information on salmon aquaculture feed and the
125 environment. Report prepared for WWF US initiated salmon aquaculture dialogue.
126 (2005).
127 19. Tacon, A. G. J., Hasan, M. R. & Metian, M. Demand and supply of feed ingredients
128 for farmed fish and crustaceans. Fisheries and aquaculture technical report for FAO.
129 (2011).
130 20. Marine Harvest ASA, Salmon Farming Industry Handbook 2018.
131 http://hugin.info/209/R/2200061/853178.pdf. (2018).
132 21. Shepherd, C. J., Monroig, O. & Tocher, D. R. Future availability of raw materials
133 for salmon feeds and supply chain implications: The case of Scottish farmed salmon.
134 *Aquaculture* **467,** 49–62 (2017). doi:10.1016/j.aquaculture.2016.08.021
135 22. Newton, R. W. & Little, D. C. Mapping the impacts of farmed Scottish salmon from
136 a life cycle perspective. *Int. J. Life Cycle Assess.* **23,** 1018–1029 (2018).
137 doi:10.1007/s11367-017-1386-8
138 23. Hites, R. A., Foran, J. A., Carpenter, D. O., Hamilton, M. C., Knuth, B. A. &
139 Schwager, S. J. Global Assessment of Organic Contaminants in Farmed Salmon.
140 *Science* **303,** 226–229 (2004). doi:10.1126/science.1091447
141 24. Jacobs, M. N., Covaci, J. A. & Schepens, P. Investigation of selected persistent
142 organic pollutants in farmed Atlantic salmon (Salmo salar), salmon aquaculture feed,
143 and fish oil components of the feed. *Environ. Sci. Technol.* **36,** 2797–2805 (2002).
144 doi:10.1021/es011287i
145 25. Friesen, E. N., Ikonomou, M. G., Higgs, D. A., Ang, K. P. & Dubetz, C. Use of
146 Terrestrial Based Lipids in Aquaculture Feeds and the Effects on Flesh
147 Organohalogen and Fatty Acid Concentrations in Farmed Atlantic Salmon. *Environ.*
148 *Sci. Technol.* **42,** 3519–3523 (2008). doi:10.1021/es0714843
149 26. Bell, J. G., McGhee, F., Dick, J. & Tocher, D. Dioxin and dioxin-like
150 polychlorinated biphenyls (PCBS) in Scottish farmed salmon (Salmo salar): effects
151 of replacement of dietary marine fish oil vegetable oils. *Aquaculture* **243,** 305–314
152 (2005). doi:10.1007/s10661-012-2564-6
153 27. NORA. Dioxin and dioxin like PCB in four commercially Important Pelagic Fish
154 Stocks in the North East Atlantic Ocean.

http://www.slideshare.net/FIFIsland/lokaskrsla-nora. (2003).
28. Sea Fish Industry Authority. Fishmeal and fish oil facts and figures. Sea Fish Industry Authority, UK, 2016.
29. Ytrestøyl, T., Asa, T. S. & Åsgård, T. Resource utilization of Norwegian salmon farming in 2012 and 2013. Nofima, Norway. (2014).
30. Suominen, K. *et al.* Occurrence of PCDD/F, PCB, PBDE, PFAS, and Organotin Compounds in Fish Meal, Fish Oil and Fish Feed. *Chemosphere* **85,** 300–306 (2011). doi:10.1016/j.chemosphere.2011.06.010
31. Nácher-Mestre, J., Serrano, R., Benedito-Palos, L., Navarro, J. C., López, F. J. & Pérez-Sánchez, J. Effects of fish oil replacement and re-feeding on the bioaccumulation of organochlorine compounds in gilthead sea bream (Sparus aurata L.) of market size. *Chemosphere* **76,** 811–817 (2009). doi:10.1016/j.chemosphere.2009.04.046
32. Olli, J. J. *et al.* Removal of persistent organic pollutants from Atlantic salmon (Salmo salar L.) diets: Influence on growth, feed utilization efficiency and product quality. *Aquaculture* **310,** 145–155 (2010). doi:10.1016/j.aquaculture.2010.09.044
33. Boissy, J., Aubin, J., Drissi, A., van der Werf, H. M. G., Bell, G. J. & Kaushik, S. J. Environmental impacts of plant-based salmonid diets at feed and farm scales. *Aquaculture* **321,** 61–70 (2011). doi:10.1016/j.aquaculture.2011.08.033
34. Berntssen, M. H. G., Julshamn, K. & A. Lundebye, K. Chemical contaminants in aquafeeds and Atlantic salmon (Salmo salar) following the use of traditional- versus alternative feed ingredients. *Chemosphere* **78,** 637–646 (2010). doi:10.1016/j.chemosphere.2009.12.021
35. Berntssen, M. H. G. *et al.* Reducing persistent organic pollutants while maintaining long chain omega-3 fatty acid in farmed Atlantic salmon using decontaminated fish oils for an entire production cycle. *Chemosphere* **81,** 242–252 (2010). doi:10.1016/j.chemosphere.2010.06.031
36. Ma, J., Daggupaty, S., Harner, T. & Li, Y. F. Impacts of lindane usage in the Canadian prairies on the Great Lakes ecosystem. 1. Coupled atmospheric transport model and modeled concentrations in air and soil. *Environ. Sci. Technol.* **37**, 3774–3781 (2003). doi:10.1021/es034747b
37. Zhang, L., Ma, J., Venkatesh, S., Li, Y. F. & Cheung, P. Modeling evidence of episodic intercontinental long-rang Mackay e transport of lindane. *Environ. Sci. Technol.* **42**, 8791–8797 (2008). doi:10.1021/es801271b
38. Ma, J., Daggupaty, S. M., Harner, T., Pierrette, P. & Waite, D. Impacts of lindane usage in the Canadian prairies on the Great Lakes ecosystem - 2: Modeled dry, wet depositions and net gas exchange fluxes, and loadings to the Great Lakes. *Environ. Sci. Technol.* **38**, 984–990 (2004).
39. Wallberg, P. & Andersson, A. Transfer of carbon and a polychlorinated biphenyl through the pelagic microbial food web in a coastal ecosystem. *Environ. Toxicol. Chem.* **19**, 827–835 (2000). doi:10.1002/etc.5620190407
40. Mackay, D. Multimedia environmental models: The fugacity approach. 2nd Edition, CRC Press, Boca Raton (2001).

41. Mackay, D., Shiu, W. Y., Ma, K. C. & Lee, S. C. Handbook of physical-chemical properties and environmental fate for organic chemicals. CRC Press, Boca Raton (2006).
42. MacLeod, M., Fraser, A. J. & Mackay, D. Evaluating and expressing the propagation of uncertainty in chemical fate and bioaccumulation models. *Environ. Toxicol. Chem.* **21**, 700–709 (2002). doi:10.1002/etc.562021040
43. Wöhrnschimmel, H., Macleod, M. & Hungerbuhler, K. Emissions, Fate and Transport of Persistent Organic Pollutants to the Arctic in a Changing Global Climate. *Environ. Sci. Technol.* **47**, 2323–2330 (2013). doi:10.1021/es304646n
44. Cropp, R., Kerr, G., Bengtson-Nash, S. & Hawker, D. A dynamic biophysical fugacity model of the movement of a persistent organic pollutant in Antarctic marine food webs. *Environ. Chem.* **8**, 263–280 (2011).
45. Schwede, D. B. & Paumier, J. O. Sensitivity of the industrial source complex model to input deposition parameters. *J. Appl. Meteorol.* **36**, 1096–1106 (1997). doi:10.1175/1520-0450(1997)036
46. Wania, F. & Mackay, D. A global distribution model for persistent organic chemicals. *Sci. Total Environ.* **160**, 211-232 (1995). doi:10.1016/0048-9697(95)04358-8
47. Reimers, C. E. & Suess, E. The partitioning of organic carbon fluxes and sedimentary organic matter decomposition rates in the ocean. *Mar. Chem.* **13**, 141–68 (1983). doi:10.1016/0304-4203(83)90022-1
48. Dachs, J., Eisenreich, S. J. & Hoff, R. M. Influence of Eutrophication on Air-Water Exchange, Vertical Fluxes, and Phytoplankton Concentrations of Persistent Organic Pollutants. *Environ. Sci. Technol.* **34**, 1095–102 (2000). doi:10.1021/es990759e
49. Vallina1, S. M., Follows, M. J., Dutkiewicz, S., Montoya, J. M., Cermeno, P. & Loreau, M. Global relationship between phytoplankton diversity and productivity in the ocean. *Nat. Commun.* 5, 4299 (2014). doi:10.1038/ncomms5299
50. Gabric, A. J., Cropp, R., Hirst, T. & Marchant, H. The sensitivity of dimethyl sulfide production to simulated climate change in the Eastern Antarctic Southern Ocean. *Tellus B: Chem. Phys. Meteorol.* **55**, 966–981 (2003). doi:10.1034/j.1600-0889.2003.00077.x
51. Gobas, F. A. P. C., McNeil, E. J., Lovett-Doust, L. & Haffner, G. D. Bioconcentration of chlorinated aromatic hydrocarbons in aquatic macrophytes. *Environ. Sci. Technol.* **2**5, 924–929 (1991). doi: 10.1021/es00017a015
52. Mailhot, H. Prediction of algal bioaccumulation and uptake rate of nine organic compounds by ten physicochemical properties. *Environ. Sci. Technol.* **21**, 1009–1013 (1987). doi:10.1021/es50001a016
53. Gobas, F. A. P. C., Zhang, X. & Wells, R. Gastrointestinal magnification: the mechanism of biomagnification and food chain accumulation of organic chemicals. *Environ. Sci. Technol.* **27,** 2855–2863 (1993). doi:10.1021/es00049a028
54. Gobas, F. A. P. C. A model for predicting the bioaccumulation of hydrophobic organic chemicals in aquatic food-webs: application to Lake Ontario. *Ecol. Model.* **69**, 1–17 (1993). doi:10.1016/0304-3800(93)90045-T
55. Gobas, F. A. P. C., Bedard, D. C., Ciborowski, J. J. H. & Haffner, G. D. Bioaccumulation of chlorinated hydrocarbons by the mayfly (*Hexagenia limbata*) in

Lake St. Clair. *J. Great Lakes Res.* **15**, 581–588 (1989). doi:10.1016/S0380-1330(89)71512-4
56. Shea, D. Developing national sediment quality criteria. *Environ. Sci. Technol.* **22**, 1256–1261 (1988). doi:10.1021/es00176a002
57. Clark, K. E., Gobas, F. A. P. C. & Mackay, D. Model of organic chemical uptake and clearance by fish from food and water. *Environ. Sci. Technol.* **24**, 1203–1213 (1990). doi:10.1021/es00078a008
58. Thomann, R. V. & Connolly, J. P. Model of PCB in the Lake Michigan lake trout food chain. *Environ. Sci. Technol.* **18**, 65–71 (1984). doi:10.1021/es00120a003
59. Jing, W. *et al.* Contamination of short-chain chlorinated paraffins to the biotic and abiotic environments in the Bohai Sea. *Environ. Pollut.* **233**, 114–124 (2018). doi:10.1016/j.envpol.2017.10.034
60. Arnot, A. & Gobas, F. A. P. C. A food web bioaccumulation model for organic chemicals in aquatic ecosystems. *Environ. Toxicol. Chem.* **23**, 2343–2355 (2004). doi:10.1897/03-438
61. Gobas, F. A. P. C. & Arnot, J. A. Food web bioaccumulation model for polychlorinated biphenyls in San Francisco Bay, California, USA. *Environ. Toxicol. Chem.* **29**, 1385–-1395 (2010). doi:10.1002/etc.164.
62. Arnot, J. A. & Gobas, F. A. P. C. A review of bioconcentration factor (BCF) and bioaccumulation factor (BAF) assessments for organic chemicals in aquatic organisms. *Environ. Rev.* **14**, 257–297. (2006). doi:10.1139/a06-005
63. Gobas, F. A. P. C. & MacKay, D. Dynamics of hydrophobic organic chemical bioconcentration in fish. *Environ. Toxicol. Chem.* **6**, 495–504 (1987). doi:10.1002/etc.5620060702
64. Fisk, A. T., Norstrom, R. J., Cymbalisty, C. D. & Muir, D. C. G. Dietary accumulation and depuration of hydrophobic organochlorines: Bioaccumulation parameters and their relationship with the octanol/water partition coefficient. *Environ. Toxicol. Chem.* **17**, 951–961 (1998). doi:10.1002/etc.5620170526
65. Gobas, F. A. P. C., Muir, D. C. G. & Mackay, D. Dynamics of dietary bioaccumulation and faecal elimination of hydrophobic organic chemicals in fish. *Chemosphere* **17**, 943–962 (1988). doi:10.1016/0045-6535(88)90066-5
66. Parkerton, T. Estimating toxicokinetic parameters for modeling the bioaccumulation of non-ionic organic chemicals in aquatic organisms. Ph. D. dissertation, Rutgers University. New Brunswick, NJ (1993).
67. Weininger, D. Accumulation of PCBs by lake trout in Lake Michigan. PhD dissertation, University of Wisconsin, Madison, WI (1978).
68. Thomann, R., Connolly, J. & Parkerton, T. Modeling accumulation of organic chemicals in aquatic food webs. In: Gobas, F. A. P. C. & Mccorquodale, J. A. (Editors). Chemical Dynamics in Fresh Water Ecosystems. Lewis, Chelsea, MI, USA, 153–186 (1992).
69. Katsoyiannis, A. & Samara, C. Persistent organic pollutants (POPs) in the sewage treatment plant of Thessaloniki, Northern Greece: occurrence and removal. *Water Res.* **38,** 2685–2698 (2004). doi:10.1016/j.watres.2004.03.027
70. Needham, T. P. & Ghosh, U. Four decades since the ban, old urban wastewater

treatment plant remains a dominant source of PCBs to the environment. *Environ. Pollut.* **246,** 390–397 (2019). doi:10.1016/j.envpol.2018.12.016
71. Morris, S. & Lester, J. N. Behaviour and fate of polychlorinated biphenyls in a pilot wastewater treatment plant. *Water Res.* **28,** 1553–1561 (1994). doi:10.1016/0043-1354(94)90222-4
72. Melymuk, L. *et al.* Diamond, From the city to the lake: Loadings of PCBs, PBDEs, PAHs and PCMs from Toronto to Lake Ontario. *Environ. Sci. Technol.* **48,** 3732–3741 (2014). doi:10.1021/es403209z
73. Zhang, L., Shi, S., Dong, L., Zhang, T., Zhou, L. & Zhang, Y. Concentrations and possible sources of polychlorinated biphenyls in the surface water of the Yangtze River Delta, China. *Chemosphere* **85,** 399–405 (2011). doi:10.1016/j.chemosphere.2011.07.064
74. Xu, Y. *et al.* An improved inventory of polychlorinated biphenyls in China: A case study on PCB-153. *Atmos. Environ.* **183,** 40–48 (2018). doi:10.1016/j.atmosenv.2018.04.013
75. Chang, J. & Hanna, S. Air quality model performance evaluation. *Meteorol. Atmos. Phys.* **87,** 167-196 (2004). doi: 10.1007/s00703-003-0070-7
76. Cortes, D. *et al.* Temporal trends in gas-phase concentrations of chlorinated pesticides measured at the shores of the Great Lakes. *Environ. Sci. Technol.* **32**, 1920–1927 (1998). doi:10.1021/es970955q
77. Hung, H. *et al.* Temporal trends of Persistent Organic Pollutants (POPs) in arctic air: 20 years of monitoring under the Arctic Monitoring and Assessment Programme (AMAP). *Environ. Pollut.* **217**, 52-61 (2016). doi:10.1016/j.envpol.2016.01.079
78. Friedman, C. L. & Selin, N. E. PCBs in the Arctic atmosphere: determining important driving forces using a global atmospheric transport model. *Atmos. Chem. Phys*. **16**, 3433–3448 (2016). doi:10.5194/acp-16-3433-2016
79. Ma, J., Venkatesh, S., Li, Y. & Daggupaty, S. M. Tracking toxaphene in the North American Great Lakes basin-1. Impact of toxaphene residues in the U.S. soils. *Environ. Sci. Technol.* **39**, 8132–8141 (2005). doi:10.1021/es050945m
80. Calabrese, E. J. Commemoration of the 50th anniversary of Monte Carlo. *Hum. Ecol. Risk Assess.* **2**, 627–1038 (1996). doi:10.1080/10807039609383638
81. Slob, W. Uncertainty Analysis in Multiplicative Models. *Risk Anal.* **14,** (1994). doi: https://doi.org/10.1111/j.1539-6924.1994.tb00271.x.
82. Breivik, K., Sweetman, A., Pacyna, J. M. & Jones, K. C. Towards a global historical emission inventory for selected PCB congeners — a mass balance approach 2. Emission. *Sci. Total Environ.* **290**, 199–224 (2002). doi: 10.1016/S0048-9697(01)01076-2
83. Asnte, K. A. *et al.* Occurrence of halogenated contaminants in inland and coastal fish from Ghana: Levels, dietary exposure assessment and human health implications. *Ecotox. Environ. Safe.* **94**, 123–130 (2013). doi:10.1016/j.ecoenv.2013.05.008
84. Stewart, M., Phillips, N. R., Olsen, G., Hickey, C. W., Tipa, G. Organochlorines and heavy metals in wild caught food as a potential human health risk to the indigenous Māori population of South Canterbury, New Zealand. *Sci. Total Environ.* **409**, 2029–

2039 (2011). doi:10.1016/j.scitotenv.2011.02.028